

Università degli Studi di Salerno

Dipartimento di Chimica e Biologia

“Adolfo Zambelli”



Corso di Dottorato di Ricerca in Chimica

XIV CICLO NUOVA SERIE

Cavity Filling and Chirality Effects in Calixarene Threading

Candidato:

Concilio Gerardo

Matr. 8880700196

Relatore:

Prof. Placido Neri

Coordinatore:

Prof. Gaetano Guerra

Anno Accademico: 2014-2015

INDEX

INTRODUCTION.....	1
1.1 SUPRAMOLECULAR CHEMISTRY AND MOLECULAR RECOGNITION.....	1
1.2 MACROCYCLIC HOSTS: CALIXARENES	5
1.2.1 Calixarenes in molecular recognition	8
CHAPTER II	10
CAVITY FILLING OF THE CALIX[6]ARENE MACROCYCLE WITH DIALKYLAMMONIUM GUESTS	10
2.1 RECOGNITION OF ALKYLAMMONIUM GUESTS BY CALIXARENES MACROCYCLES	10
2.2 AIMS	13
2.3 RESULT AND DISCUSSION	14
2.3.1 Packing Coefficient Calculation	29
2.3.2 Contacting Coefficient Calculation	34
2.3 CONCLUSION.....	38
2.4 EXPERIMENTAL SECTION.....	39
CHAPTER III.....	74
CHIRALITY AND CHIRAL MOLECULAR RECOGNITION IN THE CALIXARENE THREADING	74
3.1 CHIRAL RECOGNITION IN SUPRAMOLECULAR STRUCTURES 	74
3.2.2 Chiral recognition in gas phase.	78
3.3 AIMS	82
3.4 RESULTS AND DISCUSSIONS.....	82

3.4.1 Synthesis of chiral hosts and guest	86
3.4.2 Gas-phase study	96
3.4.3 Synthesis of enantiopure hosts.....	97
3.4.4 Synthesis of labelled enantiopure guest.....	100
3.4.5 MS experiments	103
3.4.6 Concentration Effect.....	105
3.4.7 Isotopic Effects	105
3.4.8 Chiral Recognition.....	109
3.5 CONCLUSION.....	113
3.6 EXPERIMENTAL SECTION.....	114
CHAPTER IV	155
SYNTHESIS OF NEW CALIXARENE AND RESORCINARENE BASED CHIRAL HOSTS	155
4.1 CHIRALITY AND INHERENT CHIRALITY IN CALIXARENES AND RESORCINARENES.....	155
4.1.1 Inherently chiral calixarenes.....	156
4.1.2 <i>Meta</i> -functionalization of Calixarenes: the “ <i>p</i> - bromodienone route”	159
4.1.3 Chiral and inherently chiral resorcinarenes	163
4.2 AIMS	164
4.2 RESULTS AND DISCUSSION	165
4.2.1 Synthesis of calixarene hosts via <i>p</i> -bromodienone route	165
4.2.2 Synthesis of inherently chiral resorcin[4]arene	176
4.2.3 HPLC-EDC analysis and Computational Spectroscopy	181

4.3 CONCLUSION.....	186
4.4 EXPERIMENTAL SECTION.....	187

CHAPTER I

INTRODUCTION

1.1 SUPRAMOLECULAR CHEMISTRY AND MOLECULAR RECOGNITION

Supramolecular Chemistry has been defined by Jean Marie Lehn as “*the chemistry beyond the molecule*”,¹ and refers to the study of the complex systems resulting from the aggregation of more chemical entities (molecules or ions) through non-covalent forces such as: ion-ion interactions (100-350 kJ mol⁻¹); ion-dipole (50-200 kJ mol⁻¹); hydrogen bonding (4-120 kJ mol⁻¹); dipole-dipole (5-50 kJ mol⁻¹); cation- π (5-80 kJ mol⁻¹); π - π (1-50 kJ mol⁻¹) Van der Waals (< 5 kJ mol⁻¹).²

Non-covalent interactions are weaker with respect to covalent bonds, however, this lability allows the occurrence of novel phenomena such as self-assembly³, that provide a valid approach to the synthesis of molecular systems on nanometric scale.

¹ J. M. Lehn, “*Supramolecular Chemistry: Concepts and Perspectives*”, VCH, Weinheim, **1995**.

² W. J. Steed, L. Atwood, “*Supramolecular Chemistry*”, Wiley, New York, **2000**.

³ D. Philip, J. F. Stoddart, *Angew. Chem. Int. Ed. Engl.* **1996**, 35, 1154-1196.

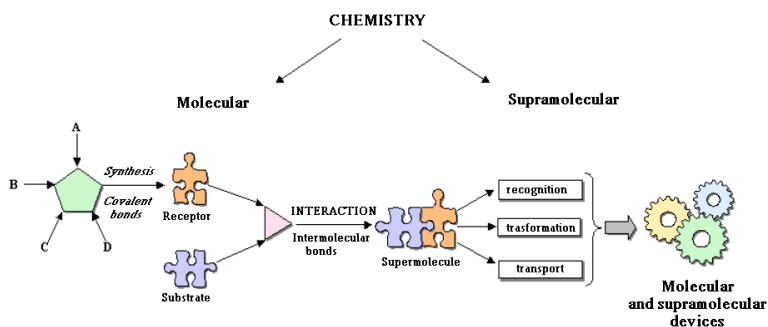


Figure 1.1 Supramolecular Chemistry.

In analogy with biological systems like enzyme-substrate Cram defined *host-guest complex*⁴, in which a host (receptor) is able to selectively complexes (recognizes) a guest (substrate). This process is a bedrock of supramolecular chemistry and it is called “*molecular recognition*”.

Emil Fisher was the first who gave the interpretation of the molecular recognition phenomenon introducing the *lock-and-key*⁵ model in 1894.

The model describes the specificity and the bond strength as the result of complementary interactions between the host and guest structures.

The most important requirements to obtain a high selectivity in the recognition process are:

- a) Geometric size and shape complementarity between

⁴ D. J. Cram, *Angew. Chem. Int. Ed. Engl.* **1988**, 27, 1009-1020.

⁵ E. Fischer, *Ber. Deutsch. Chem. Ges.* **1894**, 27, 2985-2993.

host and guest.

- b) Interactional complementarity which is achieved when an optimal match between the two interacting molecules is accomplished, even via electronic interactions such as van der Waals, ion-ion; etc.;
- c) Vast contact areas to enhance the host-guest interactions;
- d) Multiple interaction sites;
- e) Strong bond energies to realize a good stability of the complex and enhance the selectivity towards a certain guest.

Furthermore the discovery that proteins have an high flexibility and the observation that they can change their conformation during protein-substrate interactions, led to the extension of the *lock-and-key* model and the formulation of the *induced-fit* principle.⁶

The *induced-fit* process was described for the first time by Koshland in 1958 and it was mainly used to describe the interactions that are established between enzymes and substrates in biological systems. In this case the enzymatic action requires a specific orientation of the catalytic groups first and then the substrate causes a significant three-

⁶ (a) D. E. Koshland Jr., *Proc. Natl. Acad. Sci. USA* **1958**, *44*, 98-104; (b) D. E. Koshland Jr., *Adv. Enzym.* **1960**, *22*, 45.

dimensional modification of the active site in order to bring the catalytic groups in the correct position. (Figure 2)

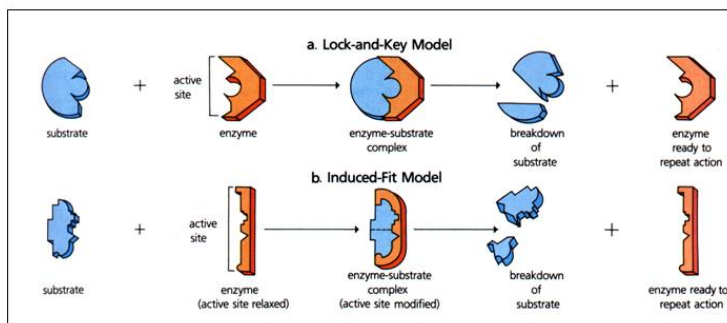


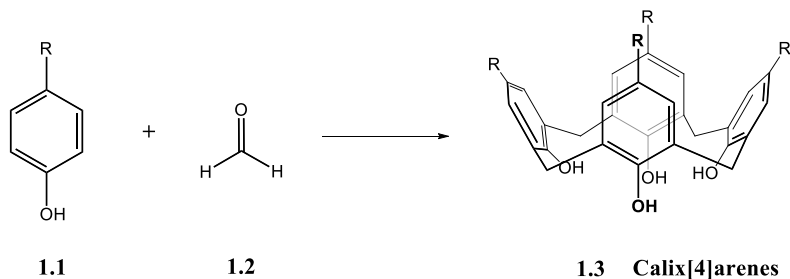
Figure 1.2 Difference between: a) *lock-and-key* model, and b) *induced-fit* model.

The *induced-fit* model in biological systems was demonstrated by a huge number of experiments and nowadays it is accepted that almost all enzymes show conformational changes after the interaction with substrates. Although in Supramolecular Chemistry, the *induced-fit* process has provided a good model to explain the host-guest interactions.

The substantial difference between the *lock-and-key* model and the *induced-fit* one is that the first model requires rigid molecules, the substrate in particular, whereas the *induced-fit* needs a certain flexibility that allows a conformational change in the molecular architectures to promote the molecular recognition process.

1.2 MACROCYCLIC HOSTS: CALIXARENES

Calixarenes⁷ have been widely studied in molecular recognition processes as versatile hosts because of their conformational properties and synthetic versatility.



Scheme 1.1 Synthesis of calix[4]arene.

Calix[*n*]arene are metacyclophanes obtained by condensation of phenols with formaldehyde in different conditions. The name of these compounds has been attributed by C. D. Gutsche because the cyclic tetramer, the *p*-*tert*-butylcalix[4]arene, adopts both in solution and solid state, a cup-like shape that reminded a Greek vase which name is “*calyx krater*”.

⁷ D. Gutsche, *Calixarenes*; The Royal Society of Chemistry, Cambridge, UK, 1989.

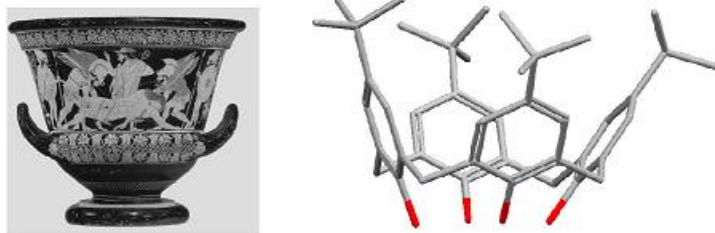


Figure 1.3 *Calix krater* (left), *p-tert-butylcalix[4]arene* structure (right).

The “*n*” in brackets means the number of aromatic units of the macrocycle.

Calixarenes co called “*major*”⁸ are those made of 4, 6 and 8⁹ phenolic units, they are easy to obtain and for this reason they have been found more applications in many fields. Contrary calixarenes “*minor*” are composed of 5 and 7 units and they are less studied because of the tediousness of the reactions and the low yields in which these compounds are obtained.

However calixarenes having phenolic units from 9 to 20⁸ have been fully characterized but are less used.

The calix[6]arene conformation have been described as distorted cone,¹⁰ compressed cone,¹¹ pinched cone,¹² double

⁸ D. R. Stewart, C. D. Gutsche, *J. Am. Chem. Soc.* **1999**, *121*, 4136-4146.

⁹ A. Ikeda, S. Shinkai, *Chem. Rev.* **1997**, *97*, 1713-1734.

¹⁰ G. D. Andreotti, G. Calestani, F. Ugozzoli, A. Arduini, E. Ghidini, A. Pochini, R. Ungaro, *J. Inclusion Phenom.* **1987**, *5*, 123-126.

¹¹ A. N. Novikov, V. A. Bacherikov, A. I. Gren, *Russian J. Gen. Chem.* **2002**, *72*, 1396-1400.

¹² a) M. Halit, O. Oehler, M. Perrin, A. Thozet, R. Perrin, J. Vicens and M. Bourakhodar, *J. Inclusion Phenom.*, **1988**, *6*, 613-623; b) P. Thuéry, N. Keller, M. Lance, J. D. Vigner, M. Nierlich, *J. Inclusion Phenom. Molec.*

partial cone,¹³ winged,¹⁴ 1,2,3-alternate,¹⁵ 1,3,5-alternate and distorted 1,2,3-alternate.¹⁶

Bott and coworkers demonstrated that the calix[6]arene conformation, in the solid state, depends strongly on the solvent used for the crystallization. Because the solvent is involved in the hydrogen bonds formation that drives the obtaining of a certain structure adopted by the calixarene.

The calixarene functionalization is the key step in the design and realization of a host capable to selectively recognize a certain guest.

Calixarenes can be functionalized by means of a transformation of the substituent at *lower rim (endo rim)* or at *upper rim (exo rim)*.

The lower rim functionalization can be achieved through a simple etherification and can be extended by considering transformation reactions of phenol in alkoxy esters, alkoxy amides, alkoxy ketones and phosphonates¹⁷.

As regards the functionalization at the *upper-rim* the most

Recognit. Chem. **1994**, *20*, 373-379.

¹³ A. Ettahiri, A. Thozet, M. Perrin, *Supramolec. Chem.* **1994**, *3*, 191-196.

¹⁴ G. D. Andreetti, F. Ugozzoli, A. Casnati, E. Ghidini, A. Pochini, R. Ungaro, *Gazz. Chim. Ital.* **1989**, *119*, 47-50.

¹⁵ W. J. Wolfgong, L. K. Talafuse, J. M. Smith, M. J. Adams, F. Adeobga, M. Valenzuela, E. Rodriguez, K. Contreras, D. M. Carter, A. Bacchus, A. R. McGuffey, S. G. Bott, *Supramol. Chem.* **1996**, *7*, 67-78.

¹⁶ P. Thuéry, N. Keller, M. Lance, J. D. Vigner, M. Nierlich, *J. Inclusion Phenom. Molec. Recognit. Chem.* **1994**, *20*, 89-96.

¹⁷ J. Lipkowski, Y. Simonov, V. I. Kalchenko, M. A. Vysotsky, L. N. Markovskiy, *An. Quim. Int. Ed.* **1998**, *94*, 328-331.

common strategies provide a wide range of electrophilic aromatic substitutions including sulfonation¹⁸, acylation¹⁹, nitration²⁰, halogenation²¹, formylation²², chloro-sulfonation²³, the *Claisen rearrangement route*²⁴, the *p*-quinone-methide-route²⁵ and *p*-chloromethylation-route²⁶.

1.2.1 Calixarenes in molecular recognition

The synthetic versatility of the calixarene macrocycles allows to obtain derivatives with significant recognition properties towards cations/anions, organic and biomolecular guests. Thus novel calixarene-hosts have been reported for the development of biosensors,²⁷ DNA chip,²⁸ and inhibitors in the field of drug discovery.²⁹

¹⁸ S. Shinkai, H. Koreishi, K. Ueda, T. Arimura, O. Manabe, *J. Am. Chem. Soc.* **1987**, *109*, 6371-6376.

¹⁹ C. D. Gutsche, L. G. Lin, *Tetrahedron* **1986**, *42*, 1633-1640.

²⁰ W. Verboom, A. Durie, R. J. M. Egberink, Z. Asfari, D. N. Reinhoudt, *J. Org. Chem.* **1992**, *57*, 1313-1316.

²¹ C. D. Gutsche, P. F. Pagoria, *J. Org. Chem.* **1985**, *50*, 5795-5802.

²² A. Arduini, S. Fanni, G. Manfredi, A. Pochini, R. Ungaro, A. R. Sicuri, F. Uguzzoli, *J. Org. Chem.* **1995**, *60*, 1448-1453.

²³ A. Casnati, Y. Ting, D. Berti, M. Fabbi, A. Pochini, R. Ungaro, D. Scotto, G. G. Lombardo, *Tetrahedron* **1993**, *49*, 9815-9822.

²⁴ C. D. Gutsche, J. Levine, *J. Am. Chem. Soc.* **1982**, *104*, 2652-2653.

²⁵ C. D. Gutsche, K. C. Nam, *J. Am. Chem. Soc.* **1998**, *110*, 6153-6162.

²⁶ M. Almi, A. Arduini, A. Casanati, A. Pochini, R. Ungaro, *Tetrahedron* **1989**, *45*, 2177-2182.

²⁷ K. S. Song, S. Nimse, J. Kim, J., V. T. Nguyen, V. T. Ta, T. Kim, *Chem Commun.* **2011**, *47*, 7101-7103.

²⁸ a) V. T. Nguyen, S. B. Nimse, K. S. Song, J. Kim, V. T. Ta, H. W. Sung, T. Kim, *Chem Commun.* **2012**, *48*, 4582-4584; b) R. Zadnard, T. Schrader, *Angew Chem.* **2006**, *118*, 2769-2772.

²⁹ a) G. M. Consoli, G. Granata, V. Cafiso, S. Stefani, C. Geraci,

A special attention has been dedicated to the recognition properties of water soluble calixarenes because water represents the natural environment in which biological processes take place.

An example of such molecular recognition is reported below³⁰ and it shows the particular affinity of *p*-sulfonatocalix[4]arene against several biochemically important analytes (**Figure 4**).

In detail the inclusion complex between *p*-sulfonatocalix[4]arene (**1.4**) and 2,3-diazabicyclo[2.2.2]oct-2-ene (**1.5**) was used as sensor system to sense the binding of choline and carnitine derivatives and tetraalkylammonium cations (**1.6**) over a large pH range.

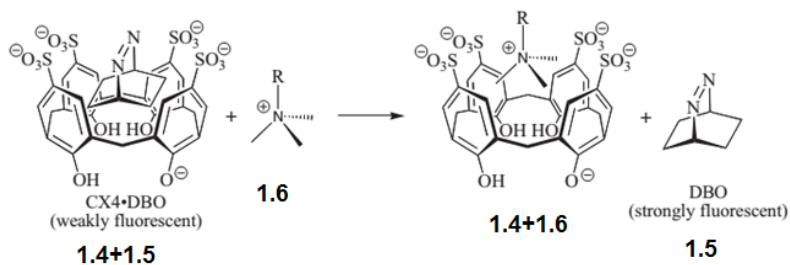


Figure 1.4 *p*-sulfonatocalix[4]arene sensor.

Tetrahedron Lett. **2011**, *44*, 5831–5834; b) A. I. Vovk, L. A. Kononets, V. Y. Tanchuk, S. O. Cherenok, A. B. Drapailo, V. I. Kalchenko, V. P. Kukhar, *Bioorg. Med. Chem. Lett.* **2010**, *20*, 483–487.

³⁰ H. Bakirci, W. M. Nau, *Adv. Funct. Mater.* **2006**, *16*, 237–242.

CHAPTER II

CAVITY FILLING OF THE CALIX[6]ARENE MACROCYCLE WITH DIALKYLAMMONIUM GUESTS

2.1 RECOGNITION OF ALKYLAMMONIUM GUESTS BY CALIXARENES MACROCYCLES

In 2010, the our group³¹ showed that the calix[6]arene hosts **2.1a,b** and **2.2a** (**Figure 2.1**) were able to recognize dialkylammonium axle **2.3a-f⁺·TFPB⁻** when they were coupled with the weakly coordinating Tetrakis[3,5-bis(tri-Fluoromethyl)Phenyl]Borate (TFPB⁻) “superweak anion” (**Figure 2.1**) that gives very loose ion-pairs with dialkylammonium cations in solution.

³¹ C. Gaeta, F. Troisi, P. Neri, *Org. Lett.* **2010**, *12*, 2092–2095.

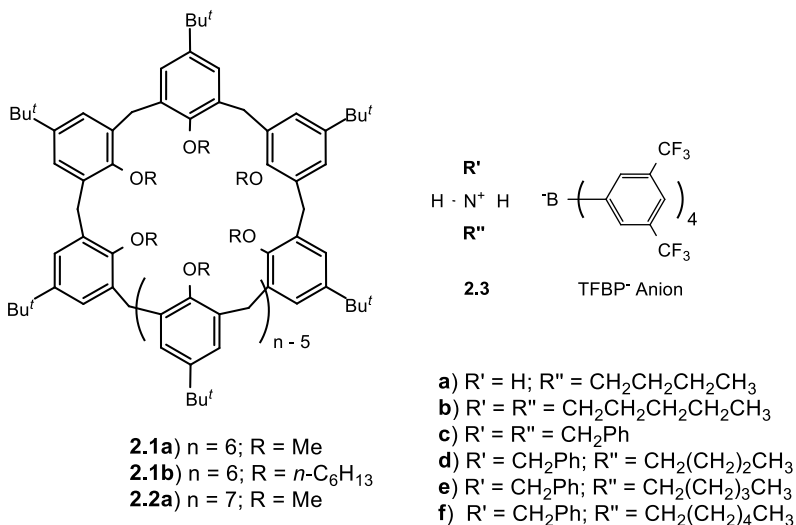


Figure 2.1. Calix[6]arene hosts and ammonium guests.

Thus, in presence of dipentylammonium **2.3b**⁺·TFPB⁻ or dibenzylammonium **2.3c**⁺·TFPB⁻ guests the calix[6]arene macrocycle **2.1a** gave complexes in which the cationic guest was "threaded" into the calix[6]arene-wheel (**Figure 2.2**). These interpenetrated structures have been defined in supramolecular chemistry as pseudorotaxane and can be considered as synthetic precursors of catenane and rotaxane architectures³² which have showed appealing properties as

³² a) G. Schill, *Catenanes, Rotaxanes, and Knots*, Academic Press, New York, USA, **1971**; b) J. P. Sauvage, C. Dietrich-Buchecker, eds. *Molecular Catenanes, Rotaxanes and Knots: A Journey through the World of Molecular Topology*, Wiley VCH, Weinheim, **1999**; c) G. G. Ramírez, D. A. Leigh, A. J. Stephens, *Angew. Chem. Int. Ed.* **2015**, *54*, 6110-6150.

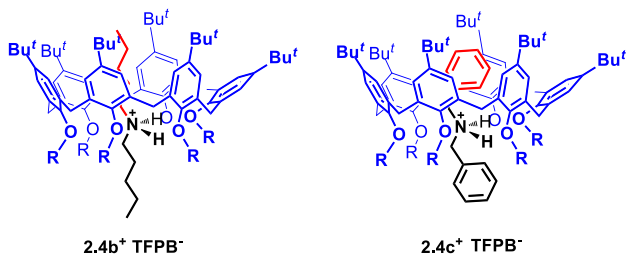


Figure 2.2. Calixarene-based pseudorotaxane structures obtained by *through-the-annulus* threading of calixarenes with TFPB⁻ salts of dialkylammonium cations.

Interestingly, the threading of *directional* alkylbenzylammonium guests **2.3d-f**⁺ with calix[6]arene wheels, in principle would give rise to two diastereoisomeric pseudorotaxane complexes, one with an *endo*-cavity alkyl chain (*endo*-alkyl stereoisomer) and the other with an *endo*-cavity benzyl moiety (*endo*-benzyl stereoisomer) (**Figure 2.3**). Thus, the experiments performed with *n*-alkylbenzylammonium cations bearing shorter alkyl chains, such as butyl **2.4d**⁺·TFPB⁻ and pentyl **2.4e**⁺·TFPB⁻, led to an *endo*-alkyl/*endo*-benzyl ratio of 30:1 and 10:1, respectively.

³³ E. R. Kay, D. A. Leigh, F. Zerbetto, *Angew. Chem. Int. Ed.* **2007**, *46*, 72-191.

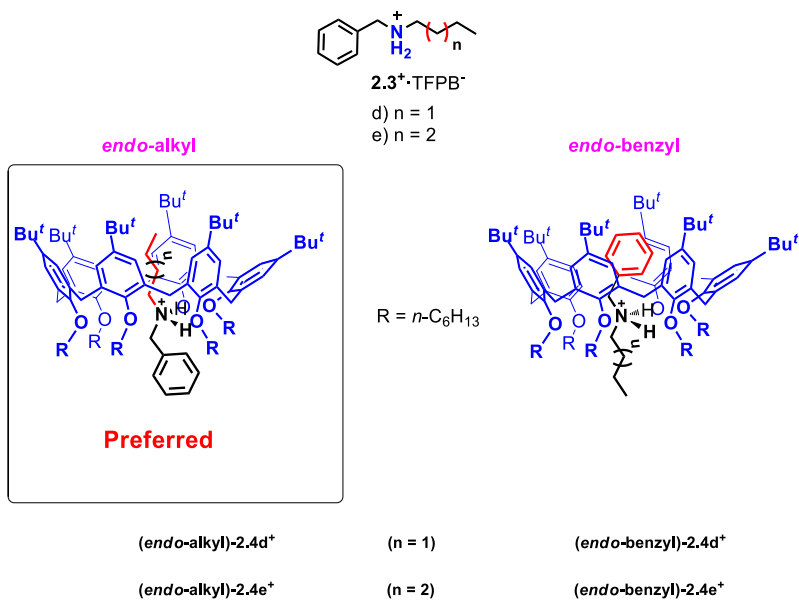


Figure 2.3. *Endo*-alkyl and *endo*-benzyl calixarene-based pseudorotaxane stereoisomers.

The observed stereo-selectivity brought to the definition of the so called “*endo*-alkyl rule”: *threading of a directional alkylbenzylammonium axle through a hexaalkoxycalix[6]arene occurs with an endo-alkyl preference.*³⁴⁻³⁵

2.2 AIMS

On these basis we have studied the recognition abilities of the calix[6]arene derivatives **2.1a** toward alkylbenzylammonium guests **2.3d⁺·TFPB⁻**, **2.3f⁺·TFPB⁻** and **2.3g-p⁺·TFPB⁻**

³⁴ R. Cioa, C. Talotta, C. Gaeta, P. Neri, *Supramolecular Chemistry* **2014**, 26, 569-578.

³⁵ C. Talotta, C. Gaeta, Z. Qi, C. A. Schalley, P. Neri, *Angew. Chem., Int. Ed.* **2013**, 125, 7585-7589.

bearing aliphatic chains with different shape and length (**Figure 2.4**). In particular, we studied the validity of the *endo*-alkyl rule with alkylbenzylammonium axes **2.3g,h,d** and f^+ bearing alkyl chains with different lengths with respect to **2.3d,e⁺** and finally using the guests **2.3i-p⁺** bearing branched alkyl chains.

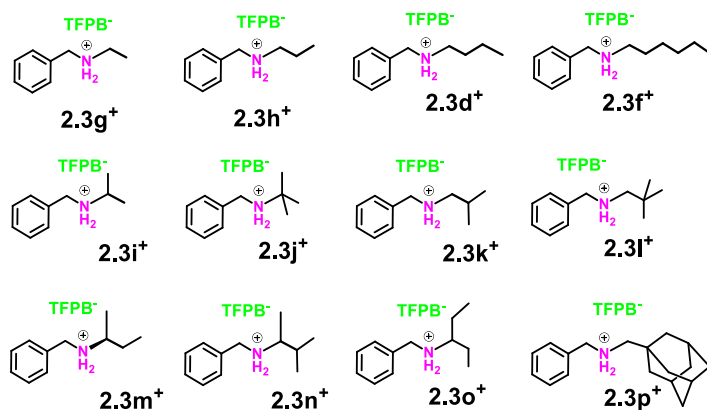


Figure 2.4 Guests studied.

2.3 RESULT AND DISCUSSION

The starting point was the synthesis of the different axes (reported in **Figure 2.4**). They were synthesised, in most cases, starting from a coupling primary amine/aldehyde or amine/ketone to obtain an imine successively reduced with NaBH_4 to obtain the secondary amine. Then the resulting secondary amine was treated with HCl (37%) to obtain the corresponding chloride that was subjected to the anion

exchange with sodium tetrakis[3,5-bis(trifluoromethyl)phenyl]borate (NaTFPB) (see experimental section for more details).

Then it was studied the threading ability of the calix[6]arene **2.1a** with alkylbenzylammonium cations **2.3d⁺·TFPB⁻**, **2.3f⁺·TFPB⁻**, **2.3g⁺·TFPB⁻** and **2.3h⁺·TFPB⁻** bearing linear aliphatic chain having a number of carbon atoms ranging from 2 to 6.

A mixture of *p*-*tert*-butylhexamethoxycalix[6]arene **2.1a** and 1 equivalent of the corresponding axle was prepared dissolving the two compound in 0.5 mL of CDCl₃.

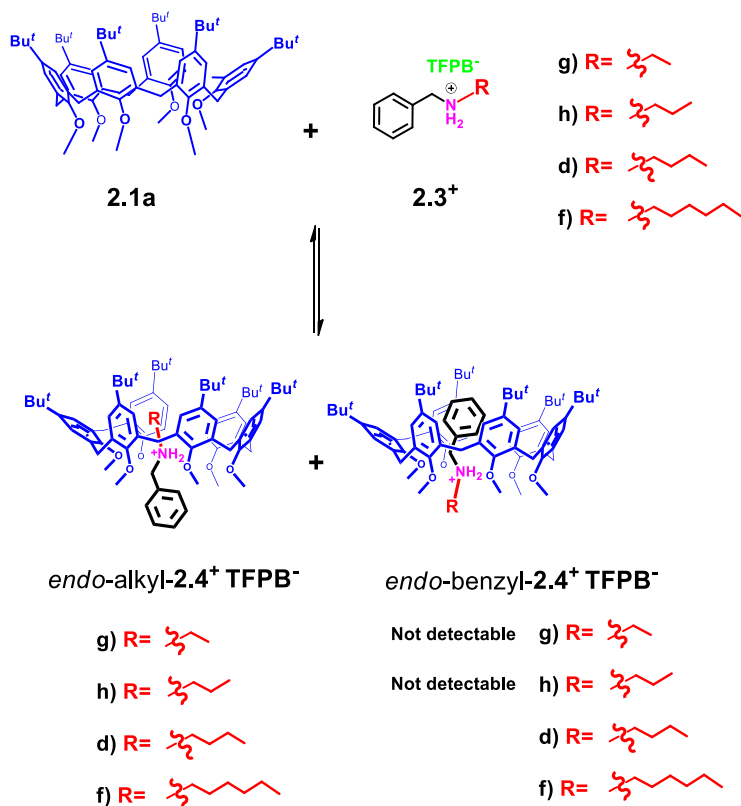


Figure 2.5 Complexation experiments between *p*-tert-butylhexamethoxycalix[6]arene and linear guests.

As it can be seen from the ^1H NMR spectra, in **Figure 2.6** the cations **2.3d⁺·TFPB⁻**, **2.3f⁺·TFPB⁻**, **2.3g⁺·TFPB⁻** and **2.3h⁺·TFPB⁻** are able to give *endo*-alkyl complexation in presence of calix **2.1a**.

Indeed the NMR signals at negative chemical shifts are related to the axle's alkyl moiety settled into the calixarene cavity that shields its protons.

The “*endo*-alkyl rule” was respected also in these cases but the important aspect was in presence of alkylbenzylammonium cations with a shorter alkyl chain **2.3g⁺·TFPB⁻** and **2.3h⁺·TFPB⁻**, the selectivity was absolutely in favour of the alkyl moiety, no evidence of *endo*-benzyl **2.4g-h⁺·TFPB⁻** stereoisomers was observed (**Figure 2.6 A and B**) , while increasing the chain length, with the **2.3d⁺·TFPB⁻** and **2.3f⁺·TFPB⁻** guests also the *endo*-benzyl- **2.4d-f⁺·TFPB⁻** stereoisomer appeared (**Figures 2.6 C and D**).

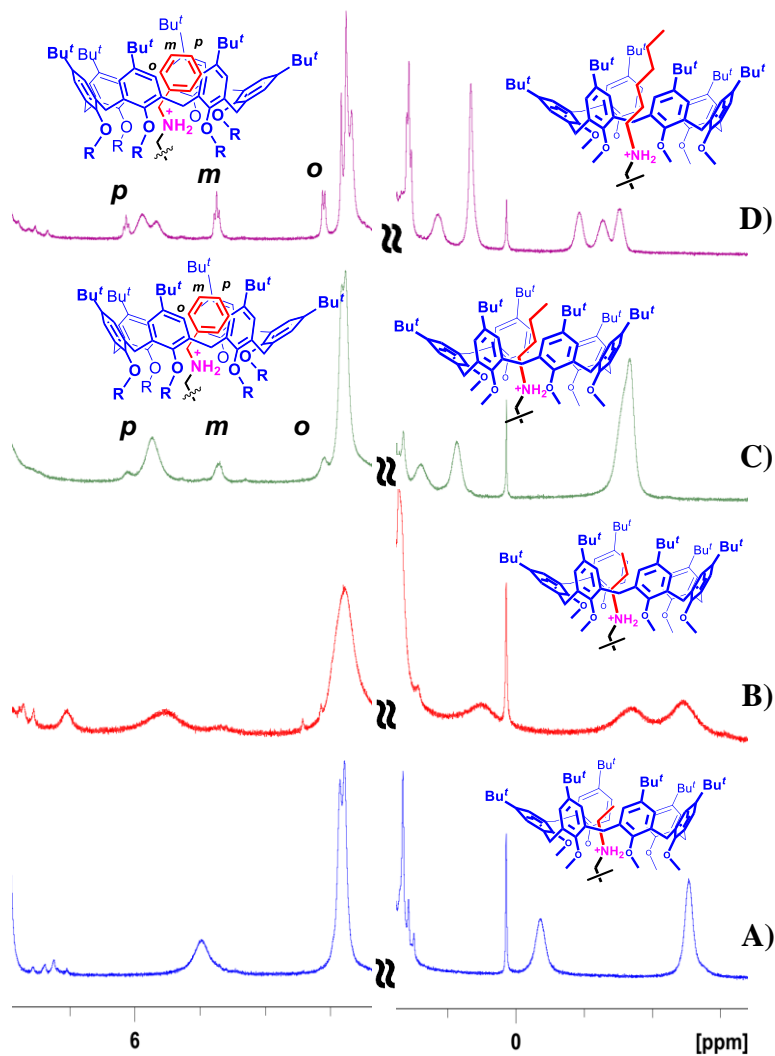


Figure 2.6 Significant portions of the ^1H NMR spectra (400 MHz, 298 K CDCl_3) of (A) 1:1 mixture of **2.1a** ($3.8 \cdot 10^{-3} \text{ M}$) and **2.3g $^+$ ·TFPB $^-$** ($3.8 \cdot 10^{-3} \text{ M}$); (B) 1:1 mixture of **2.1a** ($3.8 \cdot 10^{-3} \text{ M}$) and **2.3h $^+$ ·TFPB $^-$** ($3.8 \cdot 10^{-3} \text{ M}$); (C) 1:1 mixture of **2.1a** ($3.8 \cdot 10^{-3} \text{ M}$) and **2.3d $^+$ ·TFPB $^-$** ($3.8 \cdot 10^{-3} \text{ M}$); (D) 1:1 mixture of **2.1a** ($3.8 \cdot 10^{-3} \text{ M}$) and **2.3f $^+$ ·TFPB $^-$** ($3.8 \cdot 10^{-3} \text{ M}$).

At this point the association constants in **Table 2.1** for pseudorotaxane complexes **2.4d $^+$ ·TFPB $^-$** , **2.4f $^+$ ·TFPB $^-$** , **2.4g-**

$\mathbf{h^+ \cdot TFPB^-}$ were determined by analysis of the ^1H NMR spectra of the complexation experiments, which showed slowly exchanging signals for both free and complexed host (see experimental section for the ^1H NMR complexation experiments).

As reported in **Table 2.1** with the loss of selectivity a decrease in the constant value was observed.

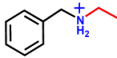
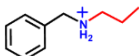
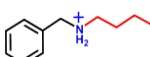
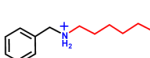
Guest	<i>Endo-Alkyl</i>	<i>Endo-Benzyl</i>	<i>endo-alkyl/endo-benzyl ratio</i>	$K_{\text{endo-alkyl}}$ (M^{-1})
2.3g⁺ 	Yes	No	-	$1.2 \pm 0.2 \times 10^6$
2.3h⁺ 	Yes	No	-	$5.0 \pm 0.8 \times 10^3$
2.3d⁺ 	Yes	Yes	3:1	$6.5 \pm 0.9 \times 10^4$
2.3f⁺ 	Yes	Yes	1:1	$5.5 \pm 0.6 \times 10^1$

Table 2.1 Linear derivatives.

Successively we have studied the binding abilities of calix[6]arene **2.1a** with alkylbenzylammonium cations bearing α -branched aliphatic chains $\mathbf{2.3g^+ \cdot TFPB^-}$, $\mathbf{2.3i^+ \cdot TFPB^-}$ and $\mathbf{2.3j^+ \cdot TFPB^-}$.

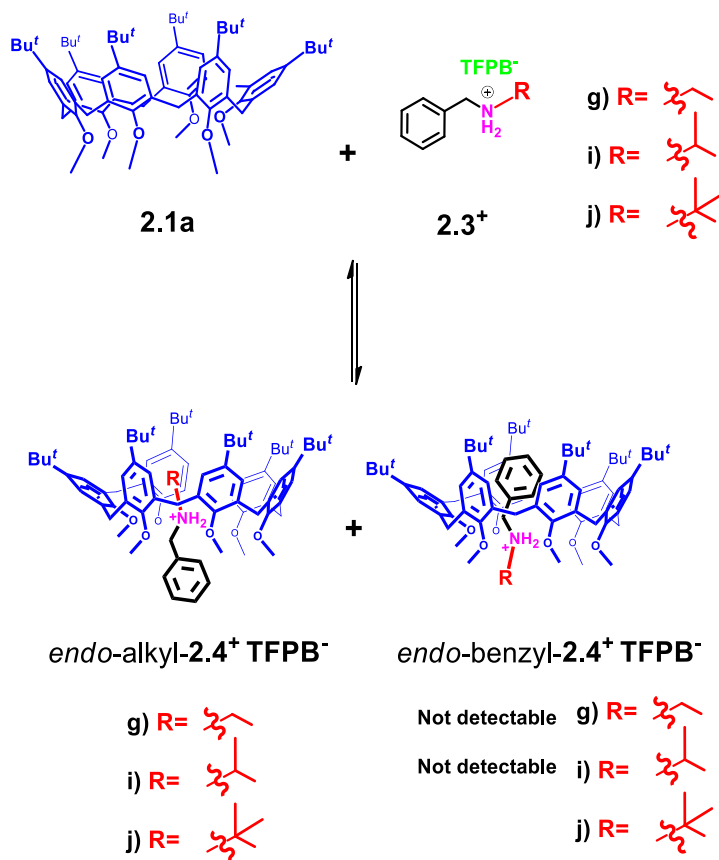


Figure 2.7 Complexation experiments between *p*-*tert*-butylhexamethoxycalix[6]arene and α -branched guests.

¹H NMR spectra in **Figure 2.7** evidenced that in presence of the *i*-propylbenzylammonium cations **2.3g⁺·TFPB⁻** the calix[6]arene **2.1a** gave exclusively the *endo*-alkyl stereoisomer. Differently in presence of *t*-butylbenzylammonium cation **2.3j⁺·TFPB⁻** a mixture of *endo*-alkyl/*endo*-benzyl stereoisomers was obtained in a 3/1 ratio.

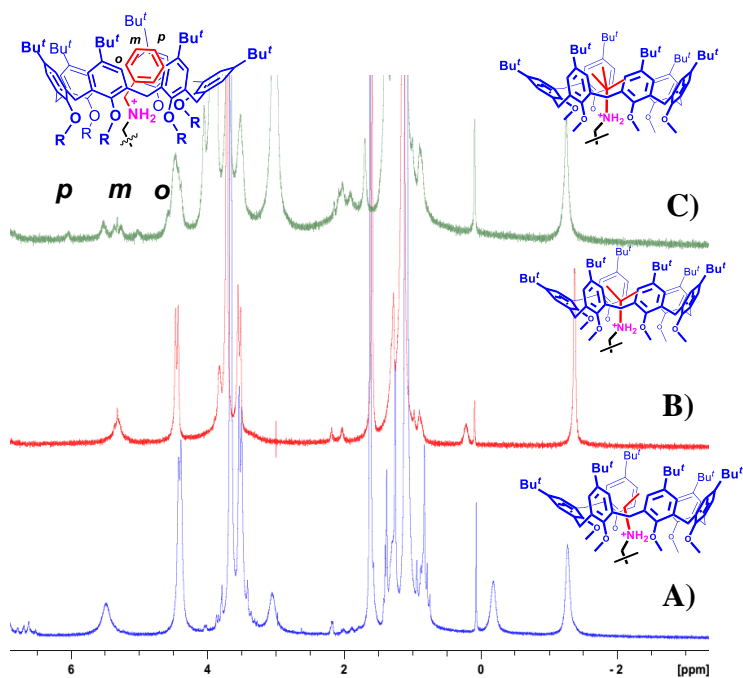
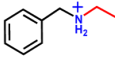
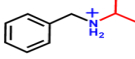
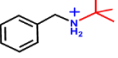


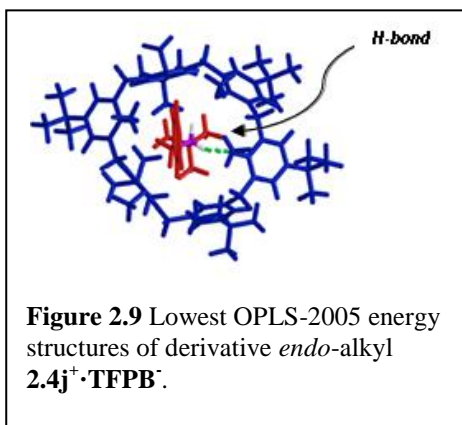
Figure 2. 8 Significant portions of the ^1H NMR spectra (400 MHz, 298 K CDCl_3) of (A) 1:1 mixture of **2.1a** ($3.8 \cdot 10^{-3}$ M) and **2.3g⁺·TFPB⁻** ($3.8 \cdot 10^{-3}$ M); (B) 1:1 mixture of **2.1a** ($3.8 \cdot 10^{-3}$ M) and **2.3i⁺·TFPB⁻** ($3.8 \cdot 10^{-3}$ M); (C) 1:1 mixture of **2.1a** ($3.8 \cdot 10^{-3}$ M) and **2.3j⁺·TFPB⁻** ($3.8 \cdot 10^{-3}$ M).

For the cations **2.3i⁺·TFPB⁻** and **2.3j⁺·TFPB⁻** there was also a decrease in the complexation constants values.

Table 2. 2 α -branched derivatives.

Guests	<i>Endo</i> -Alkyl	<i>Endo</i> -Benzyl	<i>endo</i> -alkyl/ <i>endo</i> -benzyl ratio	$K_{\text{endo-alkyl}}$ (M^{-1})
2.3g⁺ 	Yes	No	-	$1.2 \pm 0.2 \times 10^6$
2.3i⁺ 	Yes	No	-	$4.2 \pm 0.6 \times 10^4$
2.3j⁺ 	Yes	Yes	3:1	$3.6 \pm 0.5 \times 10^2$

Interestingly 1H NMR analysis of the 1H NMR spectrum of



the 1:1 mixture in $CDCl_3$ of **2.3j⁺·TFPB⁻** and calix[6]arene **2.1a** led to an association constant of $3.6 \pm 0.5 \times 10^2$ a value lower than that observed for **2.3i⁺·TFPB⁻** and **2.3g⁺·TFPB⁻**. In accord

with this, the lowest energy structure of the complex *endo*-alkyl **2.4j⁺·TFPB⁻** obtained by molecular mechanics calculations (OPLS, Macro Model $CHCl_3$) evidenced that the excessive branching allowed the formation of one single hydrogen bonding instead than two as in the *endo*-alkyl

2.4g,j⁺·TFPB⁻ pseudorotaxanes.

Successively, we studied the binding abilities of the calix[6]arene **2.1a** toward alkylbenzylammonium guests **2.3g⁺·TFPB⁻**, **2.3i⁺·TFPB⁻** and **2.3j⁺·TFPB⁻** bearing alkyl moiety with branching at the β-position.

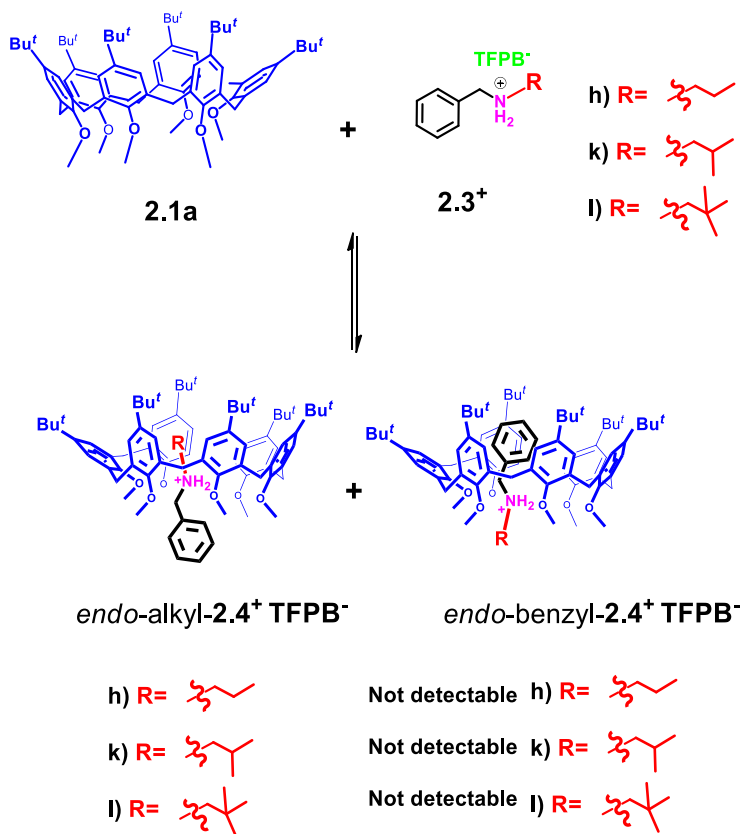


Figure 2.10 Complexation experiments between *p*-*terz*-butylhexamethoxycalix[6]arene and β-branched guests.

From the complexation experiments in **Figure 2.11** resulted

that the β -ramification did not lead to the formation of *endo*-benzyl stereoisomers but influenced the stability of the pseudorotaxane complexes as shown by the decrease of their complexation constants (**Table 2.3**).

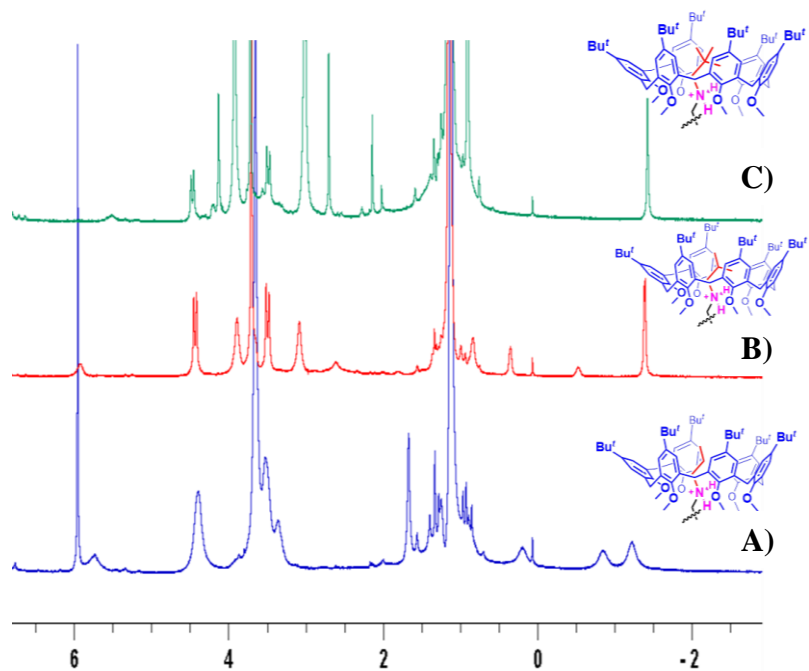
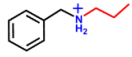
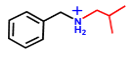
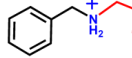


Figure 2.11 Significant portions of the ^1H NMR spectra (400 MHz, 298 K CDCl_3) of (A) 1:1 mixture of **2.1a** ($3.8 \cdot 10^{-3}\text{M}$) and **2.3h⁺·TFPB⁻** ($3.8 \cdot 10^{-3}\text{M}$); (B) 1:1 mixture of **2.1a** ($3.8 \cdot 10^{-3}\text{M}$) and **2.3k⁺·TFPB⁻** ($3.8 \cdot 10^{-3}\text{M}$); (C) 1:1 mixture of **2.1a** ($3.8 \cdot 10^{-3}\text{M}$) and **2.3l⁺·TFPB⁻** ($3.8 \cdot 10^{-3}\text{M}$).

Table 2.3 β -branched derivatives.

Axle	<i>Endo</i> -Alkyl	<i>Endo</i> -Benzyl	<i>endo</i> -alkyl/ <i>endo</i> -benzyl ratio	$K_{\text{endo-alkyl}}$ (M^{-1})
2h⁺ 	Yes	No	-	$5.0 \pm 0.8 \times 10^3$
2k⁺ 	Yes	No	-	$5.1 \pm 0.6 \times 10^3$
2l⁺ 	Yes	No	-	$1.7 \pm 0.2 \times 10^2$

Then with the intention to explore a mixed α,β -ramification the guests **2.3m⁺·TFPB⁻**, **2.3n⁺·TFPB⁻**, **2.3o⁺·TFPB⁻** and **2.3p⁺·TFPB⁻**, (**Figure 2.12**) were synthesised and the binding abilities of calix[6]arene **2.1a** was explored.

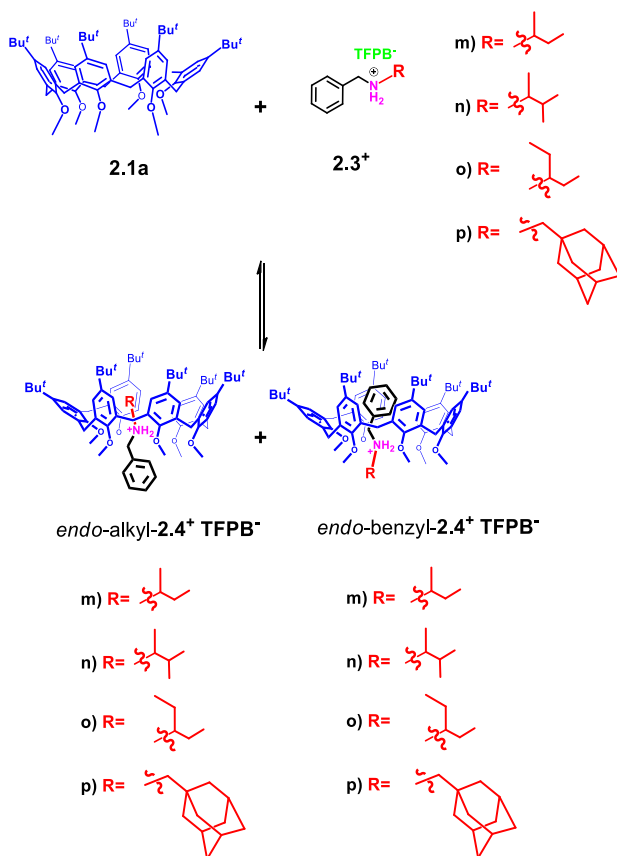


Figure 2.12 α -, β - mixed branched derivatives

In this case it was not observed a significant trend concerning the calixarene cavity selectivity because there were no signals related to *endo*-benzyl-**2.4⁺**·TFPB⁻ stereoisomers in the ¹H NMR spectra (**Figure 2.13** and **Figure 2.14**).

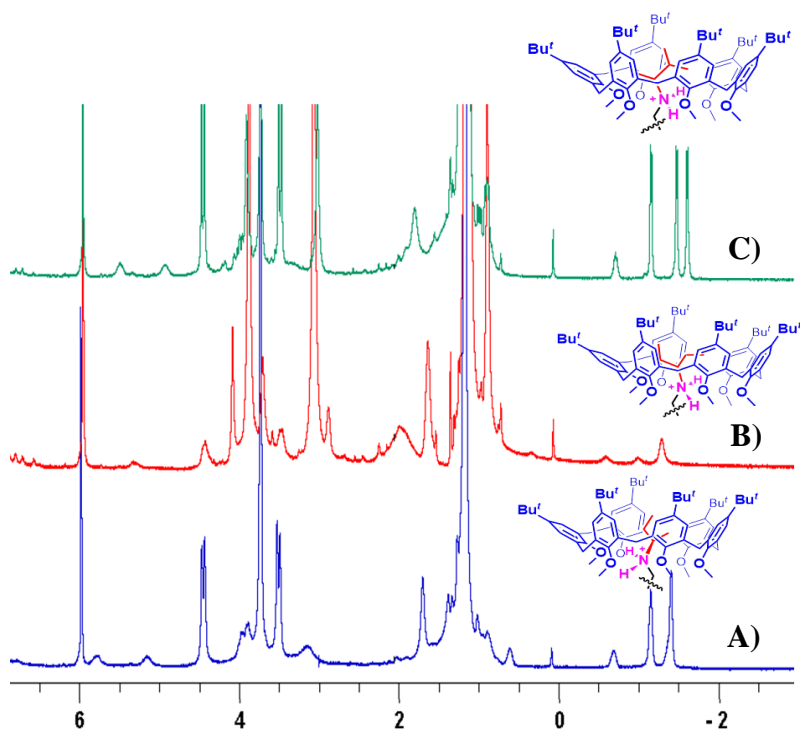


Figure 2. 13 Significant portions of the ^1H NMR spectra (400 MHz, 298 K CDCl_3) of (A) 1:1 mixture of **2.1a** ($3.8 \cdot 10^{-3}\text{M}$) and **2.3m⁺·TFPB⁻** ($3.8 \cdot 10^{-3}\text{M}$); (B) 1:1 mixture of **2.1a** ($3.8 \cdot 10^{-3}\text{M}$) and **2.3n⁺·TFPB⁻** ($3.8 \cdot 10^{-3}\text{M}$); (C) 1:1 mixture of **2.1a** ($3.8 \cdot 10^{-3}\text{M}$) and **2.3o⁺·TFPB⁻** ($3.8 \cdot 10^{-3}\text{M}$).

However the steric encumbrance of the alkyl chain effects the complexation constant to a point that no complexation was observed for the derivative **2.3p⁺·TFPB⁻** (Figure 2.14).

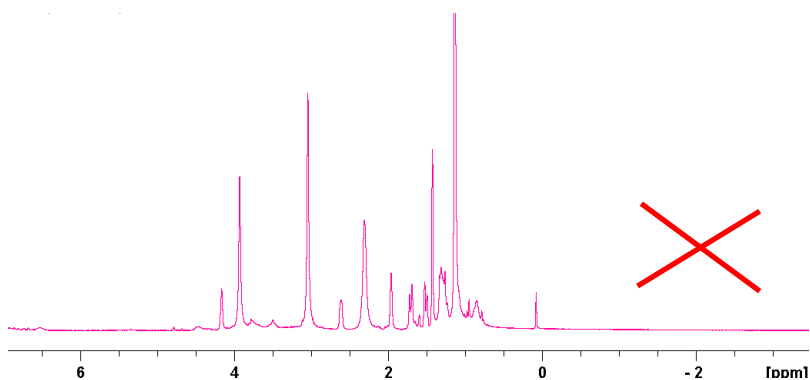


Figure 2. 14 Significant portions of the ^1H NMR spectra (400 MHz, 298 K CDCl_3) of 1:1 mixture of **2.1a** ($3.8 \cdot 10^{-3}\text{M}$) and **2.3p⁺·TFPB⁻** ($3.8 \cdot 10^{-3}\text{M}$).

Table 2. 4 α -, β - mixed branched derivatives

Guest	<i>Endo</i> -Alkyl	<i>Endo</i> -Benzyl	<i>endo</i> -alkyl/ <i>endo</i> -benzyl ratio	$K_{\text{endo-alkyl}}$ (M^{-1})
2.3m⁺ 	Yes	No	-	6.9 ± 0.8 $\times 10^3$
2.3n⁺ 	Yes	No	-	2.9 ± 0.4 $\times 10^3$
2.3o⁺ 	Yes	No	-	2.7 ± 0.4 $\times 10^2$
2.3p⁺ 	No	No	-	-

Examination of the data in the **tables 2.1-2.4** evidenced that the shape and size of the alkyl moiety of the axle influences the stability of the complex. Certainly the ability of the alkyl group to fill the cavity of the calix[6]arene-wheel plays a fundamental role in the stabilization of the pseudorotaxane.

Thus we have envisioned to correlate the association constant of the pseudorotaxanes to two parameters related to cavity filling of the calixarene:

- ✓ **Packing Coefficient**
- ✓ **Contacting Coefficient**

2.3.1 Packing Coefficient Calculation

At this point the data in Tables **2.1-2.4** relative to association constants for the formation of the calixarene-based pseudorotaxanes were correlated with the packing coefficient of the [2]pseudorotaxanes.

The term packing coefficient (**PC**) was introduced for the first time by Rebek³⁶ and it is defined as the ratio between the sum of the van der Waals volumes (**vW**) of the n molecules in a given volume and the volume (**V**)

$$PC = \frac{\sum_{i=1}^n v_w^i}{V} = \frac{V_w}{V} \quad (1)$$

Studying resorcinarene derivatives (**Figure 2.15**), Rebek

³⁶ J. Jr. Rebek, *Chem Soc. Rev.* **1996**, 25, 255-264.

demonstrated that they were able to give self-assembly only when the guest hosted in the cavity occupied a given volume. In particular when PCs fell in the range 0.55 ± 0.09 defining the so called “55% rule”.³⁷

³⁷ a) S. Mecozzi, J. Jr. Rebek, *Chem. Eur. J.* **1998**, *4*, 1016-1022; b) A. Scarso, L. Trembleau, J. Jr. Rebek, *Angew. Chem.* **2003**, *115*, 5657–5660; c) A. Scarso, L. Trembleau, J. Jr. Rebek, *Angew. Chem. Int. Ed.* **2003**, *42*, 5499–5502; d) L. Trembleau, J. Jr. Rebek, *Science* **2003**, *301*, 1219–1220; e) A. Scarso, L. Trembleau, J. Jr. Rebek, *J. Am. Chem. Soc.* **2004**, *126*, 13512–13518; f) B. W. Purse, J. Jr. Rebek, *Proc. Natl. Acad. Sci. U.S.A.* **2006**, *103*, 2530-2534; g) M. P. Schramm, J. Jr. Rebek, *Chem. Eur. J.* **2006**, *12*, 5924–5933; h) R. J. Hooley, J. Jr. Rebek, *Org. Lett.* **2007**, *9*, 1179-1182; i) D. Ajami, J. Jr. Rebek, *Angew. Chem.* **2008**, *120*, 6148–6150.

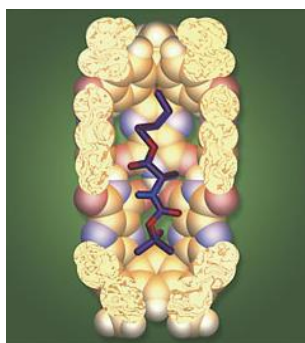
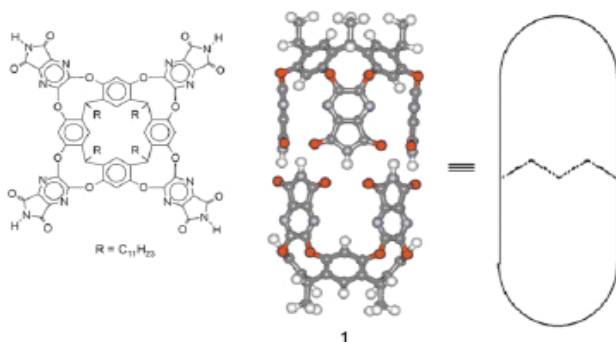


Figure 2. 15 Rebek's resorinarene-based capsule

When packing coefficients are less than 45% (40% for gaseous guest) the encapsulation does not occur because the guest is characterized by intermolecular interactions with the host that are less strong than those with solvent molecules. From the opposing point of view when the packing coefficient are higher than 65 % the guest is not encapsulated because it pays the price of an unnatural immobilization inside the capsule.

2.3.1.1 Calculation of the packing coefficients of the pseudorotaxanes *endo*-alkyl-**2.4g**⁺·**TFPB**⁻

Pseudorotaxane structures were built using the MacroModel-Maestro and minimized with the force field OPLS 2005.

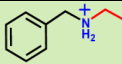
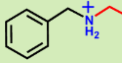
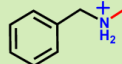
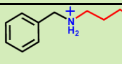
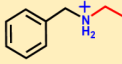
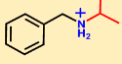
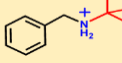
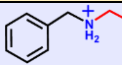
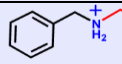
Subsequently the structures obtained in this way were used as input data to perform DFT calculations. In detail, DFT calculations were performed using B3LYP/6-31G level of the theory and Grimme's dispersion corrections IOP(3/124 = 3).³⁸ The van der Waals molecular volumes were calculated with the program Swiss-PdbViewer³⁹ with a probe size of 1.4 Å as diameter.

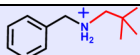
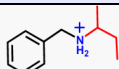
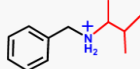
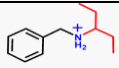
The volume of the calixarene cavity for each pseudorotaxane system was obtained removing the guest from it and then it was measured the volume of the guest hosted in the cavity. Employing these values, packing coefficients (**PCs**) were calculated for all pseudorotaxane systems and they are reported in **Table 2.5** (see experimental section, pp. 72-73, for more details on the **PCs** calculation procedure).

³⁸ (a) S. Grimme, *J. Comput. Chem.* **2004**, 25, 1463–1473. (b) S. Grimme, *J. Comput. Chem.* **2006**, 27, 1787–1799.

³⁹ Swiss-PdbViewer application is used to analyze several proteins at the same time. In particular, proteins can be superimposed in order to deduce structural alignments and compare their active sites or any other relevant parts. Amino acid mutations, H-bonds, angles and distances between atoms are easy to obtain thanks to the intuitive graphic and menu interface.

Table 2.5 PCs and K_{ass} for all [2]pseudorotaxane structures

<i>(endo-alkyl)</i> -Pseudorotaxane		K_{ass} (M^{-1})	PC (%)
LINEAR DERIVATIVES	 2.4g⁺·TFPB⁻	$1.2 \pm 0.2 \times 10^6$	45
	 2.4h⁺·TFPB⁻	$5.0 \pm 0.8 \times 10^3$	41
	 2.4d⁺·TFPB⁻	$6.5 \pm 0.9 \times 10^4$	46
	 2.4f⁺·TFPB⁻	$5.5 \pm 0.6 \times 10^1$	46
α -BRANCHED DERIVATIVES	 2.4g⁺·TFPB⁻	$1.2 \pm 0.2 \times 10^6$	45
	 2.4i⁺·TFPB⁻	$4.2 \pm 0.6 \times 10^4$	41
	 2.4j⁺·TFPB⁻	$3.6 \pm 0.5 \times 10^2$	45
α -BRANCHED DERIVATIVES	 2.4h⁺·TFPB⁻	$5.0 \pm 0.8 \times 10^3$	41
	 2.4k⁺·TFPB⁻	$5.1 \pm 0.6 \times 10^3$	44

	 2.4i⁺·TFPB⁻	$1.7 \pm 0.2 \times 10^2$	58
α-BRANCHED DERIVATIVES	 2.4m⁺·TFPB⁻	$6.9 \pm 0.8 \times 10^3$	38
	 2.4n⁺·TFPB⁻	$2.9 \pm 0.4 \times 10^3$	42
	 2.4o⁺·TFPB⁻	$2.7 \pm 0.4 \times 10^2$	44

Close inspection of data in **Table 2.5** evidenced that the packing coefficients of the pseudorotaxanes **2.4g-o⁺** fall in the range 46-64% in accord with the Rebek's rule, however they were not closely related to the K_{ass} values. In fact the pseudorotaxanes **2.4g⁺** and **2.4j⁺** which have different stability constants ($1.2 \pm 0.2 \times 10^6$ and $3.6 \pm 0.5 \times 10^2 \text{ M}^{-1}$) showed similar packing coefficients (45 and 45% respectively).

2.3.2 Contacting Coefficient Calculation

At this point, for the first time we have studied the relationship between the association constant of the pseudorotaxanes and the contact surface between the aromatic cavity of the calix[6]arene host and the alkyl moiety inside the cavity. This novel parameters has been defined by us as the

ratio between the guest's surface in close contact with the calixarene cavity surface (portion of the alkylbenzylammonium guest inside the calix-cavity) and the total surface of the guest portion hosted in the cavity (**Eq. 2**), and should take account of the ability of the guest to fill the calix-cavity establishing van der Waals and C-H... π interactions with it.

$$CC = \frac{S_{\text{host-guest contact}}}{S_{\text{guest}}} \quad (2)$$

Thus, through the program Swiss-PdbViewer it was calculated the **CC** value for the ethyl moiety inside the calixarene cavity for the pseudorotaxane **2.4g⁺**. Thus we evidenced that the 97% (**Table 2.6**) of the surface of the ethyl moiety (see **Figure 2.16** left) was in close contact with the surface of the calixarene cavity, a value significantly higher than the **CC** value of 62 % (**Table 2.6** and **Figure 2.16**) measured for the neopentyl moiety inside the calix-cavity of **2.4l⁺**.

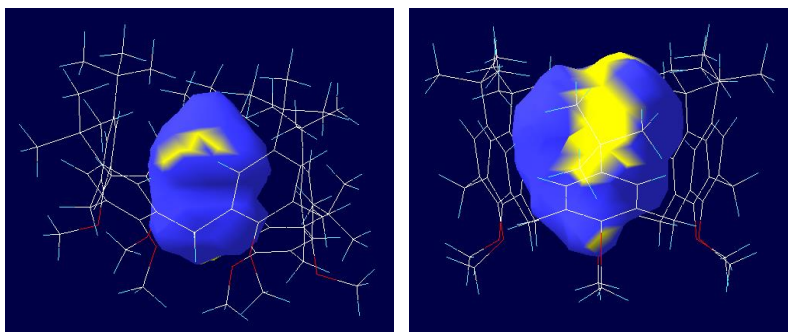
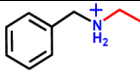
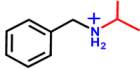
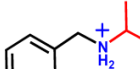
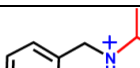
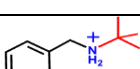
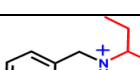
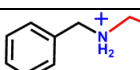
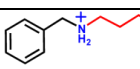


Figure 2.16 Swiss-PdbViewer representation of the contact surface (in blu) between **2.1a** and **2.4g⁺** (left) and between **2.1a** and **2.4l⁺** (right) (in yellow the free guest's surface).

Interestingly the two **CC** values of **2.4g⁺** and **2.4l⁺** of 97 and 62 % (**Table 2.6**) were well related to the association constants of two pseudorotaxanes of $1.2 \pm 0.2 \times 10^6$ and $1.7 \pm 0.2 \times 10^2 \text{ M}^{-1}$ respectively. Thus to a high **CC** value corresponds a greater stability of the complex, likely due to the increased contribution of Van der Waals interactions between host and guest. In **Figure 2.16** (left) we report the structure of the pseudorotaxane **2.4g⁺**, in yellow the free surface of the ethyl moiety of the guest not in contact with the calixarene cavity, in blu the portion in contact. Comparison with the analogue structure of **2.4l⁺** evidences a higher free surface (yellow) for the neopentyl moiety in **2.4l⁺**.

Table 2.6 PCs, CCs, and K_{ass} for [2]pseudorotaxane structures

(endo-alkyl) Pseudorotaxane	K_{ass} (M^{-1})	PC(%)	CC(%)
 2.4g⁺·TFPB⁻	$1.2 \pm 0.2 \times 10^6$	45	97
 2.4i⁺·TFPB⁻	$4.2 \pm 0.6 \times 10^4$	41	88
 2.4m⁺·TFPB⁻	$6.9 \pm 0.8 \times 10^3$	38	79
 2.4n⁺·TFPB⁻	$2.9 \pm 0.4 \times 10^3$	42	78
 2.4j⁺·TFPB⁻	$3.6 \pm 0.5 \times 10^2$	45	65
 2.4o⁺·TFPB⁻	$2.7 \pm 0.4 \times 10^2$	44	78
 2.4l⁺·TFPB⁻	$1.7 \pm 0.2 \times 10^2$	58	62
 2.4f⁺·TFPB⁻	$5.5 \pm 0.6 \times 10^1$	46	61

Close inspection of the data reported in **Table 2.6** evidenced a

good relationship between the association constants and **CC** values. Thus at high K_{ass} values corresponds high **CC** values.

2.3 CONCLUSION

In conclusion there were synthesised alkylbenzylamonium axles differently substituted and the branching effect on calixarene threading was studied.

The complexation experiment showed that, in the formation of pseudorotaxane structures the *endo*-alkyl orientation was always preferred, and *endo*-benzyl adducts were observed only for the guests $2.3d^+ \cdot \text{TFPB}^-$, $2.3f^+ \cdot \text{TFPB}^-$ and $2.3j^+ \cdot \text{TFPB}^-$ (Figures 2.6 and 2.8).

For all pseudorotaxane structures **PCs** were calculated and it was seen that they were not correlated with the effectiveness of the calixarene threading, represented by complexation constants but they were in agreement with the Rebek's 55% rule.

In order to find a correlation between guest structure and threading effectiveness, a new parameter was investigated. The new parameter **CC**, defined as **Contacting Coefficient**, showed a relationship with the binding constant, so this parameter can be a valid support or an alternative to the study of the recognition properties of the calixarene hosts.

2.4 EXPERIMENTAL SECTION

ESI(+)-MS measurements were performed on a Micromass Bio-Q triple quadrupole mass spectrometer equipped with electrospray ion source, using a mixture of H₂O/CH₃CN (1:1) and 5% HCOOH as solvent. Flash chromatography was performed on Merck silica gel (60, 40-63 μm). All chemicals were reagent grade and were used without further purification. Anhydrous solvents were purchased from Aldrich. When necessary compounds were dried in vacuo over CaCl₂. Reaction temperatures were measured externally. Reactions were monitored by TLC on Merck silica gel plates (0.25 mm) and visualized by UV light, or by spraying with H₂SO₄-Ce(SO₄)₂ or phosphomolybdic acid.

Derivatives **2.1a**, **2.3c⁺·TFPB⁻** and sodium tetrakis[3,5-bis(trifluoromethyl)phenyl]borate⁴⁰ were synthesized according to literature procedures and they are not reported here in this section. 1D NMR spectra were recorded on a Bruker Avance-400 spectrometer [400 (1H) and 100 MHz (¹³C)], Bruker Avance-300 spectrometer [300 (1H) and 75 MHz (¹³C)] and Bruker Avance-250 spectrometer [250 (1H) and 63 MHz (¹³C)].; chemical shifts are reported relative to the residual solvent peak (CHCl₃: δ 7.26, CDCl₃: δ 77.23;

⁴⁰ H. Nishida, N. Takada, M. Yoshimura, T. Sonoda, H. Kobayashi, *Bull. Chem. Soc. Jpn.* **1984**, *57*, 2600-2604.

CD₃OH: δ 4.87, CD₃OD: δ 49.0).

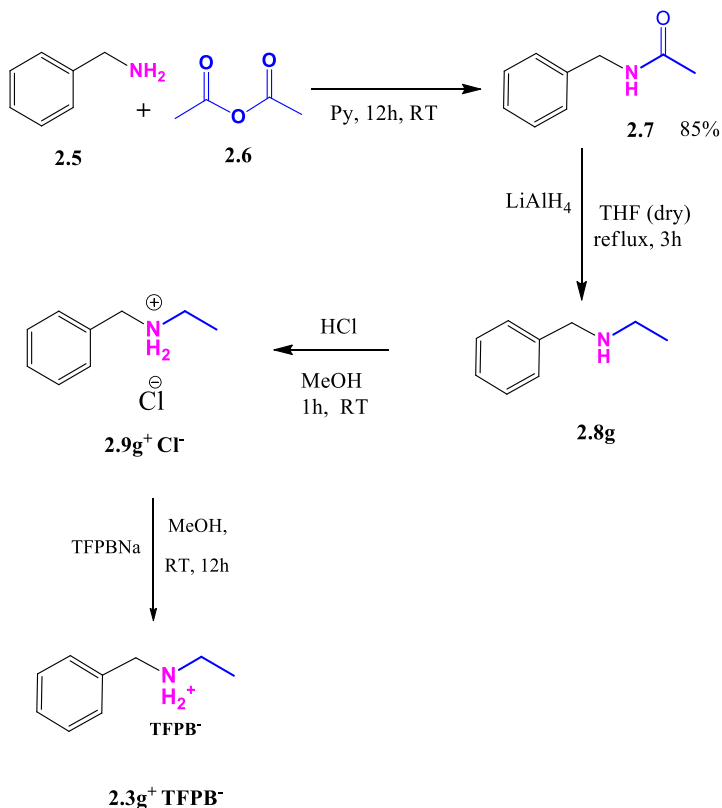
Molecular modeling studies were performed with a combined use of the MacroModel 9/Maestro-4.1⁴¹ program and the Gaussian-09 software package⁴² and Swiss-PdbViewer.⁴³

⁴¹ F. Mohamadi, N. G. Richards, W. C. Guida, R. Liskamp, M. Lipton, C. Caufield, G. Chang, T Hendrickson, W. C. Still, *J. Comput. Chem.* **1990**, *11*, 440–467.

⁴² Gaussian 09, Revision A.1, M. J. Frisch, G. W. Trucks, H. B. Schlegel, G. E. Scuseria, M. A. Robb, J. R. Cheeseman, G. Scalmani, V. Barone, B. Mennucci, G. A. Petersson, H. Nakatsuji, M. Caricato, X. Li, H. P. Hratchian, A. F. Izmaylov, J. Bloino, G. Zheng, J. L. Sonnenberg, M. Hada, M. Ehara, K. Toyota, R. Fukuda, J. Hasegawa, M. Ishida, T. Nakajima, Y. Honda, O. Kitao, H. Nakai, T. Vreven, J. A. Jr. Montgomery, J. E. Peralta, F. Ogliaro, M. Bearpark, J. J. Heyd, E. Brothers, K. N. Kudin, V. N. Staroverov, R. Kobayashi, J. Normand, K. Raghavachari, A. Rendell, J. C. Burant, S. S. Iyengar, J. Tomasi, M. Cossi, N. Rega, J. M. Millam, M. Klene, J. E. Knox, J. B. Cross, V. Bakken, C. Adamo, J. Jaramillo, R. Gomperts, R. E. Stratmann, O. Yazyev, A. J. Austin, R. Cammi, C. Pomelli, J. W. Ochterski, R. L. Martin, K. Morokuma, V. G. Zakrzewski, G. A. Voth, P. Salvador, J. J. Dannenberg, S. Dapprich, A. D. Daniels, Ö. Farkas, J. B. Foresman, J. V. Ortiz, J. Cioslowski, D. J. Fox, Gaussian, Inc., Wallingford CT, 2009.

⁴³ N. Guex, M. Peitsch, T. Schwede, A. Diemand, DeepView Swiss PDB Viewer, Glaxo Smith Klein.

Synthesis of derivative $2.3g^+ \cdot TFPB^-$



To the benzylamine (0.010 mol) was added acetic anhydride (0.010 mol) and pyridine (0.50 mL) and the reaction mixture was kept overnight under stirring at room temperature. The excess of anhydride was removed under reduced pressure to give compound **2.7** (1.2 g; R= 85%).

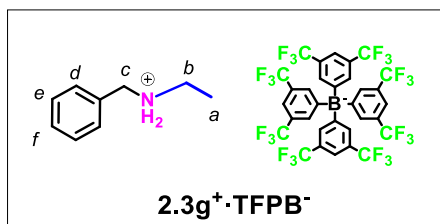
In a three necked flask, under nitrogen atmosphere, the compound **2.7** (7.7 mmol) was dissolved in THF anhydrous (70 mL) and $LiAlH_4$ (0.18 mol) was added at 0° C. The

resulting mixture was stirred at room temperature for 2 h and at reflux for 2 h.

The reaction was quenched pouring the mixture in HCl 1.0 N (0.10 L) and the organic compound was extracted with AcOEt. The organic layer was washed with water, dried over MgSO₄ and the solvent was removed under reduced pressure to give derivative **2.8g** as a yellow viscous liquid.

The crude product (8.0 mmol) was dissolved in Et₂O (20 mL) at room temperature and an aqueous solution of HCl (37% w/w, 8.0 mmol) was added dropwise. The mixture was kept under stirring for 1 h, until the formation of a white precipitate. The solid was collected by filtration, purified by crystallization with Exane/MeOH and dried under vacuum, to give derivative **2.9g⁺·Cl⁻** as a white solid.

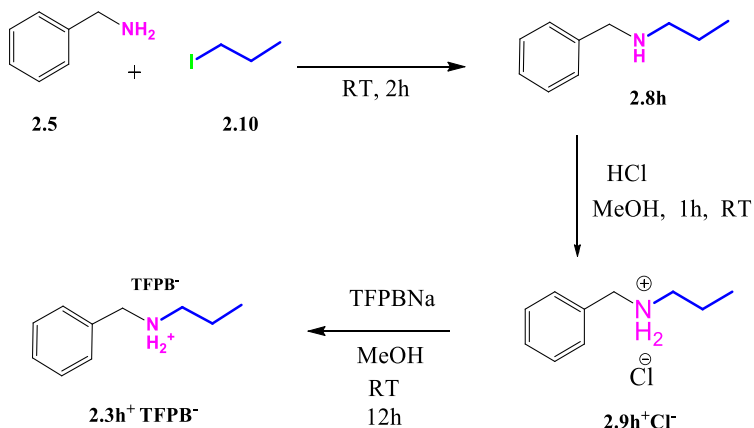
Derivative **2.9g⁺·Cl⁻** (0.15 mmol) was dissolved in dry MeOH (5.0 mL), then sodium tetrakis[3,5-bis(trifluoromethyl)phenyl]borate (0.16 mmol) was added and the mixture was kept under stirring overnight in the dark. The solvent was removed and deionized water was added, obtaining a brown precipitate that was filtered off and dried under vacuum to give derivatives **2.3g⁺·TFPB⁻**.



Derivative 2.3g⁺·TFPB⁻: (0.1310 g, 0.13 mmol, 80%).

ESI(+) MS: $m/z = 136.14$ (M^+). **¹H NMR** (250 MHz, CD₃OD, 298 K): δ 1.33 (t, $J = 7$, 3H, H_{*a*}), 3.11 (d, $J = 7$, 2H, H_{*b*}), 4.18 (s, 2H, H_{*c*}), 7.47 (s, 5H, H_{*d-f*}), 7.59 (overlapped, 12H, ArH^{TFPB}); **¹³C NMR** (100 MHz, CD₃OD, 298 K): δ 10.0, 42.4, 50.6, 117.1, 120.3, 123.0, 125.7, 128.4, 128.6, 128.9, 129.2, 129.3, 129.4, 129.5, 131.2, 134.4, 160.7, 161.2, 161.7, 162.2.

Synthesis of derivative $2.3h^+ \cdot TFPB^-$



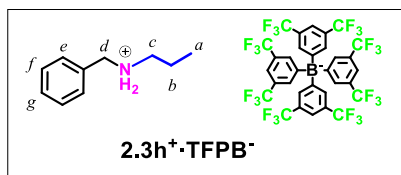
To the benzylamine (0.010 mol) was added 1-iodopropane (0.010 mol) and the reaction mixture was stirred at room temperature for 2 h.

After 2 h stirring, unreacted benzylamine was removed by crystallization with CH_2Cl_2 . The resulting crude product was subjected to flash chromatography on silica gel ($CHCl_3/MeOH$, 98/2) to give the ammonium iodide intermediate (1.7 g, 4.2 mmol, 42%).

The ammonium iodide (1.7 g, 4.2 mmol) was dissolved in AcOE (30 mL) and KOH aqueous solution 1.0 N (30 mL) and the resulting mixture was stirred at room temperature for 4 h to give the amine **2.8h**. The amine (0.15 mmol) was dissolved in Et_2O (20 mL) at room temperature and an aqueous solution of HCl (37% w/w, 1.2 eq) was added dropwise. The mixture

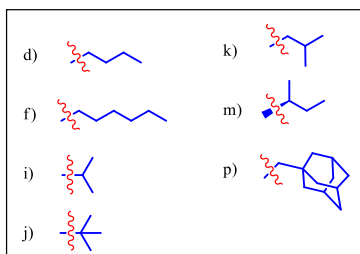
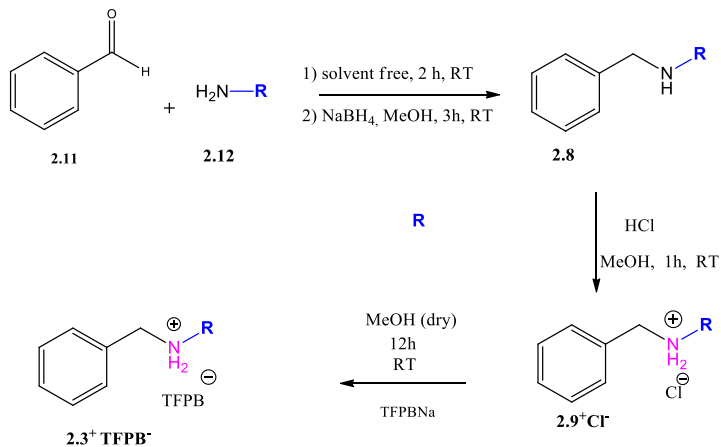
was kept under stirring for 1 h, until the formation of a white precipitate. The solid was collected by filtration, purified by crystallization with acetonitrile and dried under vacuum, to give derivative **2.9h⁺·Cl⁻** as a white solid.

Derivative **2.9h⁺·Cl⁻** (1 eq.) was dissolved in dry MeOH (C = 0.20 M), then sodium tetrakis[3,5-bis(trifluoromethyl)phenyl]borate (1.1 eq.) was added and the mixture was kept under stirring overnight in the dark. The solvent was removed and deionized water was added, obtaining a brown precipitate that was filtered off and dried under vacuum to give derivatives **2.3h⁺·TFPB⁻**.



Derivative 2.3h⁺·TFPB⁻: (0.13 g, 0.13 mmol, 78%). **ESI(+)**
MS: $m/z = 150.14$ (M^+). **¹H NMR** (300 MHz, CD₃OD, 298 K): δ 1.01 (t, $J = 7.5$, 3H, H_a), 1.73 (sext, $J = 7.2$ 2H, H_b), 2.99 (t, $J = 8$, 2H, H_c), 4.18 (s, 2H, H_d), 7.46 (overlapped, 5H, H_{e-g}), 7.59 (overlapped, 12H, ArH^{TFPB}); **¹³C NMR** (75 MHz, CD₃OD, 298 K): δ 9.9, 19.3, 48.9, 51.1, 117.2, 119.1, 122.7, 126.3, 129.1, 129.5, 129.6, 129.9, 131.3, 134.5, 160.6, 161.3, 161.9, 162.6.

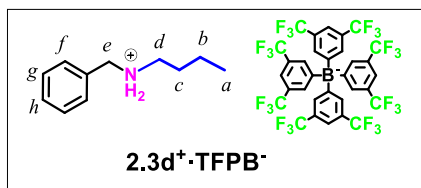
Synthesis of derivatives **2.3d,f,I,j,k,m,p**⁺·TFPB⁻



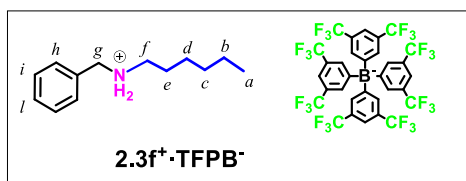
To the benzaldehyde (0.010 mol) was added the appropriate derivative amine (0.010 mol). The reaction mixture was stirred at room temperature for 2 h to give the imine intermediate in a quantitative yield. The imine was used for the next step without further purification. The imine (0.010 mol) was dissolved in dry MeOH (20 mL) under a nitrogen atmosphere and NaBH₄ (0.10 mol) was added at 0 °C and then the mixture was allowed to warm at room temperature.

The solution was kept under stirring for 3 h. The solvent was removed under reduced pressure and the residue partitioned between AcOEt and an aqueous saturated solution of NaHCO₃. The organic layer was dried over MgSO₄ and the solvent was removed, under reduced pressure, to give the secondary amine as a yellow viscous liquid. The amine was used for the next step without further purification. The crude product (0.010 mol) was dissolved in Et₂O (20 mL) at room temperature and an aqueous solution of HCl (37% w/w, 0.010 mol) was added dropwise. The mixture was kept under stirring for 1 h, until the formation of a white precipitate. The solid was collected by filtration, purified by crystallization with acetonitrile and dried under vacuum, to give the corresponding chloride as a white solid.

The corresponding chloride (1 eq.) was dissolved in dry MeOH (C= 0.20 M), then sodium tetrakis[3,5-bis(trifluoromethyl)phenyl]borate (1.1 eq) was added and the mixture was kept under stirring overnight in the dark. The solvent was removed and deionized water was added, obtaining a brown precipitate that was filtered off and dried under vacuum to give the corresponding derivative **2.3d,f,I,j,k,m,p⁺·TFPB⁻**

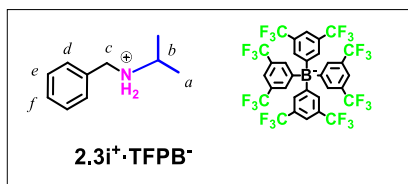


Derivative 2.3d⁺·TFPB⁻: (0.11g, 0.10 mmol, 93%). **ESI(+)**
MS: $m/z = 164.16$ (M^+). **¹H NMR** (300 MHz, CD₃OD, 298 K): δ 0.99 (t, $J = 7.5$, 3H, H_a), 1.43 (m, 2H, H_b), 1.68 (m, 2H, H_c), 3.02 (t, $J = 8$, 2H, H_d), 4.18 (s, 2H, H_e), 7.47 (overlapped, 5H, ArH_{f-h}), 7.59 (overlapped, 12H, ArH^{TFPB}); **¹³C NMR** (100 MHz, CDCl₃, 298 K): δ 13.0, 19.2, 28.1, 48.8, 53.6, 117.6, 120.5, 123.2, 125.9, 127.5, 128.5, 128.6, 128.8, 129.0, 129.4, 130.4, 131.7, 134.8, 160.9, 161.4, 161.9, 162.4.

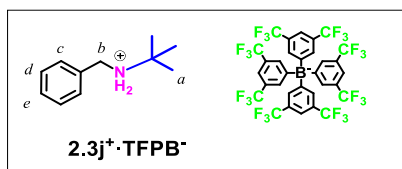


Derivative 2.3f⁺·TFPB⁻: (0.16 g, 0.15 mmol, 99%). **ESI(+)**
MS: $m/z = 192.18$ (M^+). **¹H NMR** (300 MHz, CD₃OD, 298 K): δ 0.91 (s, broad, 3H, H_a), 1.36 (s, broad, 6H, H_{b-d}), 1.72 (s, broad, 2H, H_e), 3.04 (s, broad, 2H, H_f), 4.02 (s, broad, 2H, H_g), 7.48 (s, broad, 5H, ArH), 7.64 (s, broad, 12H, ArH^{TFPB}); **¹³C NMR** (75 MHz, CD₃OD, 298 K): δ 14.2, 23.4, 27.1, 27.3,

32.3, 52.4, 118.5, 120.4, 123.0, 127.6, 129.9, 130.3, 130.7, 130.9, 131.2, 132.5, 135.8, 161.9, 162.6, 163.2, 163.9.

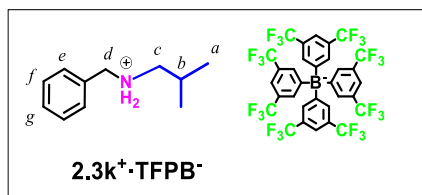


Derivative 2.3i⁺·TFPB⁻: (0.090 g, 0.10 mmol, 88%). **ESI(+)**
MS: $m/z = 150,15$ (M^+). **¹H NMR** (300 MHz, CD₃OD, 298 K): δ 1.39 (d, $J = 7$, 6H, H_a), 3.42 (m, 1H, H_b), 4.19 (s, 2H, H_c), 7.48 (overlapped, 5H, H_{c-e}), 7.61 (overlapped, 12H, ArH^{TFPB}); **¹³C NMR** (65 MHz, CD₃OD, 298 K): δ 17.0, 47.5, 49.5, 116.2, 117.0, 121.3, 125.6, 127.4, 128.0, 128.3, 128.5, 128.9, 130.0, 130.7, 133.5. **DEPT 135°** (75 MHz, CD₃OD, 298 K): δ 17.0, 47.5, 49.5, 116.1, 116.2, 116.3, 128.0, 128.3, 128.5, 133.5.

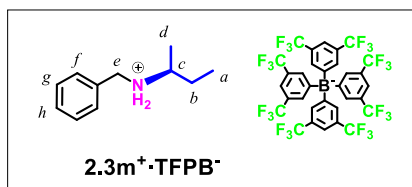


Derivative 2.3j⁺·TFPB⁻: (0.090 g, 0.10 mmol, 88%). **ESI(+)**
MS: $m/z = 164,15$ (M^+). **¹H NMR** (400 MHz, CD₃OD, 298 K): δ 1.45 (s, 9H, H_a), 4.17 (s, 2H, H_b), 7.48 (overlapped, 5H,

H_{c-e}), 7.60 (overlapped, 12H, ArH^{TFPB}); ^{13}C NMR (100 MHz, CD_3OD , 298 K): δ 24.4, 45.2, 57.1, 117.1, 120.3, 123.0, 125.7, 128.4, 128.6, 129.0, 129.2, 129.5, 131.6, 134.4, 160.7, 161.2, 161.7, 162.2.

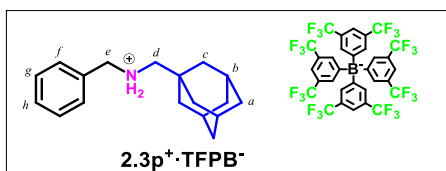


Derivative 2.3k⁺·TFPB⁻: (0.11 g, 0.11 mmol, 73%). **ESI(+)**
MS: $m/z = 164,14$ (M^+). 1H NMR (250 MHz, MeOD, 298 K): δ 1.02 (d, $J = 7$, 6H, H_a), 2.02 (m, 1H, H_b), 2.87 (d, $J = 7$, 2H, H_c), 4.20 (s, 2H, H_d), 7.47 (s, 5H, ArH_{e-g}), 7.59 (s, 12H, ArH^{TFPB}); ^{13}C NMR (100 MHz, CD_3OD , 298 K): δ 20.3, 27.2, 52.8, 55.7, 116.5, 121.7, 124.4, 127.1, 129.8, 130.3, 130.6, 130.8, 131.0, 132.4, 135.8, 162.1, 162.6, 163.1, 163.6.



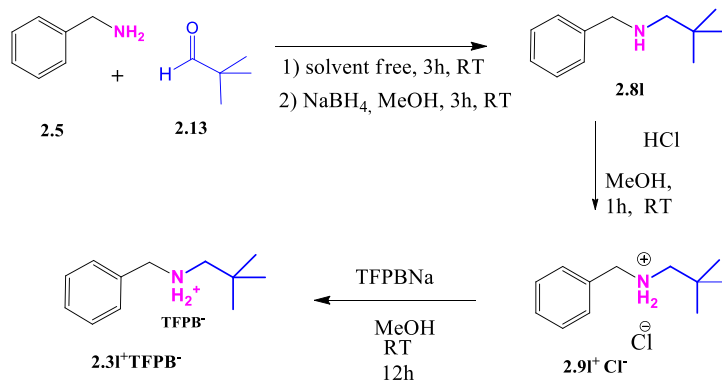
Derivative 2.3m⁺·TFPB⁻: (0.11g, 0.10 mmol, 91%). **ESI(+)**
MS: $m/z = 164.18$ (M^+). 1H NMR (400 MHz, $CDCl_3$ 298 K): δ

0.94 (t, $J = 7$, 3H, H_a), 1.34 (d, $J = 6$, 3H, H_d), 1.60 (m, broad, 1H, H_b), 1.70 (overlapped, 1H, H_b), 3.30 (s, broad, 1H, H_c), 4.13 (m, broad, 2H, H_e), 5.65-5.76 (m, broad, 2H, H_{NH_2}) 7.20 (d, $J = 7$, 2H, ArH) 7.42-7.53 (overlapped, 3H + 4H, $ArH + ArH^{TFPB}$), 7.69 (s, 8H, ArH^{TFPB}); ^{13}C NMR (75 MHz, $CDCl_3$, 298 K): δ 27.5, 32.3, 35.9, 54.2, 60.1, 117.7, 119.3, 122.9, 126.5, 128.0, 128.4, 128.9, 129.2, 129.7, 130.1, 130.4, 131.6, 134.9, 160.8, 161.5, 162.2, 162.8.



Derivative 2.3p⁺·TFPB⁻: (0.096 g, 0.085 mmol, 83%).
ESI(+) MS: $m/z = 256,23$ (M^+). 1H NMR (400 MHz, $CDCl_3$, 298 K): δ 1.41 (s, 6H, H_a), 1.55 (d, $J = 13$, 3H, H_c), 1.76 (d, $J = 13$, 3H, H_c), 2.02 (s, 3H, H_b), 2.72 (m, broad, 2H, H_d), 4.09 (t broad 2H, H_e), 6.23 (s broad 2H, H_{NH_2}), 7.21 (d, $J = 7$, 2H, H_f), 7.43 (t, $J = 7$, 2H, H_g); 7.48-7.58 (overlapped, 5H, H_{a-c}), 7.59 (overlapped, 12H, ArH^{TFPB}); ^{13}C NMR (75 MHz, $CDCl_3$, 298 K): δ 27.5, 32.3, 35.9, 54.2, 60.1, 117.7, 119.3, 122.9, 126.5, 128.0, 128.4, 128.9, 129.2, 129.7, 130.1, 130.4, 131.6, 134.9, 160.8, 161.5, 162.2, 162.8.

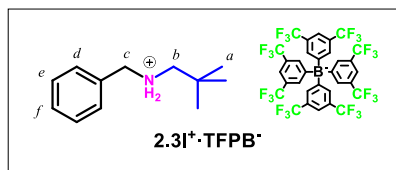
Synthesis of derivative **2.31⁺·TFPB⁻**



To the benzylamine (0.010 mol) was added 3,3-dimethylbutyraldehyde (0.010 mol) and the reaction mixture was stirred at room temperature for 3 h.

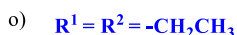
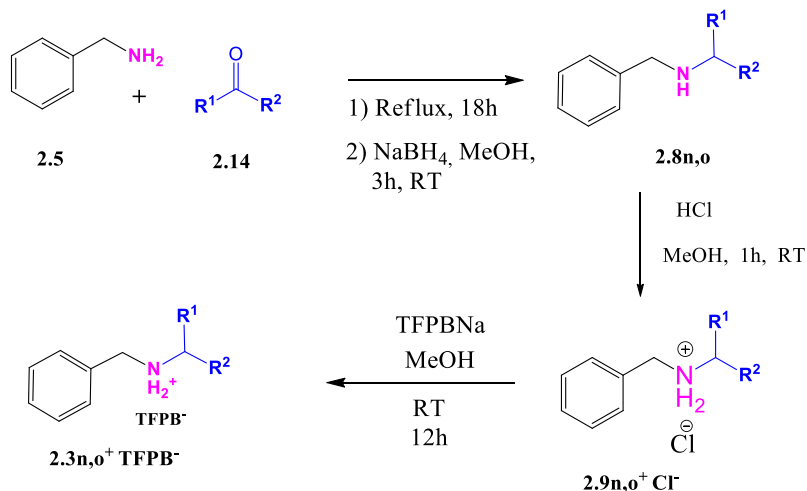
The resulting imine (0.010 mol) was dissolved in dry MeOH (20 mL) under a nitrogen atmosphere and NaBH₄ (0.10 mol) was added at 0 °C and then the mixture was allowed to warm at room temperature. The solution was kept under stirring for 3 h. The solvent was removed under reduced pressure and the residue partitioned between AcOEt (30 mL) and an aqueous saturated solution of NaHCO₃ (30 mL). The organic layer was dried over MgSO₄ and the solvent was removed under reduced pressure, to give derivative **2.81** as a yellow viscous liquid. The compound was used for the next step without further purification. The crude product (0.010 mol) was dissolved in Et₂O (20 mL) at room temperature and an

aqueous solution of HCl (37% w/w, 0.011mol) was added dropwise. The mixture was kept under stirring for 1 h, until the formation of a white precipitate. The solid was collected by filtration, purified by crystallization with Exane/MeOH and dried under vacuum, to give derivative **2.9I⁺·Cl⁻** as a white solid. Derivative **2.9I⁺·Cl⁻** (0.15 mmol) was dissolved in dry MeOH (5.0 mL), then sodium tetrakis[3,5-bis(trifluoromethyl)phenyl]borate (0.16 mmol) was added and the mixture was kept under stirring overnight in the dark. The solvent was removed and deionized water was added, obtaining a brown precipitate that was filtered off and dried under vacuum to give derivatives **2.3I⁺·TFPB⁻**.



Derivative 2.3I⁺·TFPB⁻: (0.090 g, 0.22 mmol, 95%). **ESI(+)**
MS: $m/z = 178.17$ (M⁺). **¹H NMR** (250 MHz, CD₃OD, 298 K): δ 1.01 (s, 9H, Ha), 2.78 (s 2H, Hb), 4.24 (s, 2H, Hc), 7.31-7.80 (overlapped, 5H, Hd-f + 12H, ArH_{TFPB}); **¹³C NMR** (65 MHz, CDCl₃, 298 K): δ 26.5, 31.3, 54.5, 60.2, 117.6, 117.7, 119.3, 122.9, 126.5, 127.9, 128.4, 128.79, 128.82 129.2, 129.6, 130.10, 130.4, 131.7, 134.9, 160.8, 161.4, 162.1, 162.8.

Synthesis of derivatives $2.3n,o^+ \cdot \text{TFPB}^-$

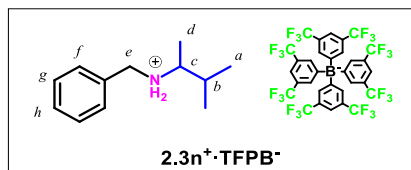


Benzylamine (0.010 mol) was dissolved into the corresponding ketone **2.14** (40 mL) and the reaction mixture was stirred at reflux for 18 h. The reaction mixture was then cooled to room temperature and the excess of ketone was removed under reduced pressure.

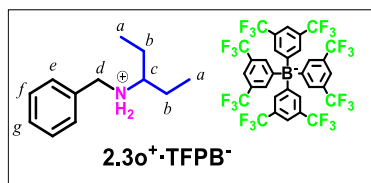
The resulting imine (0.010 mol) was dissolved in dry MeOH (20 mL) under a nitrogen atmosphere and NaBH_4 (0.10 mol) was added at 0 °C and then the mixture was allowed to warm at room temperature. The solution was kept under stirring for 3 h. The solvent was removed under reduced pressure and the

residue partitioned between AcOEt (30 mL) and an aqueous saturated solution of NaHCO₃ (30 mL). The organic layer was dried over MgSO₄ and the solvent was removed under reduced pressure, to give derivative **2.8n,o** as a yellow viscous liquid. The compound was used for the next step without further purification. The crude product (0.010 mol) was dissolved in Et₂O (20 mL) at room temperature and an aqueous solution of HCl (37% w/w, 0.011 mol) was added dropwise. The mixture was kept under stirring for 1 h, until the formation of a white precipitate. The solid was collected by filtration, purified by crystallization with Exane/MeOH and dried under vacuum, to give derivative **2.9n,o⁺·Cl⁻** as a white solid.

Derivative **2.9n,o⁺·Cl⁻** (1 eq.) was dissolved in dry MeOH (C= 0.20 M), then sodium tetrakis[3,5-bis(trifluoromethyl)phenyl]borate (1.1 eq) was added and the mixture was kept under stirring overnight in the dark. The solvent was removed and deionized water was added, obtaining a brown precipitate that was filtered off and dried under vacuum to give derivatives **2.3n,o⁺·TFPB⁻**.



Derivative 2.3n⁺·TFPB⁻: (0.14 g, 0.14 mmol, 99%). **ESI(+)**
MS: $m/z = 178,15$ (M^+). **¹H NMR** (400 MHz, CDCl₃, 298 K):
 δ 0.86-1.00 (overlapped, 6H, H_a), 1.29 (d, $J = 7$, 3H, H_d), 1.98
(m broad, 1H, H_b), 3.17 (m, broad 1H, H_c), 4.08 (m, broad
1H, H_e), 6.17 (s, broad 1H, H_{NH2}), 6.88 (s, broad 1H, H_{NH2}),
(overlapped, 5H, H_{c-e}), 7.48-7.61 (overlapped, 5H, H_f +
ArH^{TFPB}) 7.45 (t broad, $J = 7$, 2H, H_g), 7.71 (s, 8H, ArH^{TFPB}
); **¹³C NMR** (100 MHz, CD₃OD, 298 K): δ 10.0, 14.3, 18.2,
29.4, 48.8, 59.0, 117.1, 120.3, 123.0, 125.7, 128.4, 128.6,
128.9, 129.2, 129.3, 129.6, 131.1, 134.4, 160.7, 161.2, 161.7,
162.2.



Derivative 2.3o⁺·TFPB⁻: (0.12 g, 0.11 mmol, 78%). **ESI(+)**
MS: $m/z = 178,15$ (M^+). **¹H NMR** (250 MHz, CD₃OD, 298
K): δ 1.00 (t, $J = 7$, 6H, H_a), 1.81 (m, broad, 4H, H_b), 3.08 (m,
broad, 1H, H_c), 4.21 (s, 2H, H_d), 7.48 (overlapped, 5H, H_{e-g}),
7.59 (overlapped, 12H, ArH^{TFPB})); **¹³C NMR** (65 MHz,
CD₃OD, 298 K): δ 8.6, 22.8, 50.8, 63.1, 117.7, 118.2, 122.5,
126.8, 128.2, 128.8, 128.9, 129.3, 129.8, 130.6, 131.2, 131.8,
134.9, 160.6, 161.4, 162.2, 163.0.

General procedure for the preparation of [2]Pseudorotaxane **2.4⁺·TFPB⁻**

Calixarene derivative **2.1a** ($1.9 \cdot 10^{-3}$ mmol) was dissolved in 0.5 mL of CDCl₃ ($3.8 \cdot 10^{-3}$ M solution). Then, the appropriate TFPB⁻ salt **2.3⁺·TFPB⁻** was added ($1.9 \cdot 10^{-3}$ mmol, $3.8 \cdot 10^{-3}$ M) and the mixture was stirred for 15 min. Then, the solution was transferred in a NMR tube for 1D NMR spectra acquisition.

^1H NMR determination of K_{ass} values⁴⁴ for the *endo*-alkyl pseudorotaxanes $\mathbf{2.4f}^+\cdot\text{TFPB}^-$, $\mathbf{2.4j}^+\cdot\text{TFPB}^-$, $\mathbf{2.4k}^+\cdot\text{TFPB}^-$, $\mathbf{2.4l}^+\cdot\text{TFPB}^-$, $\mathbf{2.4m}^+\cdot\text{TFPB}^-$, $\mathbf{2.4n}^+\cdot\text{TFPB}^-$.

The association constant values were calculated by integration of free and complexed ^1H NMR peaks of host or guest.

The calixarene derivative $\mathbf{2.1a}$ ($1.9\cdot 10^{-3}$ mmol) was dissolved in 0.5 mL of CDCl_3 ($3.8\cdot 10^{-3}$ M solution). Then, the appropriate TFPB $^-$ salt $\mathbf{2.4}^+$ was added ($1.9\cdot 10^{-3}$ mmol, $3.8\cdot 10^{-3}$ M) and the mixture was stirred for 15 min. Then, the solution was transferred in a NMR tube for spectra acquisition.

An representative example of K_{ass} calculation is reported in **Figure 2.17**.

⁴⁴ K. Hirose, *J. Incl. Phenom. Macrocycl. Chem.* **2001**, 39, 193-209.

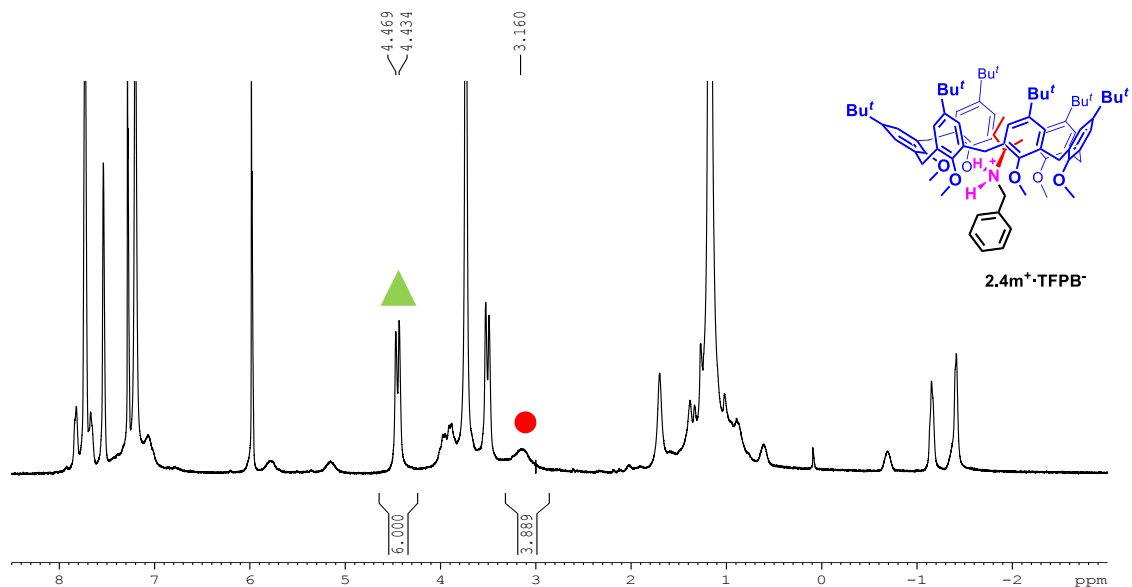


Figure 2.17 ^1H NMR spectrum (CDCl_3 , 400 MHz, 298 K) of equimolar solution ($3.8 \cdot 10^{-3}$ M) of **2.1a** and **2.3m⁺·TFPB⁻**. The association constant K_{ass} value was calculated by integration of complexed (▲) and free (●) derivative **2.1a**: $[(6.00 \times 3 / 21.89) \times 3.8 \times 10^{-3}] / [(3.89/21.89) \times 3.8 \times 10^{-3}]^2 = 6.9 \times 10^3 \text{ M}^{-1}$.

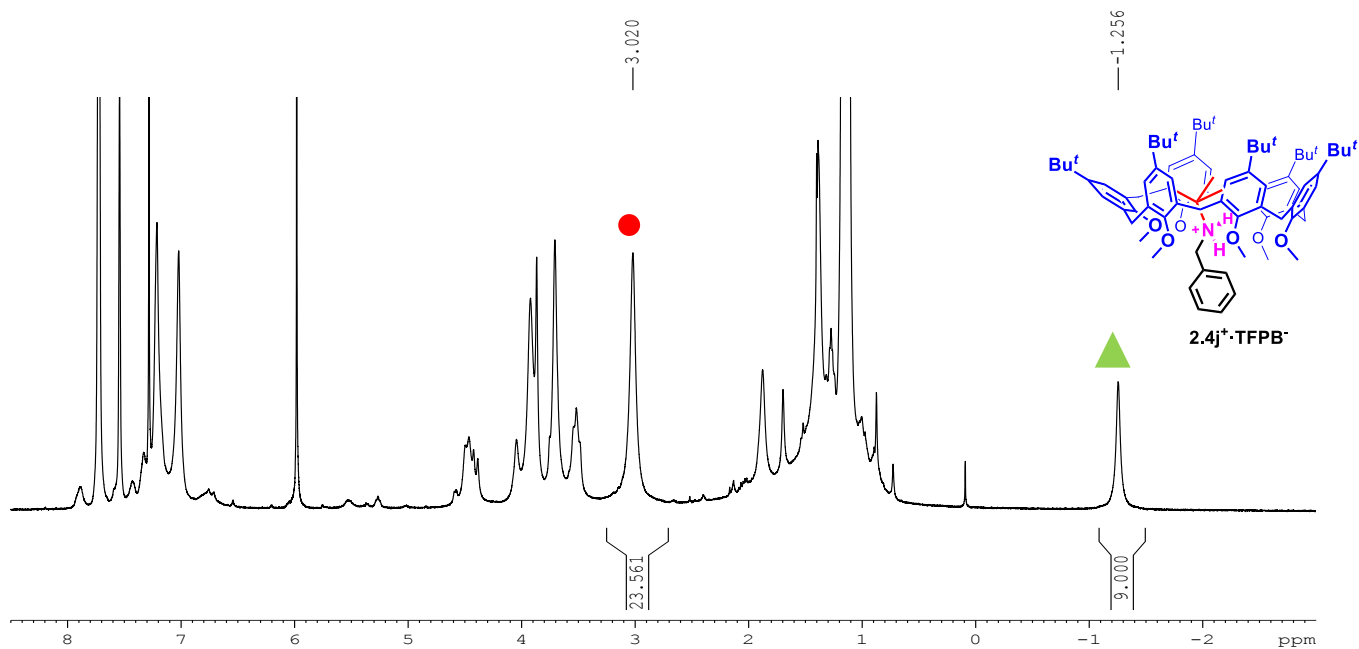


Figure 2.18 ^1H NMR spectrum (CDCl_3 , 400 MHz, 298 K) of equimolar solution ($3.8 \cdot 10^{-3}$ M) of **2.1a** and **2.3j⁺·TFPB⁻**. The association constant K_{ass} value was calculated by integration of complexed (▲) and free derivative **2.1a** (●).

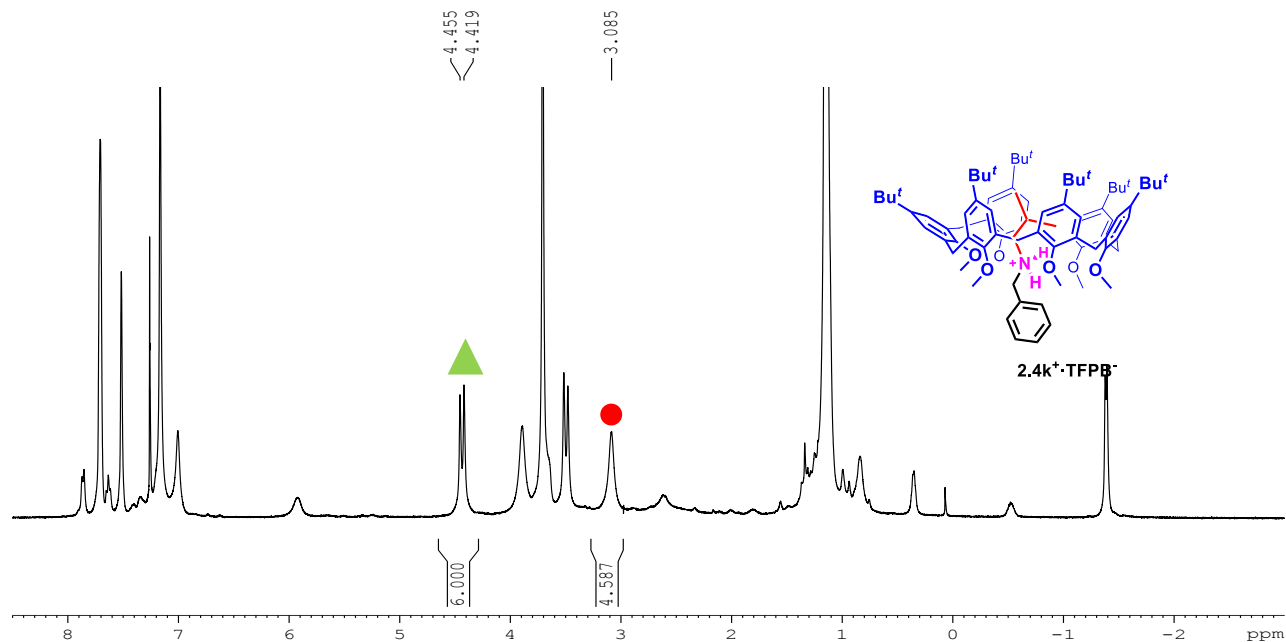


Figure 2.19 ^1H NMR spectrum (CDCl_3 , 400 MHz, 298 K) of equimolar solution ($3.8 \cdot 10^{-3}$ M) of **2.1a** and **2.3k⁺·TFPB⁻**. The association constant K_{ass} value was calculated by integration of complexed (▲) and free (●) derivative **2.1a**.

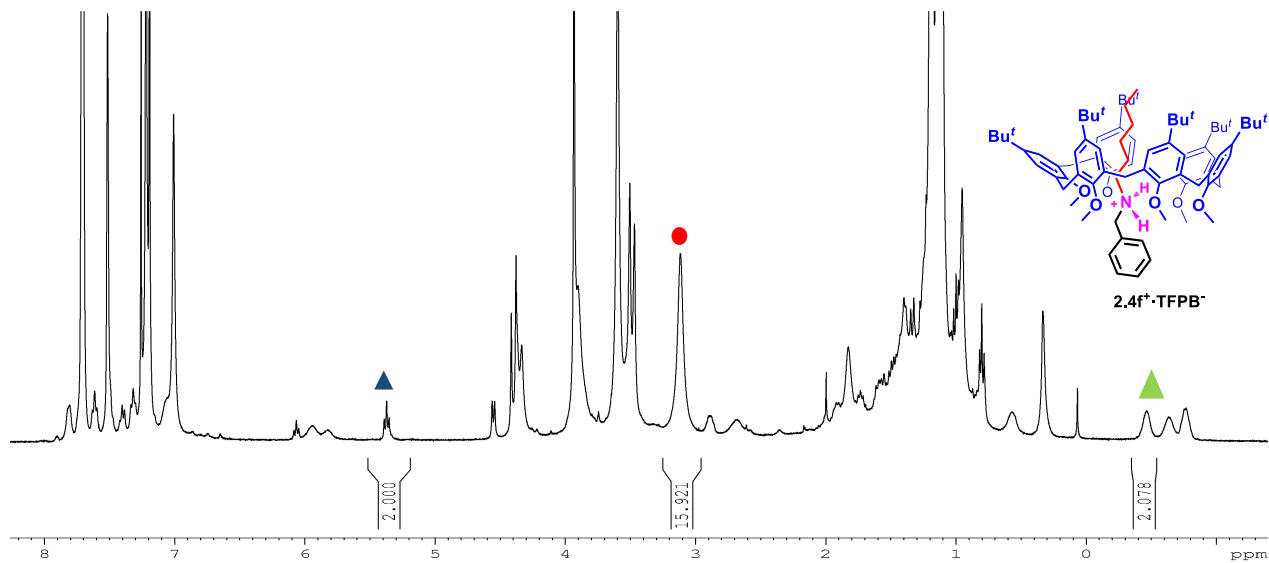


Figure 2.20 ^1H NMR spectrum (CDCl_3 , 400 MHz, 298 K) of equimolar solution ($3.8 \cdot 10^{-3}$ M) of **2.1a** and **2.3f⁺·TFPB⁻**. The association constant K_{ass} value was calculated by integration of *endo*-alkyl complexed (\blacktriangle), *endo*-benzyl complexed (\blacktriangle) and free derivative **2.1a** (\bullet).

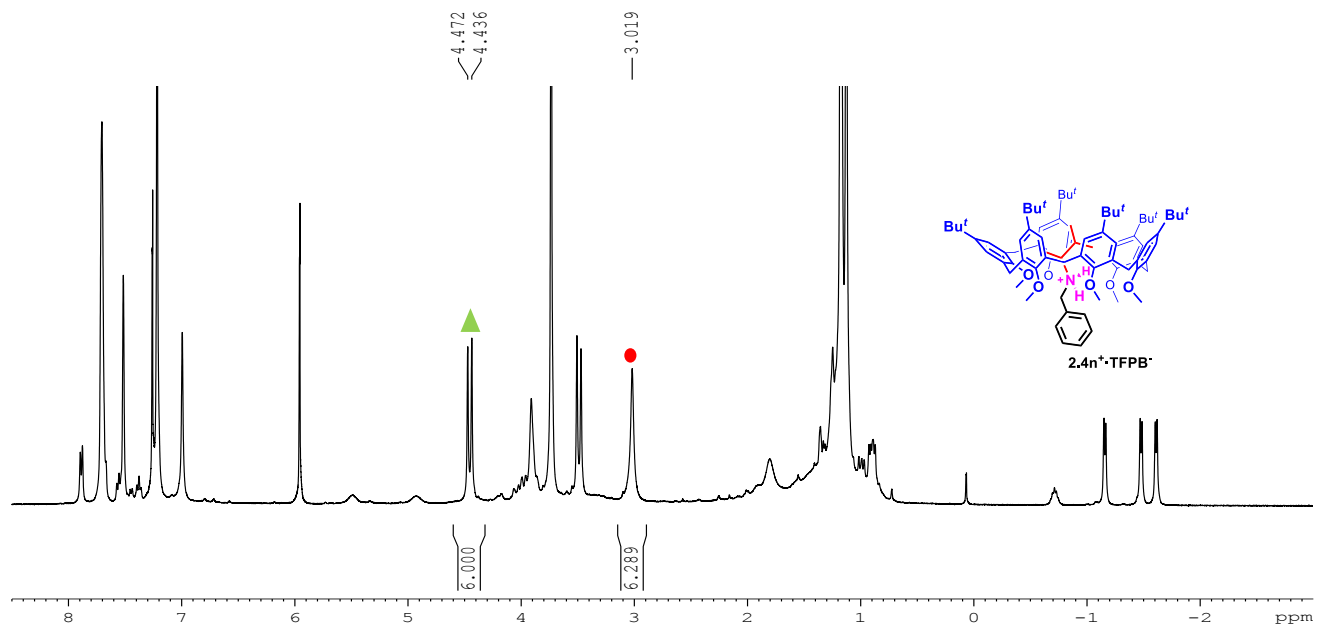


Figure 2.21 ^1H NMR spectrum (CDCl_3 , 400 MHz, 298 K) of equimolar solution ($3.8 \cdot 10^{-3}$ M) of **2.1a** and $2.3n^+\cdot\text{TFPB}^-$. The association constant K_{ass} value was calculated by integration of complexed (\blacktriangle) and free (\bullet) derivative **2.1a**.

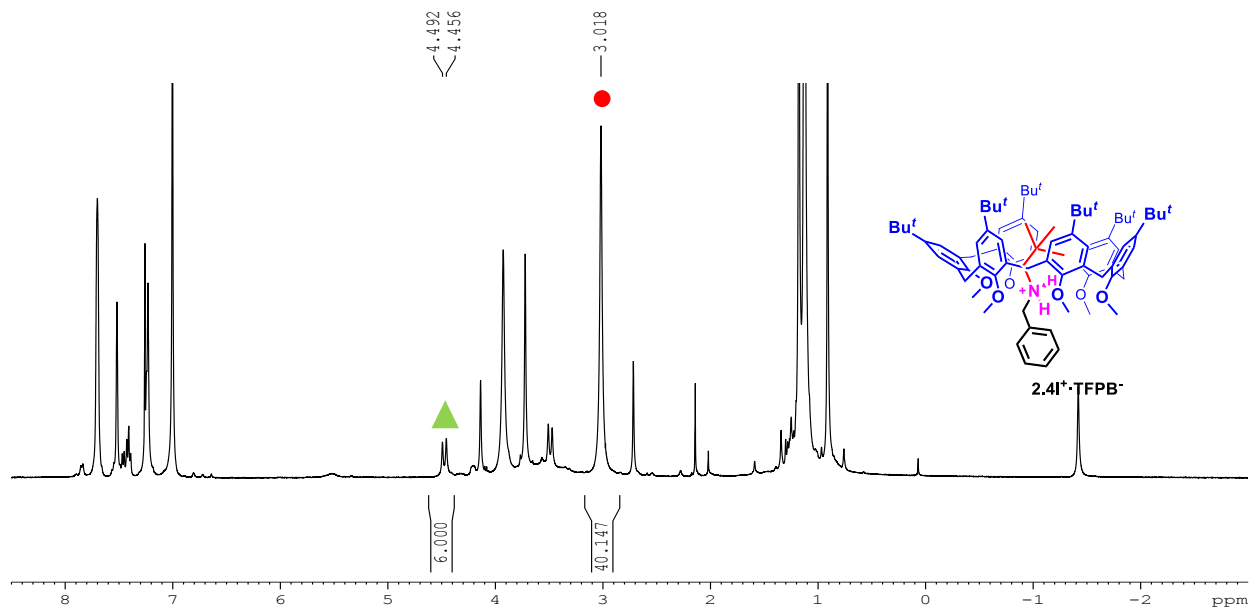


Figure 2.22 ^1H NMR spectrum (CDCl_3 , 400 MHz, 298 K) of equimolar solution ($3.8 \cdot 10^{-3}$ M) of **2.1a** and $2.3\text{I}^+\cdot\text{TFPB}^-$. The association constant K_{ass} value was calculated by integration of complexed (▲) and free (●) derivative **2.1a**.

^1H NMR determination of the K_{ass} value for the $2.4\mathbf{o}^+\cdot\text{TFPB}^-$ pseudorotaxane by quantitative NMR Analysis.

The sample was prepared by dissolving $2.1\mathbf{a}$ (1.9×10^{-3} mmol) and the $2.3\mathbf{o}^+\cdot\text{TFPB}^-$ benzylalkylammonium guest (1.9×10^{-3} mmol) in CDCl_3 (0.5 mL) containing 1 μL of 1,1,2,2-tetrachloroethane ($d = 1.59$ g/mL) as internal standard. The complex concentration was evaluated by integration of the ^1H NMR signal of $\text{CHCl}_2\text{CHCl}_2$ Vs the signal of the complex. The following equation was used to obtain the moles of the complex:

$$\frac{G_a}{G_b} = \frac{F_a}{F_b} \times \frac{N_a}{N_b} \times \frac{M_a}{M_b}$$

G_a = grams of 1,1,2,2-tetrachloroethane;

G_b = grams of complex

F_a and F_b = areas of the signals of 1,1,2,2-tetrachloroethane and the shielded signal of the guest

N_a and N_b = numbers of nuclei which cause the signals (N_a for 1,1,2,2-tetrachloroethane; N_b for guest)

M_a and M_b = molecular masses of 1,1,2,2-tetrachloroethane (a) and complex (b)

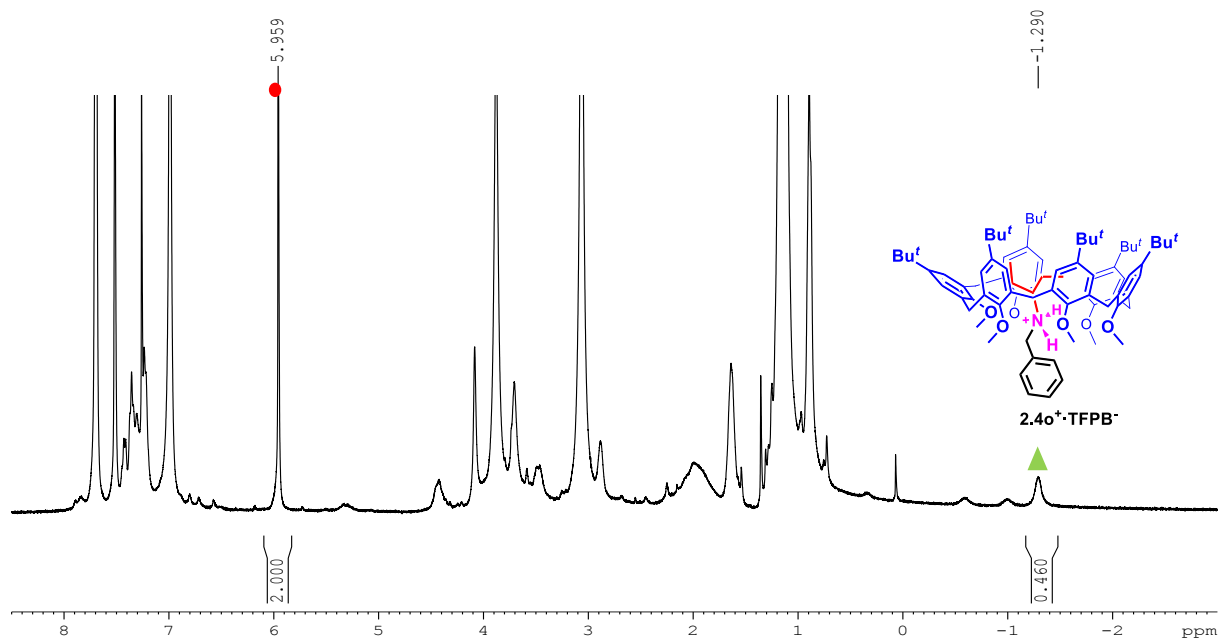


Figure 2.23. ^1H NMR spectrum (CDCl_3 , 400 MHz, 298 K) of equimolar solution ($3.8 \cdot 10^{-3}$ M) of **2.1a** and **2.3o $^+$ ·TFPB $^-$** . The association constant K_{ass} value was calculated by integration of the complexed derivative **2.1a** (\blacktriangle) and the signal of $\text{CHCl}_2\text{CHCl}_2$ (\bullet).

^1H NMR determination of the K_{ass} values for *endo*-alkyl **2.4d**⁺·TFPB⁻, **2.4i**⁺·TFPB⁻, **2.4h**⁺·TFPB⁻ and **2.4g**⁺·TFPB⁻ pseudorotaxanes by competition experiments.

^1H NMR competition experiments were performed by analysis of a 1:1:1 mixture of host H **1**, guest GA and guest GB in a NMR tube using CDCl₃ as solvent.

Calixarene derivative **2.1a** ($1.9 \cdot 10^{-3}$ mmol) was dissolved in 0.5 mL of CDCl₃ ($3.8 \cdot 10^{-3}$ M solution). Then, the appropriate guests GA ($1.9 \cdot 10^{-3}$ mmol, $3.8 \cdot 10^{-3}$ M) and GB ($1.9 \cdot 10^{-3}$ mmol, $3.8 \cdot 10^{-3}$ M) were added. Then, the solution was transferred in a NMR tube for 1D NMR spectra acquisition.

$$K_{A<H} = \frac{[HG_A]}{[H][G_A]} \quad \text{and} \quad K_{B<H} = \frac{[HG_B]}{[H][G_B]} \quad \rightarrow \quad K_{rel} = \frac{K_{A<H}}{K_{B<H}} = \frac{[HG_A][H][G_B]}{[HG_B][H][G_A]} \quad \rightarrow$$

$$\frac{[HG_A] = [G_B]}{[HG_B] = [G_A]} \quad \rightarrow \quad K_{rel} = \frac{K_{A<H}}{K_{B<H}} = \frac{[HG_A]^2}{[HG_B]^2}$$

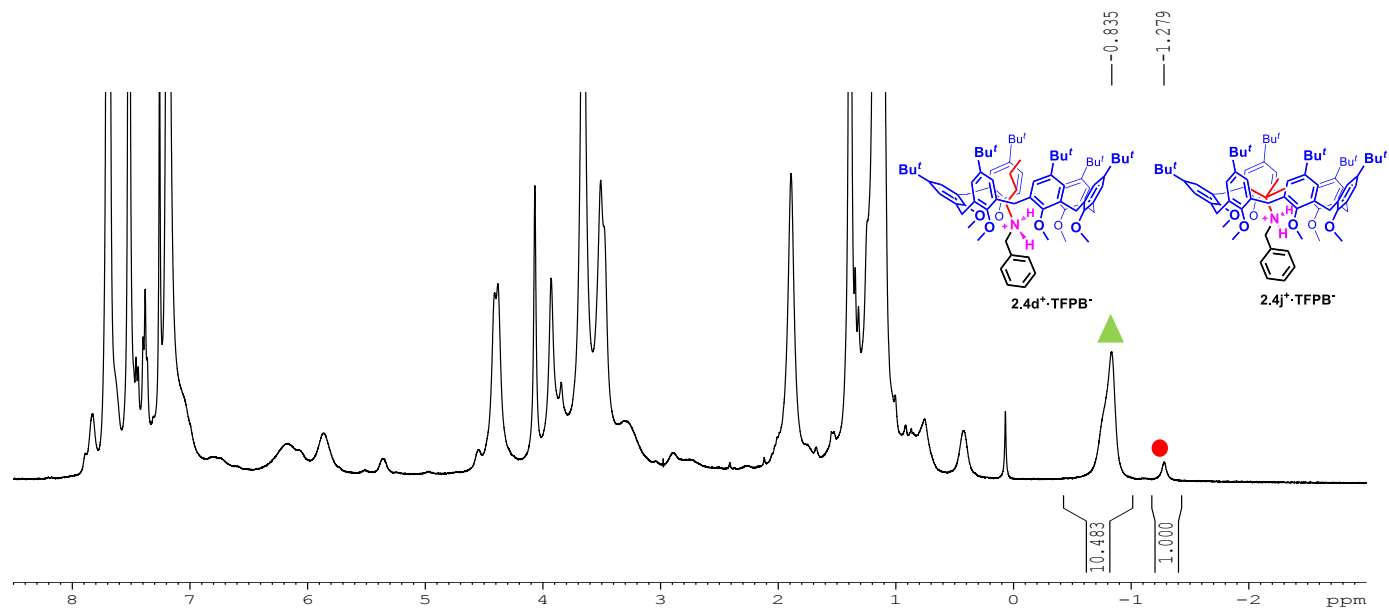


Figure 2.24 ^1H NMR spectrum (CDCl_3 , 400 MHz, 298 K) of derivative **2.1a** in presence of 1 equivalent of $2.3\text{d}^+\cdot\text{TFPB}^-$ and 1 equivalent of $2.3\text{j}^+\cdot\text{TFPB}^-$ ($3.8 \cdot 10^{-3}$ M each one). (●) Resonance relative to the *endo*-alkyl- $2.4\text{d}^+\cdot\text{TFPB}^-$ complex, (▲) resonance relative to the *endo*-alkyl- $2.4\text{j}^+\cdot\text{TFPB}^-$.

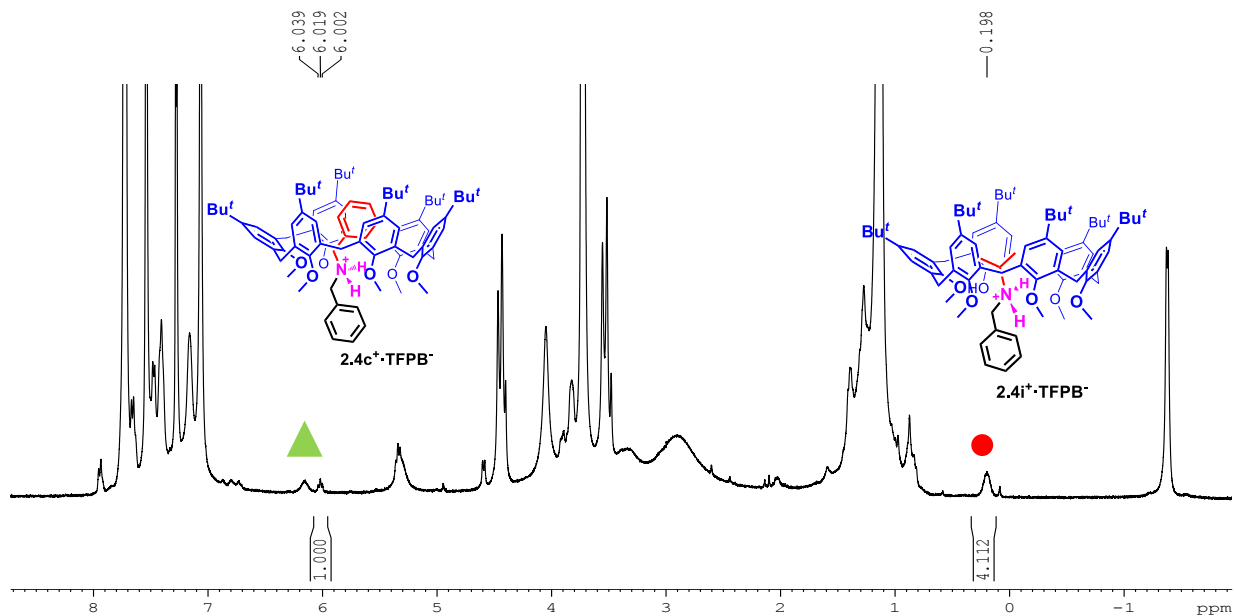


Figure 2.25 ^1H NMR spectrum (CDCl_3 , 400 MHz, 298 K) of derivative **2.1a** in presence of 1 equivalent of **2.3i⁺·TFPB⁻** and 1 equivalent of **2.3c⁺·TFPB⁻** ($3.8 \cdot 10^{-3}$ M each one). (●) Resonance relative to the *endo*-alkyl-**2.4i⁺·TFPB⁻** complex, (▲) resonance relative to **2.4c⁺·TFPB⁻** complex.

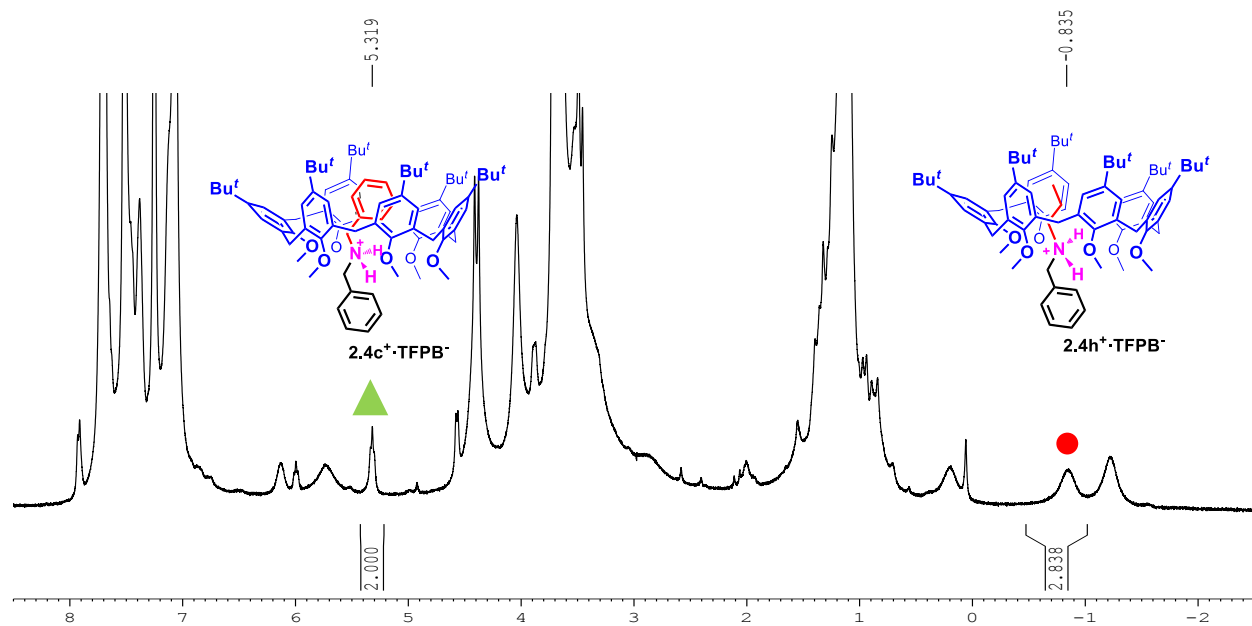


Figure 2.26 ^1H NMR spectrum (CDCl_3 , 400 MHz, 298 K) of derivative **2.1a** in presence of 1 equivalent of **2.3h $^+$ ·TFPB $^-$** and 1 equivalent of **2.3c $^+$ ·TFPB $^-$** ($3.8 \cdot 10^{-3}$ M each one). (●) Resonance relative to the *endo*-alkyl-**2.4h $^+$ ·TFPB $^-$** complex, (▲) resonance relative to the **2.4c $^+$ ·TFPB $^-$** complex.

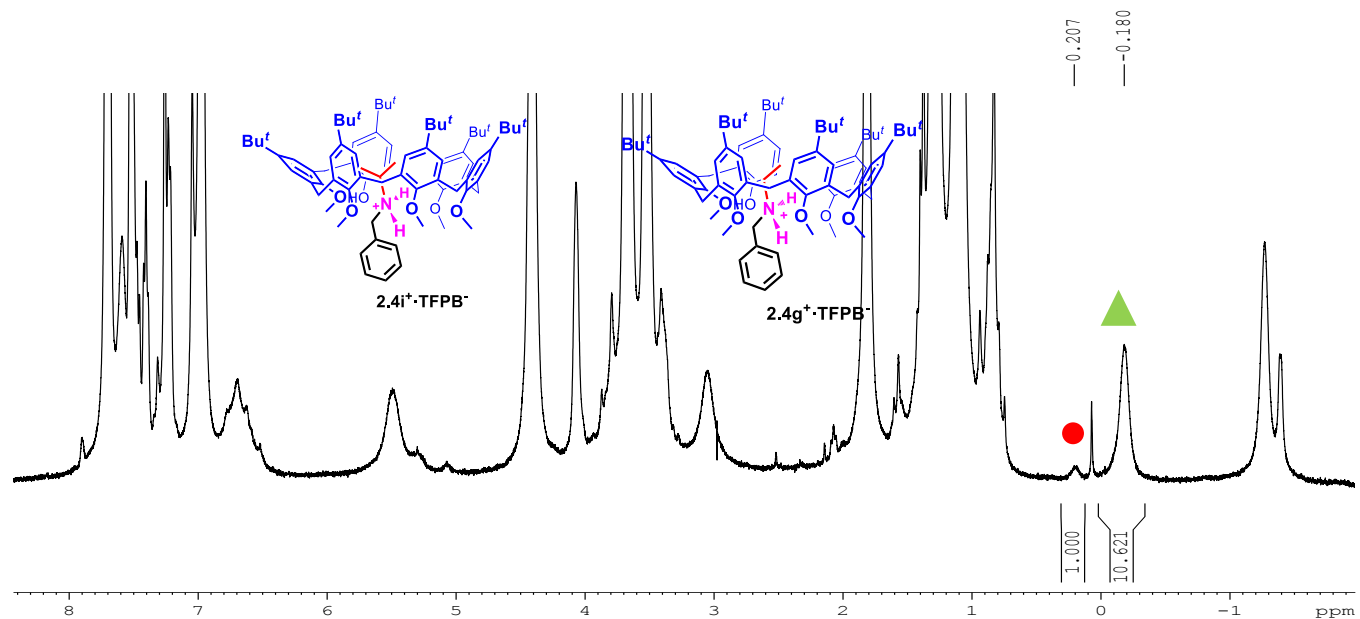


Figure 2.27 ^1H NMR spectrum (CDCl_3 , 400 MHz, 298 K) of derivative **2.1a** in presence of 1 equivalent of **2.3i⁺·TFPB⁻** and 1 equivalent of **2.3g⁺·TFPB⁻** ($3.8 \cdot 10^{-3}$ M each one). (●) resonance relative to **2.4i⁺·TFPB⁻** complex, (▲) resonance relative to **2.4g⁺·TFPB⁻** complex.

Packing Coefficient and CCs calculation.

- A. Pseudorotaxane structures *endo*-alkyl-**2.4⁺·TFPB⁻** were minimized using the force field OPLS-2005 in the MacroModel program. The structures obtained were subsequently defined by DFT calculations using B3LYP/6 31G level of the theory and Grimme's dispersion corrections (IOp(3/124 = 3).
- B. The Swiss-pdb program was used to calculate the volume of the internal calixarene cavity and the guest volume. In detail, the guest was removed from each pseudorotaxane, the resulting calixarene was capped with a meta xylene unit and the inner volume was calculated with a probe of 1.4 Å as diameter. The guest volume was obtained considering only the portion hosted in the cavity by cutting the guest at the ammonium site level
- C. **Packing Coefficients.** PCs were calculated dividing the guest volume by the calixarene volume, both calculated as described in section B.
- D. **Contacting Coefficients.** Using the Swiss-pdb program each pseudorotaxane was divided in two portions: calixarene and guest and their surfaces were calculated (for the guest surface, S_{guest} , it was considered only the portion hosted in the cavity by

cutting the guest at the ammonium site level). Again with the Swiss-pdb program, these two surface values were used to define the contact surface between host and guest ($S_{\text{host-guest contact}}$). The **CC** values, for each pseudorotaxane, were obtained dividing the contact surface $S_{\text{host-guest contact}}$ by the guest surface S_{guest} .

CHAPTER III

CHIRALITY AND CHIRAL MOLECULAR RECOGNITION IN THE CALIXARENE THREADING

3.1 CHIRAL RECOGNITION IN SUPRAMOLECULAR STRUCTURES

One of the most important aims of the Supramolecular Chemistry is the recognition of chiral guests.⁴⁵ In fact, differently by the natural receptors the artificial chiral discrimination is quite difficult to achieve with synthetic hosts. Usually, the use of a chiral host can be a good way to distinguish between two chiral guests.

For example when an enantiopure host is added to a mixture of two enantiomers, the two diastereoisomeric complexes formed are characterized by different properties and so their separation becomes easier to achieve.

An interesting example of chiral recognition is represented by the Cram's machine (**Figure 3.1**).⁴⁶

⁴⁵ X. X. Zhang, J. S. Bradshaw, R. M. Izatt, *Chem. Rev.*, **1997**, *97*, 3313–3361.

⁴⁶ M. Newcomb, J. L. Toner, R. C. Helgeson, D. J. Cram, *J. Am. Chem. Soc.* **1979**, *101*, 4941–4947.

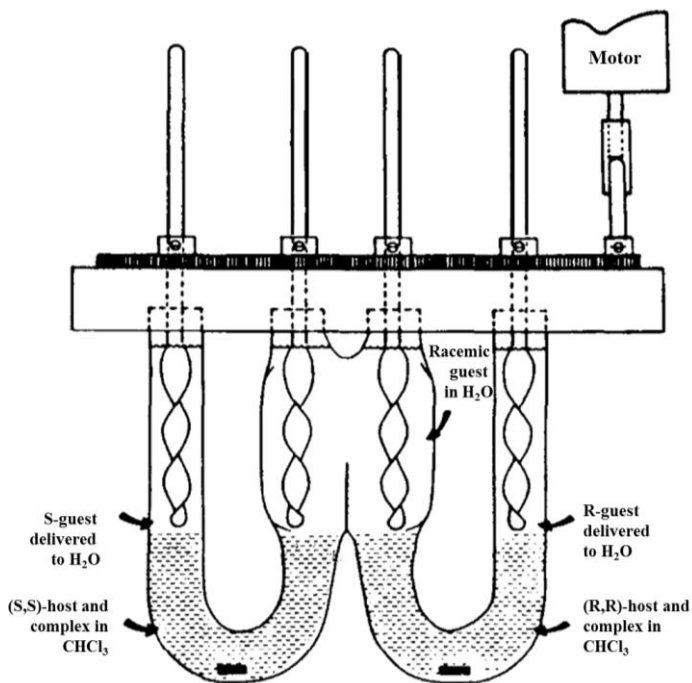


Figure 3.1 Cram's machine.

The machine operated in the way that from the central tank of the W-tube containing an aqueous solution of racemic salt **3.2** (**Figure 3.2**), the (R)-enantiomer **3.2** was delivered to the left hand aqueous layer by (S,S)-**3.1**, while the (R)-enantiomer was transported by (R,R)-**3.1** and delivered to the right hand aqueous layer. Fresh racemic guest was continuously added to the central tank and (S)- and (R) - $C_6H_5H(CO_2CH_3)NH_3PF_6$ of 86-90 % enantiomeric excess were continuously removed from the left and right hand aqueous tanks, respectively.

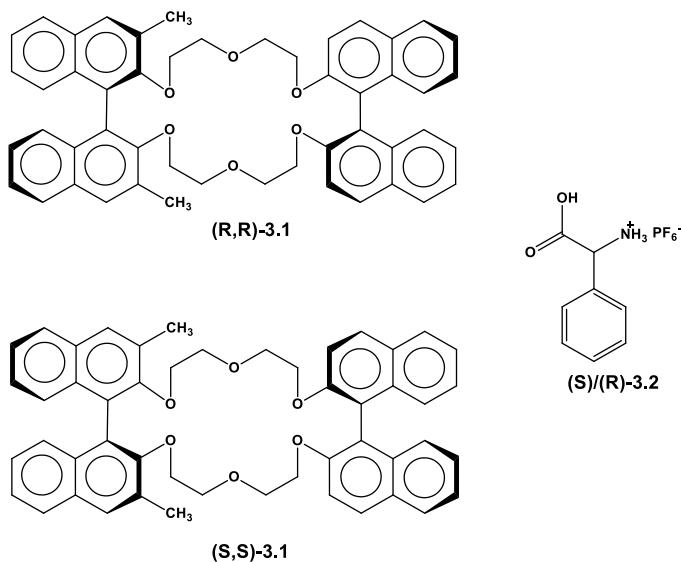


Figure 3.2. Hosts and guests studied by Cram.

There are several spectroscopic techniques that have been used to study the chiral recognition, naturally the most common are those who study chiroptical properties such as electron circular dichroism (ECD), vibrational circular dichroism (VCD) and optical rotary dispersion (ORD).

All these techniques represent also an useful tool for the assignment of the absolute configuration.

Interestingly, Habata and co-workers showed that an achiral crown-ether macrocycle was able to recognize chiral *sec*-ammonium cations and that an amplification of the chirality was observed due to the formation of a chiral pseudo[2]rotaxane (**Figure 3.3**).

In detail with the intent to investigate the chirality

transcription and amplification by the [2]pseudorotaxanes, the UV-vis and CD spectra of the crown ether **3.3**, ammonium salts (R)/(S)-**3.4a-b**, and [2]pseudorotaxanes were measured (**Figure 3.3**).

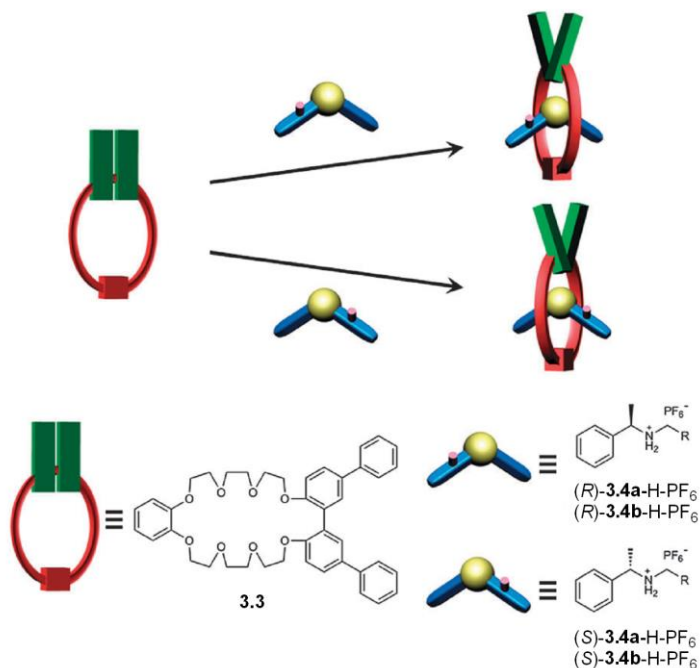


Figure 3.3 Diagram of the formation of [2]pseudorotaxanes.

The host **3.3** was achiral and no Cotton effect was observed. The chiral ammonium salt (R) -**3.4a**-H-PF₆ showed CD Cotton effects around 260 nm (aromatic ¹L_b band) but the amplitude was very low. On the other hand, the [2]pseudorotaxane [**3.3**· (R) -**3.4a**-H][PF₆] displayed significant CD Cotton effects due to the exciton coupling between the two biphenyl chromophores in the 2',2''-quaterphenyl group.

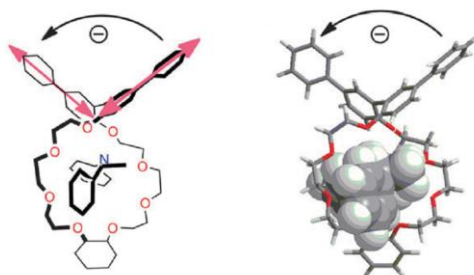


Figure 3. 4 Optimized structure of [3.3·(R)-3.4a-H][PF₆] by *ab initio* B3LYP/6-31G*

3.2.2 Chiral recognition in gas phase.

Supramolecular species are sometimes quite big, with high molecular masses and their subunits are weakly bound and easy to destroy during the ionization process in mass spectrometry. For this reason the conventional mass spectrometry methods, in particular the harsh ionization methods such as EI and CI have delayed the development of mass spectrometry as tool to characterize supramolecular aggregates.

However since the introduction of the soft ionization methods in FAB, MALDI and ESI, mass spectrometry has gained a position among the analytical tools used to characterize noncovalent species.

As it is well-known, MS is insensitive to chirality differences; thus, MS cannot provide enantiomer differentiation but there

are several methods to use this technique to differentiate diastereomers.

The first method is the “*Enantiomer Labelled*” guest method (EL). In this case the enantiopure host is mixed with the guest in racemic form. One of the two enantiomers is isotopically labelled, and the other not, so the signals for the two diastereomeric host-guest complexes appear at different m/z values in a MS spectra.

Directly from the intensity ratio of the two complexes, it is possible to determine the stereochemical effect in absence of the isotopic effect.

This method was successfully applied to some crown ethers by Sawada et al. using FAB⁴⁷ and ESI-MS⁴⁸ ionization techniques and it was extensively reviewed by Schalley in 2001.⁴⁹

⁴⁷ a) M. Sawada, Y. Takai, H. Yamada, T. Kaneda, K. Kamada, T. Mizooku, K. Hirose, Y. Tobe, K. Naemura, *J. Chem. Soc. Chem. Comm.* **1994**, 2497–2498; b) M. Sawada, Y. Takai, H. Yamada, S. Hirayama, T. Kaneda, T. Tanaka, K. Kamada, T. Mizooku, S. Takeuchi, K. Ueno, K. Hirose, Y. Tobe, K. Naemura, *J. Am. Chem. Soc.* **1995**, *117*, 7726–7736.

⁴⁸ a) M. Sawada, Y. Takai, H. Yamada, T. Kaneda, R. Arakawa, M. Okamoto, H. Doe, T. Matsuo, K. Naemura, K. Hirose, Y. Tobe, *Chem. Commun.* **1996**, 1735–1736. b) M. Sawada, Y. Takai, H. Yamada, J. Nishida, T. Kaneda, R. Arakawa, M. Okamoto, K. Hirose, T. Tanaka, K. Naemura, *J. Chem. Soc. Perkin. Trans 2*, **1998**, *3*, 701–710.

⁴⁹ C. A. Schalley, *Mass Spectrom. Rev.* **2001**, *20*, 253-309.

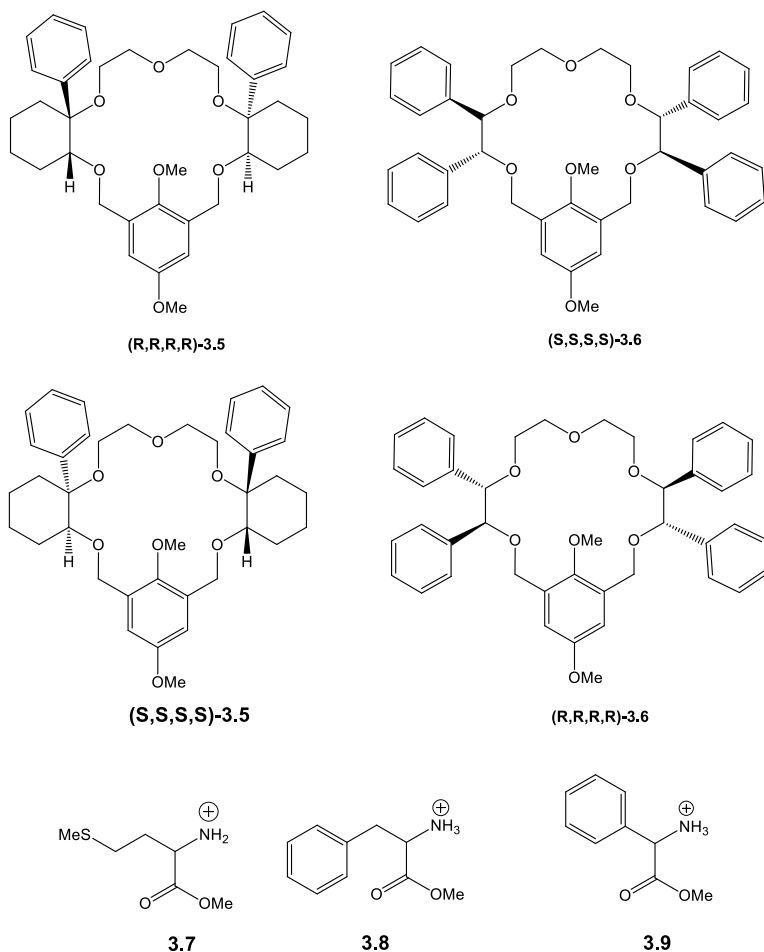


Figure 3.5 Chiral crown ethers and ammonium guest ions studied by Sawada with EL method.

This study revealed that in the FAB experiments the crown **(R,R,R,R)-3.5** recognized the guest **(R)-3.7** (**Figure 3.5**) with a large excess compared to the **S**-isomer, but in ESI experiment this difference was less evident.

This trend was found to be common to all host-guest pairs

investigated and was ascribed to the electrospray process, although no valid explanation was given about how the spray procedure affected the result.

An alternative method to the EL needs two independent measurements of each host enantiomer with a given guest used as a reference. It has been used in chiral recognition experiments between some crown ethers and ammonium ion guests by Pöcsfalvi⁵⁰ and a similar work was made always by Sawada (**Figure 3.6**).⁵¹

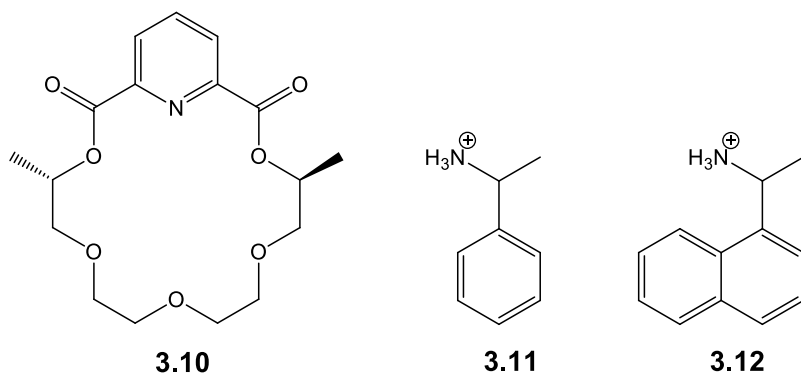


Figure 3. 6 Chiral crown ether and ammonium guest ions studied by Sawada with the reference method

⁵⁰ G. Pöcsfalvi, M. Lipták, P. Huszthy, J. S. Bradshaw, R. M. Izatt, K. Vékey, *Anal. Chem.* **1996**, *68*, 792–795.

⁵¹ a) M. Sawada, M. Shizuma, Y. Takai, H. Yamada, T. Kaneda, T. Hanafusa, *J. Am. Chem. Soc.* **1992**, *114*, 4405–4406; b) M. Sawada, Y. Okumura, M. Shizuma, Y. Takai, Y. Hidaka, H. Yamada, T. Tanaka, T. Kaneda, K. Hirose, S. Misumi, S. Takahashi, *J. Am. Chem. Soc.* **1993**, *115*, 7381–7388; c) M. Sawada, Y. Okumura, H. Yamada, Y. Takai, S. Takahashi, T. Kaneda, K. Hirose, S. Misumi, *Org. Mass. Spectrom.* **1993**, *28*, 1525–1528.

Also in this case a stereo-preference was observed and was possible to enhance the crown's enantiodiscrimination ability upon replacement of the two methyl groups with two phenyl substituents.

3.3 AIMS

In the previous chapter we have showed that the calix[6]arene macrocycle was able to thread branched dialkylammonium cations. On these basis and considering the importance of the chiral recognition, another aim of this PhD project has been the study of the chiral recognition abilities of calix[6]arene macrocycles toward chiral dialkylammonium guests.

Therefore the goal was to explore the changes in the chiroptical properties of the single components calix-wheel/dialkylammonium axle of the calixarene-based pseudorotaxane after the threading process and finally to investigate the possibility to obtain a chiral recognition between chiral hosts and guests.

3.4 RESULTS AND DISCUSSIONS

In the first instance we decided to study what happens to the chiroptical properties of the achiral calixarene host **3.13** after threading with a chiral enantiopure dibenzylammonium guest **3.14⁺·TFPB⁻**.

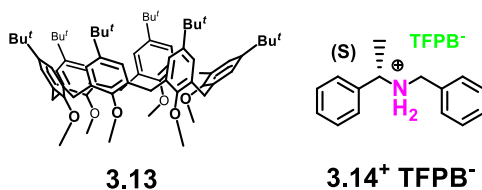


Figure 3.7 Host and guest studied in complexation experiments

The complexation experiment was conducted mixing the calixarene **3.13** and 1 equivalent of **3.14⁺·TFPB⁻** in CDCl₃ and the mixture analysed by ¹H NMR.

The first surprising results was the formation of the pseudorotaxane *endo*-alkyl-**3.15⁺·TFPB⁻** in **Figure 3.8** in which the α-methylbenzyl moiety was inside the calixarene cavity.

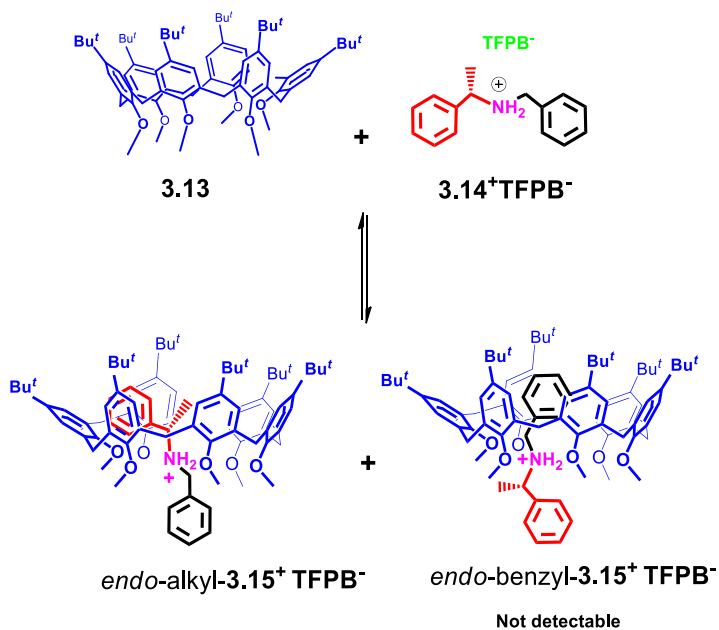


Figure 3.8. Complexation experiments between the derivative **3.13** and the derivative **3.14⁺·TFPB⁻**.

Indeed the signal at -0.9 ppm was related to the methyl group of the guest **3.14⁺·TFPB⁻** shielded inside the calixarene cavity.

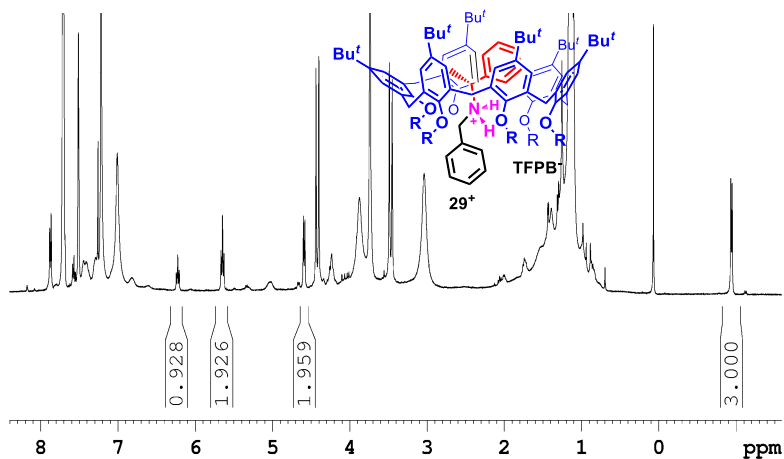


Figure 3. 9 Significant portion of the ^1H NMR spectra (400 MHz, 298 K CDCl_3) of 1:1 mixture of **3.13** ($3.8 \cdot 10^{-3}\text{M}$) and **3.14 $^+$ ·TFPB $^-$** ($3.8 \cdot 10^{-3}\text{M}$)

However the most important aspect in the formation of the [2]pseudorotaxane **3.15 $^+$ ·TFPB $^-$** was that mixing the chiral guest **3.14 $^+$ ·TFPB $^-$** with the achiral calixarene-host **3.13** it was observed a chirality induction and amplification from the guest to the entire complex. The ORD experiment reported below was made in collaboration with the Prof. Superchi from “Università degli Studi della Basilicata”.

As it can be seen from the graphic (**Figure 3.10**), moving from the axle to the complex there is a shift in the ORD spectra that indicates an induced optical rotary dispersion demonstrating an induced and amplification of chirality in the complex formation.

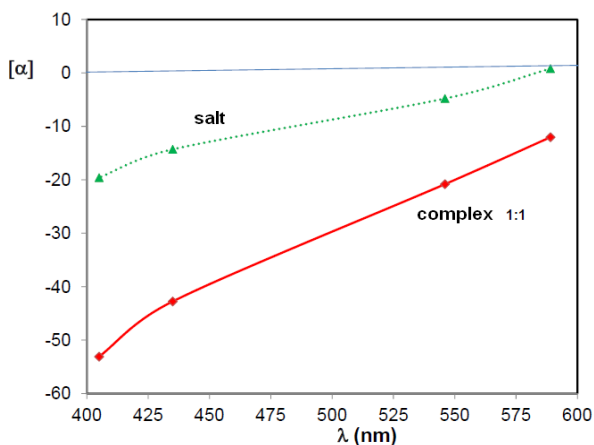


Figure 3.10 ORD spectra (CHCl_3 , 298 K) of $3.14^+\cdot\text{TFPB}^-$ (3.6 mg/mL) (\blacktriangle) and $3.15^+\cdot\text{TFPB}^-$ (3.6 mg/mL) (\blacktriangle).

3.4.1 Synthesis of chiral hosts and guest

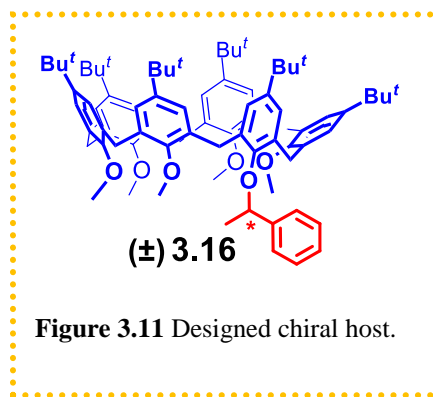


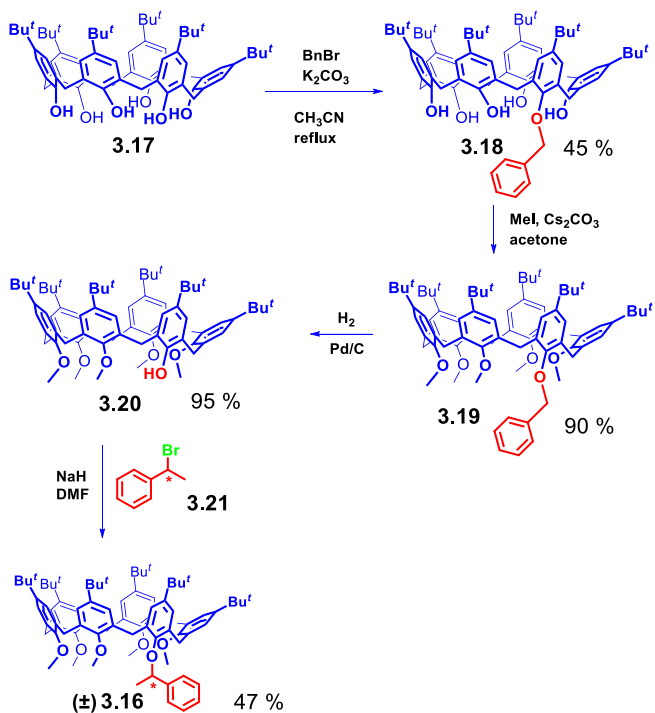
Figure 3.11 Designed chiral host.

Once having experimented a change in the chiroptical properties of the complex the study moved towards more complex chiral systems.

At this point the *through the annulus* threading was

explored using the chiral host (\pm)-**3.16** showed in **Figure 3.11** and different guests.

The synthesis of the chiral calixarene (\pm)-**3.16** was outlined in the **Scheme 3.1**.



Scheme 3.1 Synthesis of derivative **28**

p-tert-butyl-calix[6]arene **3.17** was monobenzylated with benzyl bromide in the presence of potassium carbonate as base in dry CH₃CN at reflux to give mono-benzyl ether **3.18** (45%) after usual work-up. Compound **3.18** was exhaustively methylated by treatment with MeI in acetone in presence of Cs₂CO₃.

The removal of the benzyl groups was easily accomplished by hydrogenolysis to give pentamethoxy-calix[6]arene-mono-ol

3.20 in 95% yield.

The ^1H NMR spectrum (400 MHz, CDCl_3 , 298 K) of **3.20** showed three sharp singlets due to ArCH_2Ar groups indicating a fast conformational interconversion, which is due to the small dimension of the methoxy groups at the lower rim of the macrocycle.

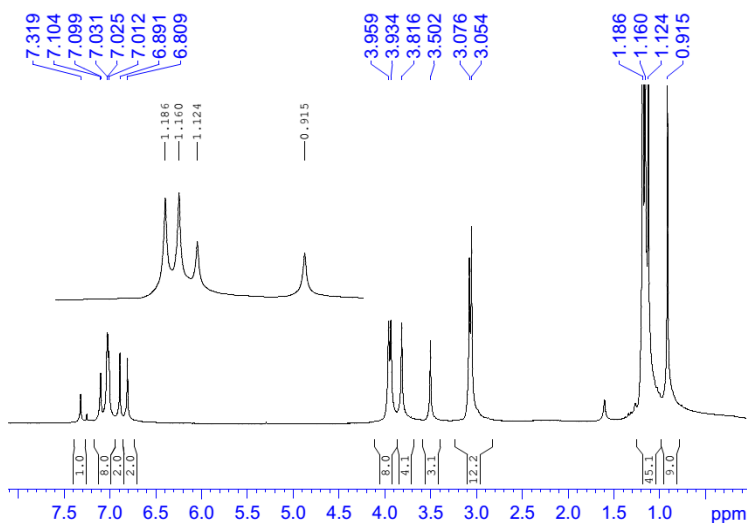


Figure 3. 12 ^1H NMR spectrum (400 MHz, CDCl_3 , 298 K) of the derivative **3.20**

Finally, the treatment of **3.20** with α -methylbenzylbromide in dry DMF and NaH as base, gave the racemic compound **3.16**.

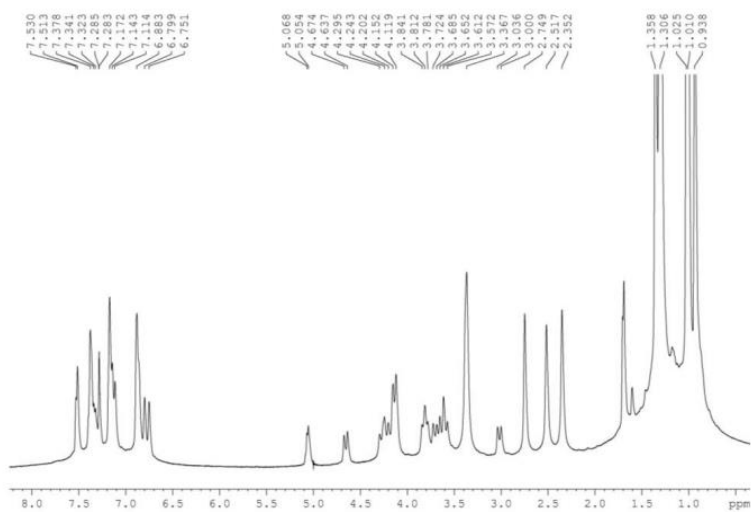


Figure 3. ^1H NMR spectrum (400 MHz, CDCl_3 , 298 K) of (\pm)-**3.16**.

ESI(+)-MS spectrum confirmed the molecular formula of (\pm)-**3.16**, in addition ^1H and ^{13}C NMR spectra confirmed the structure (**Figure 3.13**) in fact, two signals were presents at 5.05 and 1.73 ppm related, respectively to the benzylic CH and methyl CH_3 both from the chiral substituent.

The aromatic region showed a complex signal pattern (6.75-7.53) related to the benzylic protons of both calixarene scaffold and substituent. Again there were 6 AX systems due to ArCH_2Ar groups belonging to the calixarene scaffold at 4.64 and 3.63ppm ($J = 13.4$ Hz), 4.27 and 3.69 ppm ($J = 14.0$ Hz), 4.25 and 3.59 ppm ($J = 14.0$ Hz), 4.16 and 3.00 ppm ($J = 13.4$ Hz), 4.12 and 3.84 ppm ($J = 13.9$ Hz); 4.12 and 3.77 ppm ($J = 13.9$ Hz).

The compound (\pm)**3.16** was studied in complexation experiments with the chiral guest **3.14⁺·TFPB⁻**.

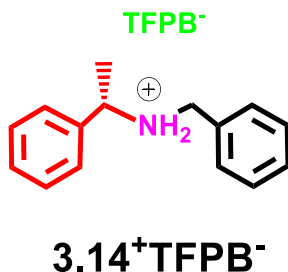


Figure 3.14. Chiral derivative **3.14⁺·TFPB⁻**.

In this case the formation of [2]pseudorotaxane could lead at four different stereoisomers.

The dibenzylammonium cation **3.14⁺·TFPB⁻** was constitutionally asymmetric so two stereoadducts were possible with the stereogenic center into the calixarene cavity for both calixarene enantiomers (being the calixarene in racemic form) and other two having the stereogenic center outside the cavity for the two calixarene enantiomers as well.

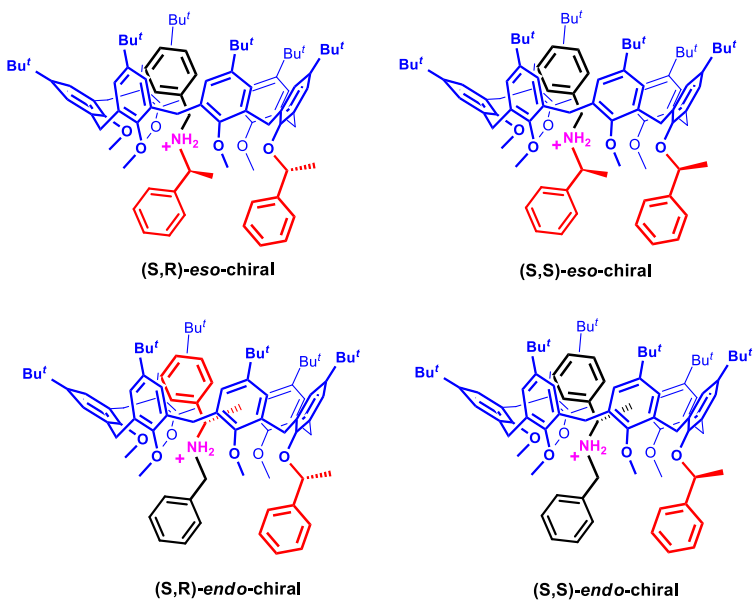
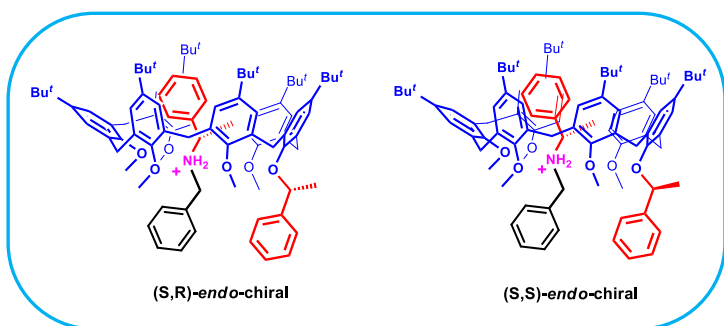


Figure 3.15 Stereoisomeric [2]pseudorotaxane obtainable.

The ^1H NMR spectrum of the complexation experiment showed the formation of the only “*endo-chiral*” stereoisomers.



Indeed there was the signal, at negative chemical shift, related to the methyl group of the α -methylbenzyl moiety into the calixarene cavity and shielded by the aromatic wall.

In addition in the range 4.8 - 6.5 ppm there was the classic pattern, already seen before, related to the benzylic hydrogens shielded by the calixarene cavity.

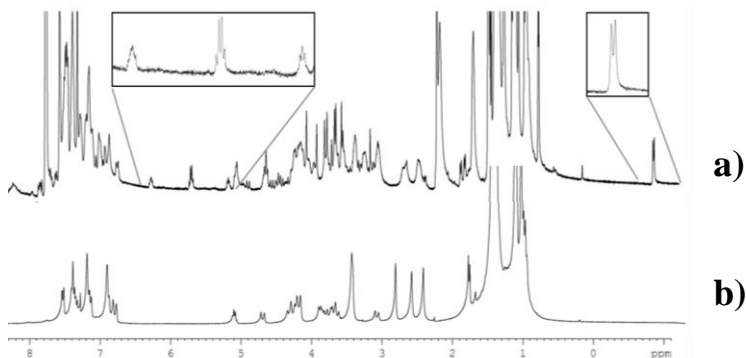
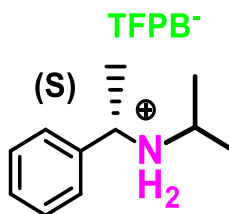


Figure 3. 16 Significant portion of the ^1H NMR spectra (400 MHz, 298 K CDCl_3) of **a)** 1:1 mixture of **3.16** ($3.8 \cdot 10^{-3}\text{M}$) and **3.14 $^+$ ·TFPB $^-$** ($3.8 \cdot 10^{-3}\text{M}$); **b)** **3.16** ($3.8 \cdot 10^{-3}\text{M}$).

Furthermore, focussing the attention on the methoxy and *terz*-butyl ^1H NMR region, a qualitative valuation about the number and the intensity of these signals, suggested that the two diastereoisomers were formed in equal ratio.

This meant that no enantiodiscrimination was observed in the formation of the [2]pseudorotaxane probably because the two chiral centres were too distant, in the space, to act as a discriminating agent.

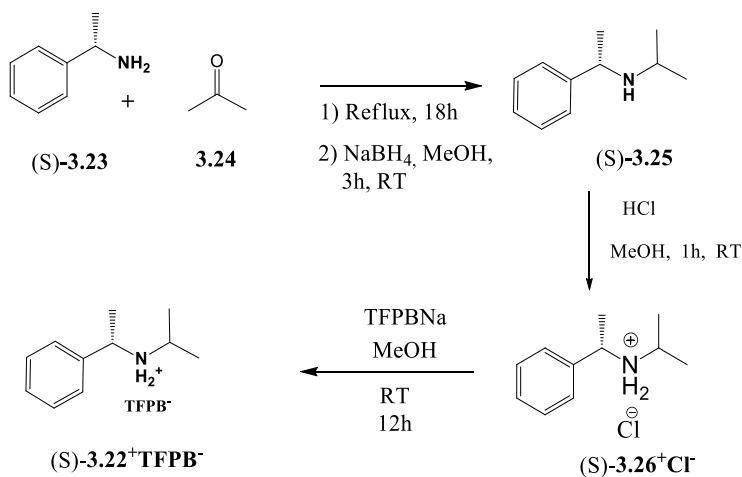


(S)-3.22⁺·TFPB⁻

Figure 3.17 Chiral derivative **3.22⁺·TFPB⁻**

With the intent to observe a discrimination effect in the formation of [2]pseudorotaxane it was designed a new derivative that would have brought the two chiral centres closer to each other after the threading. This was possible, again, assuming the validity of the *endo*-alkyl rule for the new axle **3.22⁺·TFPB⁻** reported.

The proposed guest was synthesised from α -methylbenzylamine and acetone at reflux for 18 h and reduced with NaBH₄. HCl (37%) was then used to obtain the chloride that was exchange with NaTFPB (**Scheme 3.2**).



Scheme 3.2 Synthesis of the chiral axle **3.22⁺·TFPB⁻**.

The threading between **3.22⁺·TFPB⁻** and the derivative (\pm)**3.16** could lead at four different stereoisomers as in the previous case: two stereoadducts (**R,R** and **R,S**) with the isopropyl moiety into the calixarene cavity and other two with the benzyl moiety into the cavity for the two calixarene enantiomers, **R** and **S** as well.

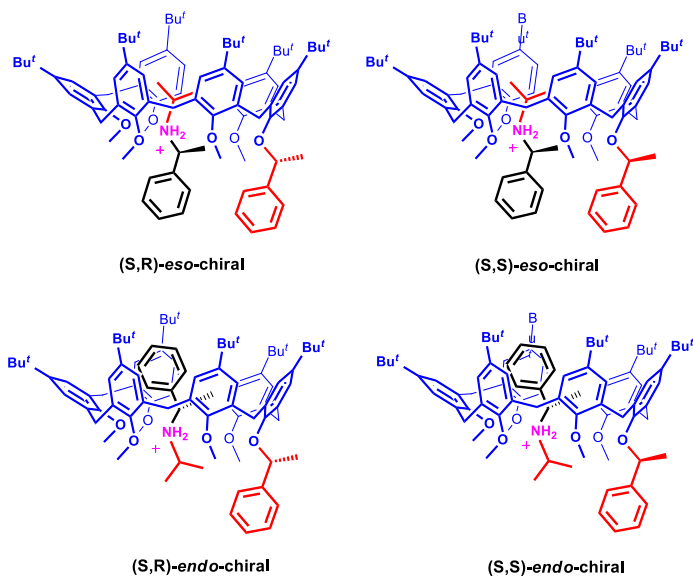


Figure 3. 18 Stereoisomeric [2]pseudorotaxane obtainable.

The ^1H NMR spectrum of the complexation experiment showed the characteristic isopropyl signal at negative chemical shift and the absence of the classic pattern related to the benzylic hydrogen shielded by the cavity. Therefore it was possible to claim that, the only stereoisomers formed were the ones with the isopropyl group into the calixarene cavity.

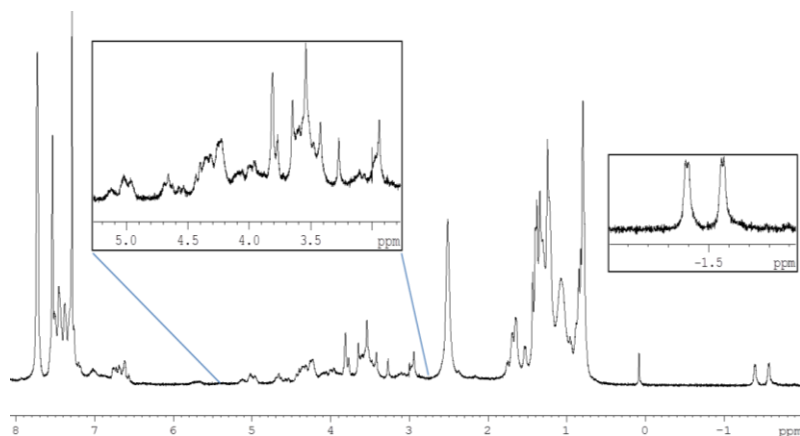


Figure 3.19 Significant portion of the ^1H NMR spectra (400 MHz, 298 K CDCl_3) of a 1:1 mixture of **3.16** ($3.8 \cdot 10^{-3}\text{M}$) and $(S)\text{-3.22}^+\cdot\text{TFPB}^-$ ($3.8 \cdot 10^{-3}\text{M}$).

The two stereo-adducts had the two chiral centres closer to each other this time but looking at the methoxy group region it was difficult to establish if there was enantiodiscrimination or not. The only 1D and 2D NMR techniques were not sufficient to discriminate and fully understand the complexation process.

For this reason it was decided to explore the enantiomeric discrimination in the calixarene threading by mass spectroscopy through the "**enantiomer labelled guest method (EL)**".

3.4.2 Gas-phase study

In this study it was applied the "**enantiomer labelled guest method (EL)**" as described in the introduction section.

An enantiopure host is mixed with an excess of a racemic mixture of the guest.

One of the enantiomeric guests is isotopically labelled, and the other is not so the signals for the two diastereomeric host-guest pairs appear at different m/z ratios.

3.4.3 Synthesis of enantiopure hosts

As well know, a good and easy way to obtain chiral calixarenes in enantiopure form is the functionalization of the calixarene lower rim with a chiral substituent.

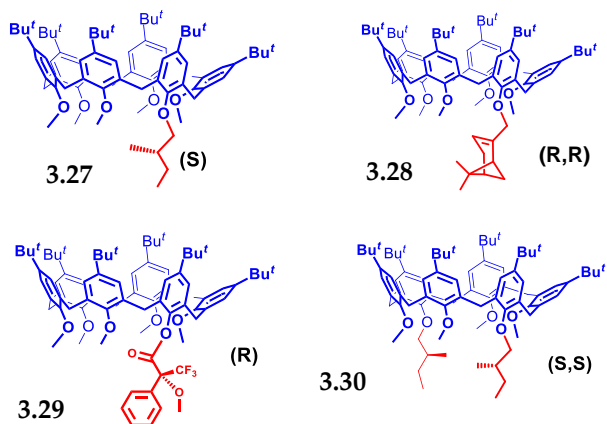
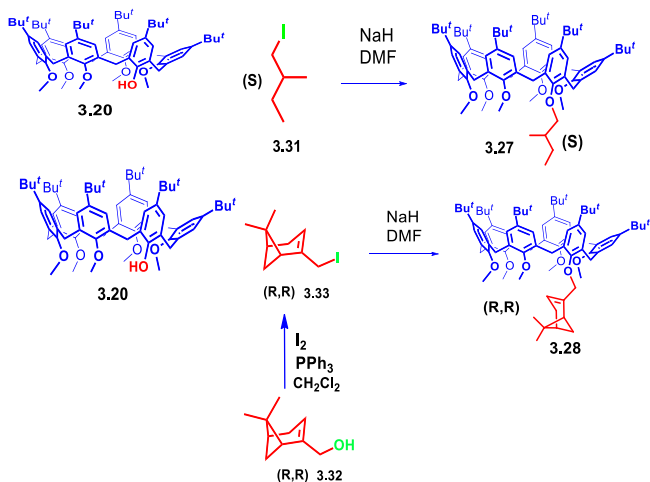


Figure 3.20 Chiral hosts synthesised

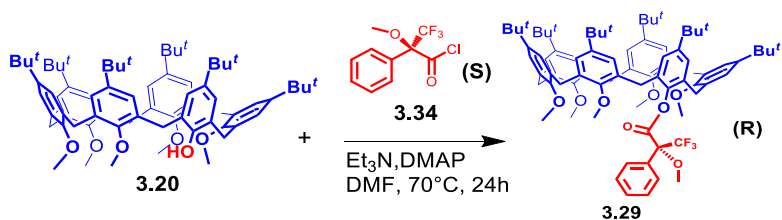
The hosts **3.27**, **3.28** and **3.29** in the **Figure 3.18** are mono-functionalised and were obtained by the functionalization of the derivative pentamethoxy-calix[6]arene-mono-ol **3.20**, in

particular, the synthesis of chiral derivatives **3.27** and **3.28** were outlined in **Scheme 3.3**.



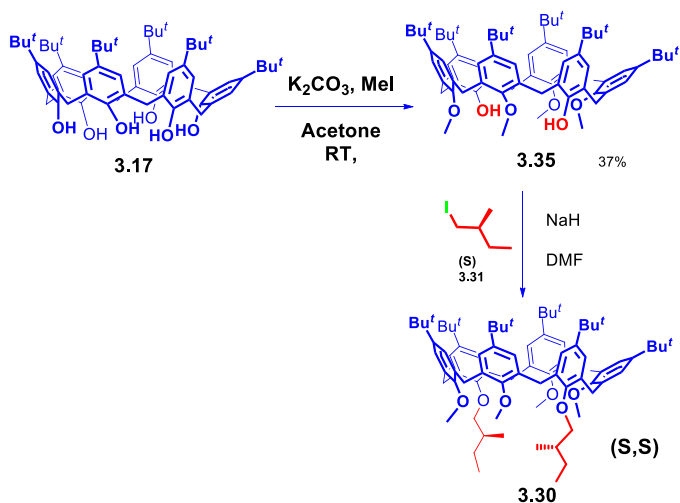
Scheme 3.3 Synthesis of derivatives **3.27** and **3.28**.

Compound **3.29** was obtained after the esterification of the hydroxyl group of the derivative **3.20** with **3.34**.



Scheme 3.4 Synthesis of derivative **3.29**

The fourth compound was obtained exploiting the reaction sequence shown in the **Scheme 3.5**.



Scheme 3.5 Synthesis of derivative **3.30**

The *p*-terz-butyl-calix[6]arene was mixed with K_2CO_3 as base and MeI in dry acetone in autoclave. Compound **3.35** was obtained after purification by recrystallization.

Compound **3.30** was obtained through a $\text{S}_{\text{N}}2$ reaction in which the derivative **3.35** was deprotonated with NaH and (*S*)-1-iodo-2-methylbutane was added in DMF.

The four compounds were fully characterized by the use of NMR and MS spectroscopy that was particularly helpful to assume the obtaining of the desired products.

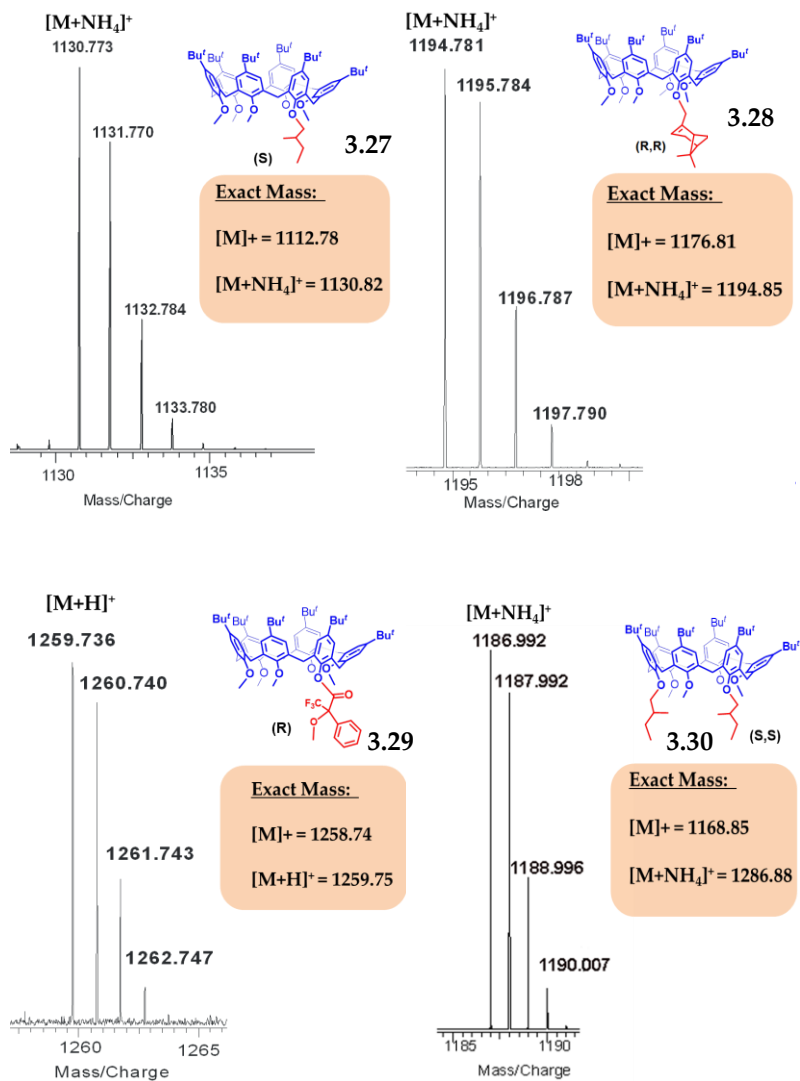


Figure 3.21 Mass spectra of compounds **3.27**, **3.28**, **3.29** and **3.30**.

3.4.4 Synthesis of labelled enantiopure guest

As already mentioned before the **EL** method requires an

isotopically labelled enantiomer of the selected guest.

On the basis of the results obtained by threading studies with the chiral ammonium cation (S)-**3.22**⁺·TFPB⁻ (see **Figure 3.16** at pag. 94) it was synthesized the labelled enantiomer (R)-**3.22-d**₆⁺·TFPB⁻

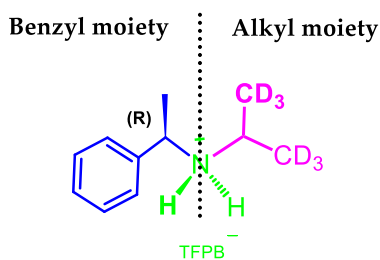
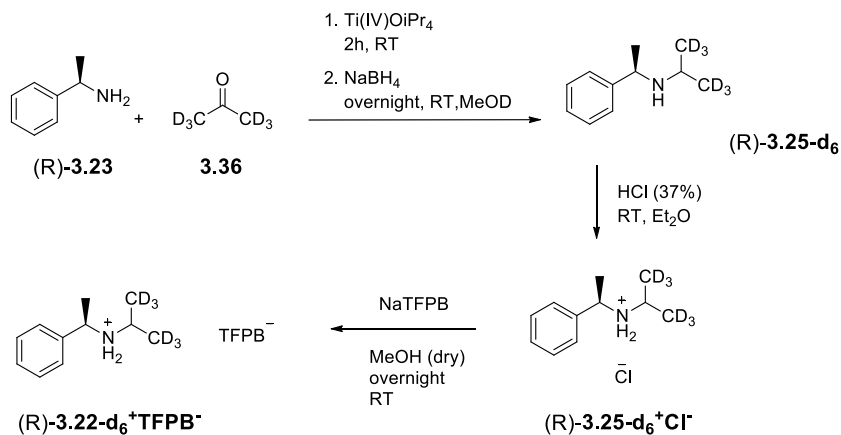


Figure 3. 22 Deuteration strategy explored for the synthesis of (R)-**3.22-d**₆⁺·TFPB⁻.

The synthesis of (R)-**3.22-d**₆⁺·TFPB⁻ was outlined in **Scheme 3.6**. The amine-acetone coupling was made by using Ti(IV)O*i*Pr₄ as catalyst. The acidification with HCl (37%) gave the ammonium chloride and the usual salt exchange gave the axle required



Scheme 3.6 Synthesis of deuterated axle **(R)-3.22-d₆⁺·TFPB⁻**.

The guest **(R)-3.22-d₆⁺·TFPB⁻** was characterized by NMR and mass spectrometry. Due to the inevitable H/D exchange in the first reaction step the resulting axle was not fully deuterated but a mixture of partially deuterated compounds (d_4 , d_5 and d_6). This was evident in the ^1H NMR (**Figure 3.23**) by the presence of the low signal at 1.3 ppm and from the MS spectra (**Figure 3.22**).

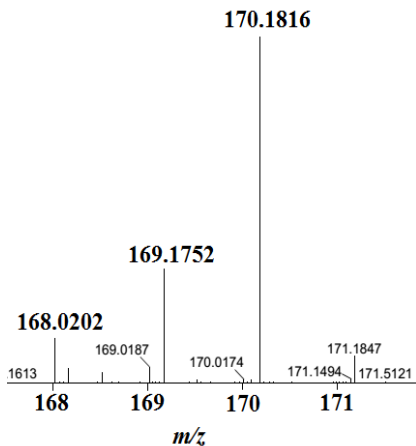


Figure 3.23 mass spectrum of derivative (R)-3.22- d_6^+ ·TFPB $^-$.

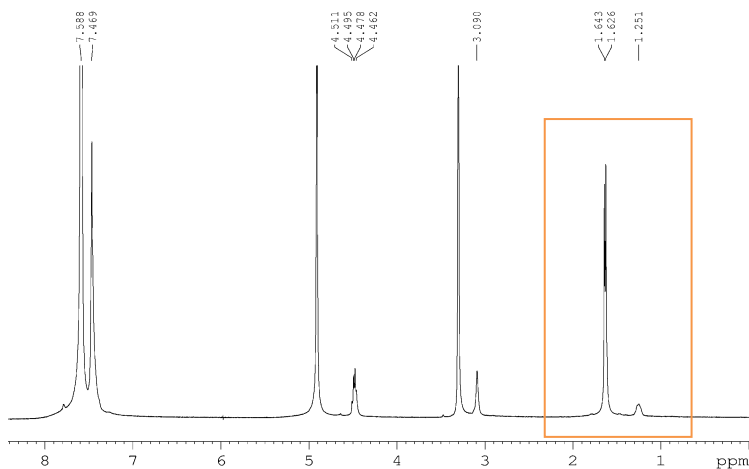


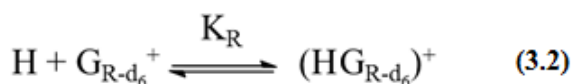
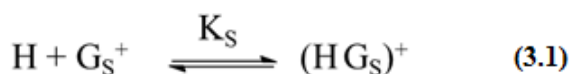
Figure 3. 24 Significant portions of the; 1H NMR spectrum (CH_3OH , 400 MHz, 298 K) of derivative (R)-3.22- d_6^+ ·TFPB $^-$.

3.4.5 MS experiments

A fundamental feature of this method is the use of an isotopically labelled enantiomer of a selected guest to

distinguish two diastereomeric host-guest complexes in a mass spectrum. A 1/1 mixture of labelled and unlabelled guest enantiomers was mixed with 0.5 equivalent of the target chiral host.

It was considered the competitive equilibrium system through eqs. **3.1** and **3.2**



Therefore, the peak intensity ratio, $I[(\text{HG}_S)^+]/I[(\text{HG}_{R-d_6})^+]$, of the diastereomeric host-guest complex ions, was expected to become a measure of the enantio-discrimination ability of the host toward the two enantiomers of the chiral guest.

- If $I_S/I_{R-d_6} > 1$ means that a given chiral host binds more strongly the (S)-enantiomer. The larger the I_S/I_{R-d_6} ratio value and higher the degree of chiral recognition of the host.
- $I_S/I_{R-d_6} < 1$ means that a given chiral host binds more strongly the R-labelled guest.

- $I_S/I_{R-d_6} = 1.0 \pm 0.1$ means that a given chiral host cannot differentiate the chirality of a given guest.

3.4.6 Concentration Effect

The concentration solution can affect the ionization process and therefore the intensity ratio $I[(H + G_S)^+]/I[(H + G_{R-d_6})^+]$.

Therefore the first step was to choose the best concentration value to use.

It was seen that the peak intensities were quite low up to a 300 μM solution and the intensity ratio did not change increasing the concentration over 300 μM . Therefore 300 μM solutions were used in determining isotopic and chiral recognition effects.

3.4.7 Isotopic Effects

In order to determine certain effects of deuterium labelling on the mass spectral intensities of the corresponding host-guest complex ions, it was used here a 1:1 mixture of a pair of labelled (R)-and unlabelled (R)-enantiomer guests and we evaluated the $[I_R/I_{R-d_6}]$ values with the corresponding host.

The unlabelled (R)-enantiomer, (R)-**3.22⁺·TFPB⁻** was

synthesised using the same procedure used for the synthesis of (S)-**3.22**⁺·TFPB⁻ described before in **Figure 3.16** and **Scheme 3.2**.

The resulting MS spectra for the investigation of the isotopic effect are reported below.

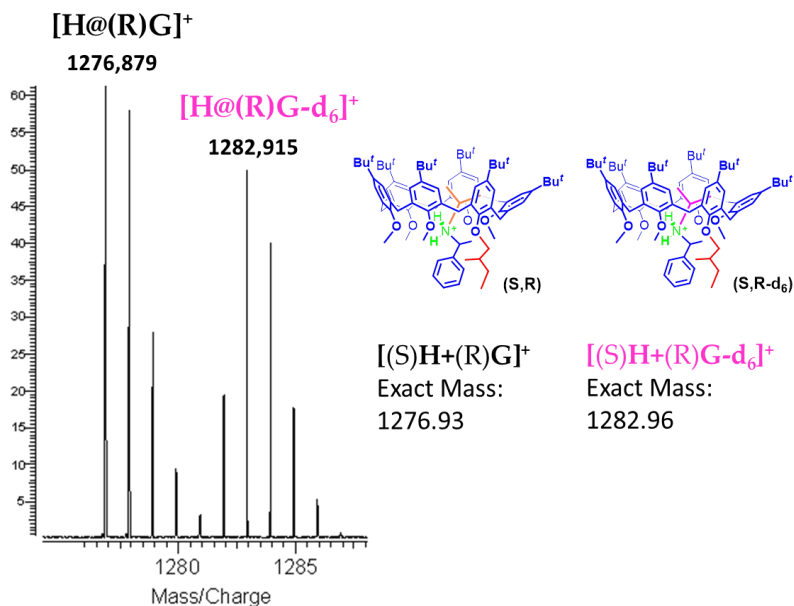


Figure 3. 25 Significant portion of the mass spectrum of a 1:2:2 mixture (CH₂Cl₂, 300 μM) of the derivatives **3.27**, (R)-**3.22**⁺·TFPB⁻ and (R)-**3.22-d**₆⁺·TFPB⁻ respectively (sample cone 25V, HV 2500 V).

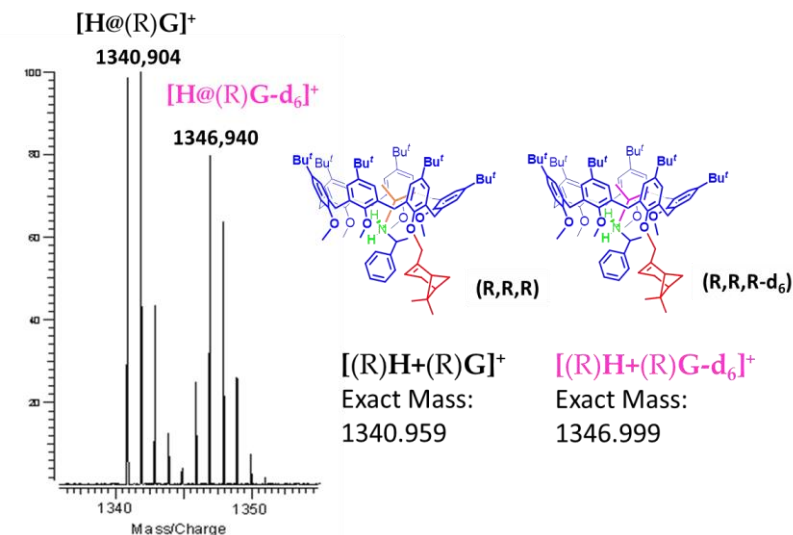


Figure 3. 26 Significant portion of the mass spectrum of a 1:2:2 mixture (CH_2Cl_2 , 300 μM) of the derivatives **3.28**, (R)-**3.22**⁺·**TFPB**⁻ and (R)-**3.22-d**₆⁺·**TFPB**⁻ respectively (sample cone 25V, HV 2500 V).

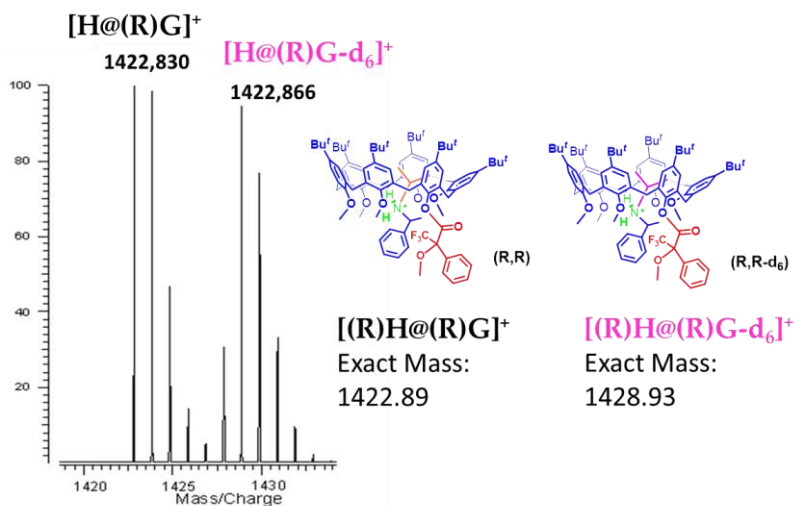


Figure 3. 27 Significant portion of the mass spectrum of a 1:2:2 mixture (CH_2Cl_2 , 300 μM) of the derivatives **3.29**, (R)-**3.22**⁺·**TFPB**⁻ and (R)-**3.22-d**₆⁺·**TFPB**⁻ respectively (sample cone 25V, HV 2500 V).

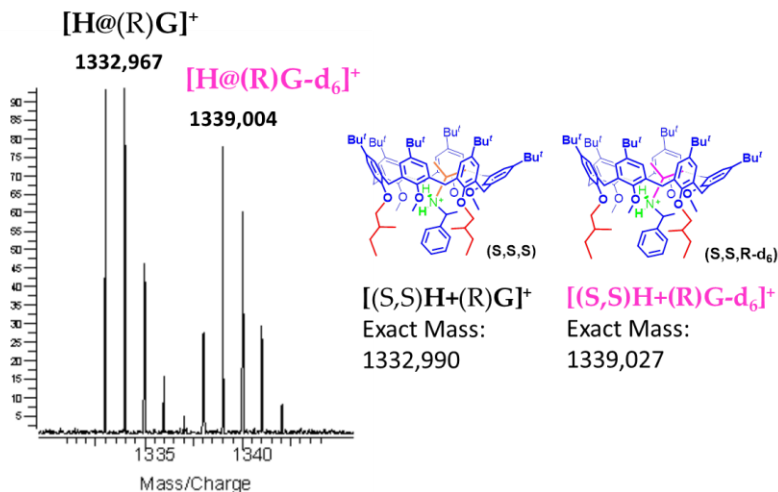


Figure 3. 28 Significant portion of the mass spectrum of a 1:2:2 mixture (CH_2Cl_2 , 300 μM) of the derivatives **3.30**, (R)-**3.22**⁺·TFPB⁻ and (R)-**3.22-d₆**⁺·TFPB⁻ respectively (sample cone 25V, HV 2500 V).

The $[\text{I}_\text{R}/\text{I}_{\text{R}-\text{d}_6}]$ values for the guest **3.30** was close to the unit indicating that no isotopic effect was observed, however the MS spectra for the compound **3.27**, **3.28** and **3.29** showed a slight isotopic effect (see experimental section for the exact values and the calculation procedures).

Accordingly to the literature, the directionality of isotope effects is difficult to predict from system to system.

The literature supports observation of deuterium IEs from both solution and gas phase.⁵²

Therefore, the observed effects in our system might be due to a decreased van der Waals interactions between the guest's

⁵² K. A. Schug, N. M. Maier, W. Lindner, *J. Mass Spectrom.* **2006**, *41*, 157–161.

deuterated moiety and the host; or a preferential ionization of one diastereomeric complex over the other one; or a different gas-phase behaviour between the deuterated and non-deuterated guests.

3.4.8 Chiral Recognition

In order to determine a chiral recognition effect of a 1:1 mixture of a pair of labelled (R)-enantiomer, (R)-**3.22-d₆⁺·TFPB⁻** and unlabelled (S)-enantiomer guest (S)-**3.22⁺·TFPB⁻** was used with 0.5 equivalent of the corresponding host and the I_S/I_{R-d_6} ratio value was measured by inspection of the mass spectrum.

The resulting MS spectra for the investigation of the isotopic effect are reported below.

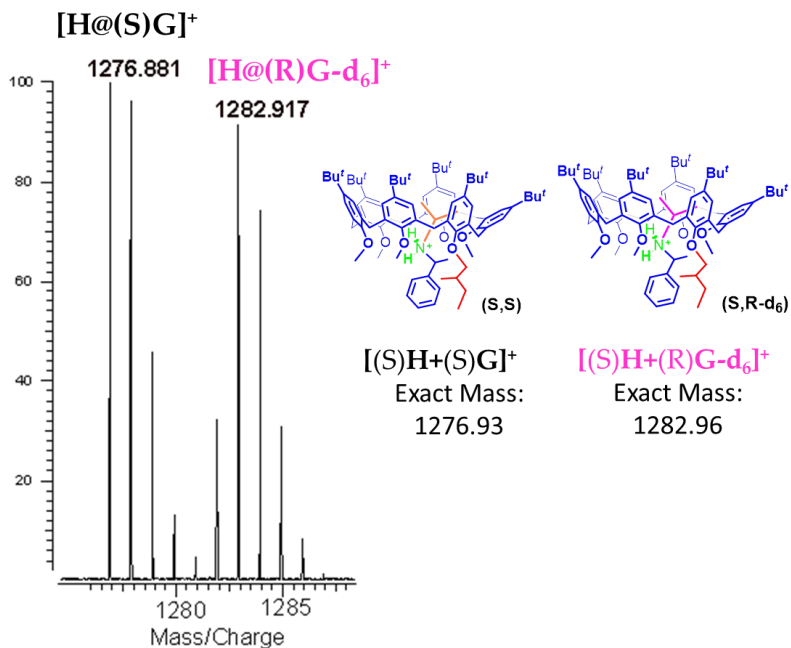


Figure 3.29 Significant portion of the mass spectrum of a 1:2:2 mixture (CH₂Cl₂, 300 μM) of the derivatives **3.27**, (S)-**3.22**⁺·TFPB⁻ and (R)-**3.22**-d₆⁺·TFPB⁻ respectively (sample cone 25V, HV 2500 V).

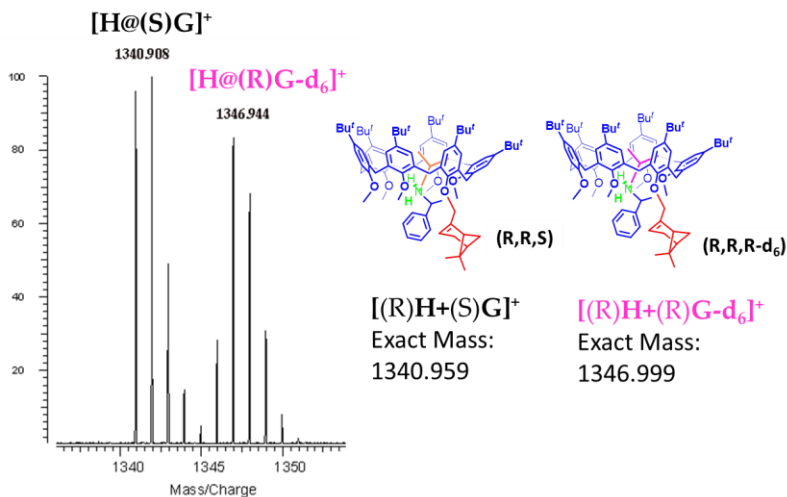


Figure 3.30 Significant portion of the mass spectrum of a 1:2:2 mixture

(CH₂Cl₂, 300 μM) of the derivatives **3.28**, (S)-**3.22**⁺·TFPB⁻ and (R)-**3.22**-d₆⁺·TFPB⁻ respectively (sample cone 25V, HV 2500 V).

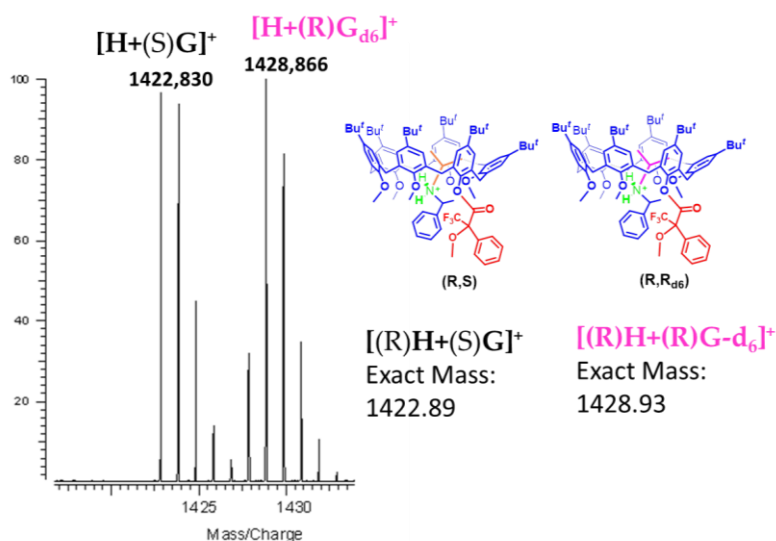


Figure 3. 31 Significant portion of the mass spectrum of a 1:2:2 mixture (CH₂Cl₂, 300 μM) of the derivatives **3.29**, (S)-**3.22**⁺·TFPB⁻ and (R)-**3.22**-d₆⁺·TFPB⁻ respectively (sample cone 25V, HV 2500 V).

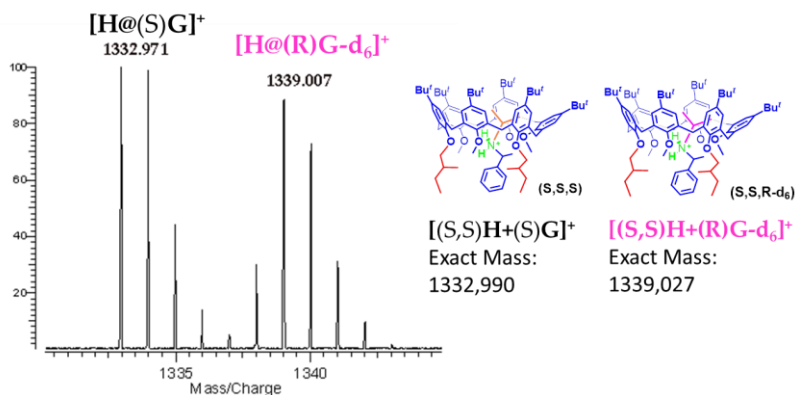


Figure 3. 32 Significant portion of the mass spectrum of a 1:2:2 mixture (CH₂Cl₂, 300 μM) of the derivatives **3.30**, (S)-**3.22**⁺·TFPB⁻ and (R)-**3.22**-d₆⁺·TFPB⁻ respectively (sample cone 25V, HV 2500 V).

For the hosts **3.30** the I_S/I_{R-d_6} was, again close to the unit so no enantiodiscrimination was observed.

For the hosts **3.27**, **3.28** and **3.29** the I_S/I_{R-d_3} were slightly different from the unit however their values were identical to those regarding the isotopic effect and therefore there was not a chiral enantiodiscrimination recognition with the hosts studied (see experimental section for the exact values and the calculation procedures).

3.5 CONCLUSION

In this chapter it was studied the calixarene threading with chiral systems. In particular it was demonstrated that in the formation of a [2]pseudorotaxane, starting from a chiral axle and an achiral calix, there was a chiral induction and transfer from the axle to the pseudorotaxane.

Soon later, the attention moved toward the possibility to obtain chiral recognition during the calixarene threading and the formation of the [2]pseudorotaxane.

In the first instance the NMR spectroscopy was selected as the technique for exploring the enantiodiscrimination formation of the [2]pseudorotaxanes. However the complexity and the difficulty to interpret the results obtained, suggested investigating the enantiodiscrimination process differently.

For this reason it was decided to explore the enantiomeric discrimination in the calixarene threading.

The enantiodiscrimination process was then studied in gas-phase by means of the MS spectrometry.

This required the synthesis of some enantiopure hosts and a pair of guests in which one of them was deuterated. Unfortunately the study did not provide the awaited results for the hosts objected of the study but it provided another way to study processes that occur in the calixarene threading.

3.6 EXPERIMENTAL SECTION

Absorption and ORD spectra were recorded on a JASCO J600 spectropolarimeter at room temperature, in acetonitrile, using 0.1 mm cells and concentrations of about 1×10^{-3} M. During the measurement, the instrument was thoroughly purged with nitrogen.

Mass spectra were recorded with a Finnigan Mat 711 (EI, 80 eV, 8 kV), an Agilent 6210 ESI-TOF, and an Agilent QFT-7 FTICR mass spectrometer with Micromass Z-Spray ESI source. Flash chromatography was performed on Merck silica gel (60, 40-63 μm). All chemicals were reagent grade and were used without further purification. Anhydrous solvents were purchased from Aldrich. When necessary compounds were dried in vacuo over CaCl_2 . Reaction temperatures were measured externally. Reactions were monitored by TLC on Merck silica gel plates (0.25 mm) and visualized by UV light, or by spraying with $\text{H}_2\text{SO}_4\text{-Ce}(\text{SO}_4)_2$ or phosphomolybdic acid.

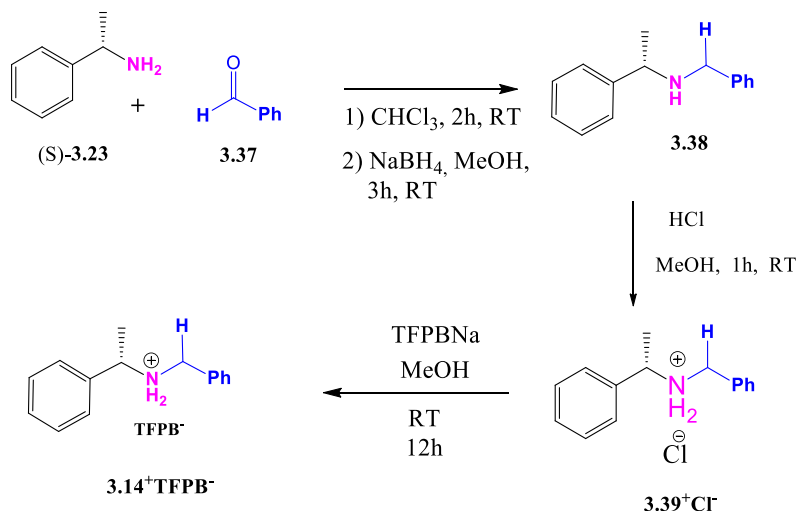
¹D NMR spectra were recorded on a Bruker Avance-400 spectrometer [400 (1H) and 100 MHz (13C)], Bruker Avance-300 spectrometer [300 (1H) and 75 MHz (13C)] and Bruker Avance-250 spectrometer [250 (1H) and 63 MHz (13C)]; chemical shifts are reported relative to the residual solvent peak (CHCl_3 : δ 7.26, CDCl_3 : δ 77.23; CD_3OH : δ 3.31,

CD₃OD: δ 49.0). Derivatives **3.17**, **3.18**, **3.19** and **3.35** were synthesized according to literature procedures.⁵³⁻⁵⁴

⁵³) R. G. Janssen, W. Verboom, D. N. Reinhoudt, A. Casnati, M. Freriks, A. Pochini, F. Ugozzoli, R. Ungaro, P. M. Nieto, M. Carramolino, F. Cuevas, P. Prados, J. de Mendoza, *Synthesis* **1993**, *4*, 380-386.

⁵⁴ J. de Mendoza, M. Carramolino, F. Cuevas, P. Manule Nieto, D. N. Reinhoudt, W. Verboom, R. Ungaro, A. Casnati, *Synthesis* **1994**, *1*, 47-50.

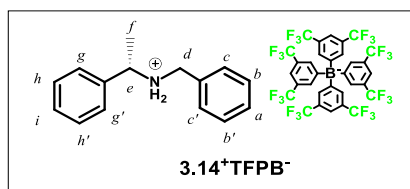
Synthesis of derivative **35⁺**



(S)- α -Methylbenzylamine (0.010 mol) was added to benzaldehyde in CHCl_3 dry (2 mL) and the reaction mixture was stirred at room temperature for 2 h to give the imine intermediate in a quantitative yield.

The resulting imine (0.010 mol) was dissolved in dry MeOH (20 mL) under a nitrogen atmosphere and NaBH_4 (0.10 mol) was added at 0 °C and then the mixture was allowed to warm at room temperature. The solution was kept under stirring for 3 h. The solvent was removed under reduced pressure and the residue partitioned between AcOEt (30 mL) and an aqueous saturated solution of NaHCO_3 (30 mL). The organic layer was dried over MgSO_4 and the solvent was removed under

reduced pressure, to give derivative **3.38** as a yellow viscous liquid. The compound was used for the next step without further purification. The crude product (0.010 mol) was dissolved in Et₂O (20 mL) at room temperature and an aqueous solution of HCl (37% w/w, 0.011 mol) was added dropwise. The mixture was kept under stirring for 1 h, until the formation of a white precipitate. The solid was collected by filtration, purified by crystallization with acetonitrile and dried under vacuum, to give derivative **3.39**⁺ as a white solid. Derivative **3.39**⁺ was dissolved in dry MeOH (C= 0.2 M), then sodium tetrakis[3,5-bis(trifluoromethyl)phenyl]borate (1.1 eq) was added and the mixture was kept under stirring overnight in the dark. The solvent was removed and deionized water was added, obtaining a brown precipitate that was filtered off and dried under vacuum to give derivatives **3.14**⁺**TFPB**⁻.



Derivative 3.14⁺**TFPB**⁻: (0.090 g, 0.22 mmol, 95%). **ESI**(+) **MS**: m/z = 212.15 (M⁺). **¹H NMR** (400 MHz, CD₃OD, 298 K): δ 1.65 (d, J = 7, 3H, H_f), 3.85 and 4.05 (d, J = 13, 2H,

Hd), 4.36 (q, $J = 6$, 1H, He), 7.32-7.42 (overlapped, 6H, ArH, + 4H, ArH^{TFPB}), 7.56-7.59 (overlapped, 4H, ArH + 12 H, ArH^{TFPB}); ¹³C NMR (100 MHz, CD₃OD, 298 K) δ 18.3, 49.3, 58.3, 117.1, 120.3, 123.0, 125.7, 127.2, 128.4, 128.6, 128.9, 129.2, 129.3, 129.4, 129.5, 130.9, 134.4, 136.0, 160.8, 161.2, 161.7, 162.2.

General Procedure for the Preparation of [2]Pseudorotaxane
3.15⁺TFPB⁻

Calixarene derivative **3.13** ($1.9 \cdot 10^{-3}$ mmol) was dissolved in 0.5 mL of CDCl_3 ($3.8 \cdot 10^{-3}$ M solution). Then, the TFPB- salt **3.14⁺TFPB⁻** was added ($1.9 \cdot 10^{-3}$ mmol, $3.8 \cdot 10^{-3}$ M) and the mixture was stirred for 15 min. Then, the solution was transferred in a NMR tube for 1D NMR spectra acquisition.

^1H NMR determination of K_{ass} values.

The association constant value was calculated by integration of free and complexed ^1H NMR peaks of host and guest.

Calixarene derivative **3.13** ($1.9 \cdot 10^{-3}$ mmol) was dissolved in 0.5 mL of CDCl_3 ($3.8 \cdot 10^{-3}$ M solution). Then, the TFPB- salt **3.14⁺TFPB⁻** was added ($1.9 \cdot 10^{-3}$ mmol, $3.8 \cdot 10^{-3}$ M) and the mixture was stirred for 15 min. Then, the solution was transferred in a NMR tube for spectra acquisition.

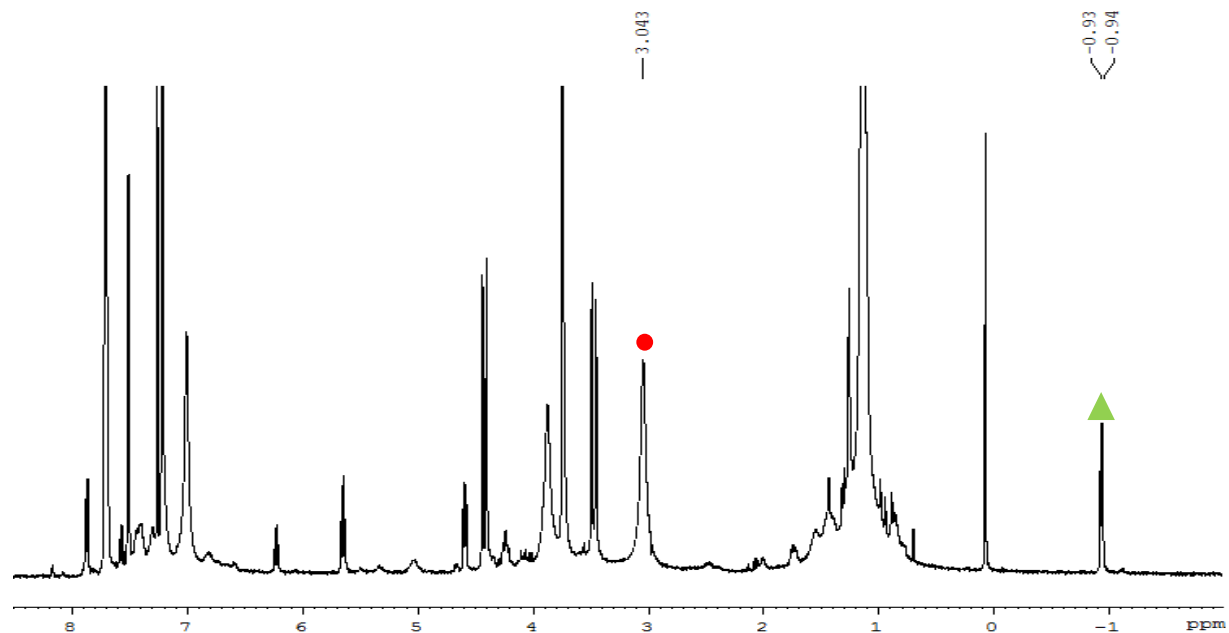


Figure 3. ^{33}H NMR spectrum (CDCl_3 , 400 MHz, 298 K) of equimolar solution ($3.9 \cdot 10^{-3}$ M) of **3.13** and $\text{3.14}^+\cdot\text{TFPB}^-$. The association constant K_{ass} value was calculated by integration of the complexed (\blacktriangle) and free derivative **3.13** (\bullet).

Procedure for ORD calculation

7.13 mg of derivative **3.14⁺TFPB⁻** were dissolved in 2mL of CHCl₃ and the ORD was measured for the guest.

Then an equimolar solution of the derivative **3.14⁺TFPB⁻** (6.96 mg) and **3.13** (6.32 mg) in 2 mL of CHCl₃ was used for the measurement of the ORD for the complex.

$$\alpha_{\text{tot}} = \alpha_{\text{comp}} + \alpha_{\text{guest}}$$

$$\alpha_{\text{comp}} = \alpha_{\text{tot}} - \alpha_{\text{guest}}$$

$$\alpha_{\text{guest}} = [\alpha]_{\text{guest}} \times C'_{\text{guest}} / 100 \quad (C' \text{ expressed in g/100mL})$$

$$\text{guest} = 6.69 \text{ mg} \quad C^{\circ}_{\text{guest}} = 3.11 \times 10^{-3} \text{ M}$$

$$\text{host} = 6.32 \text{ mg} \quad C^{\circ}_{\text{host}} = 2.99 \times 10^{-3} \text{ M}$$

From the NMR spectrum the percentage of complexation is 42% et equilibrium, then:

$$C'_{\text{comp}} = C^{\circ}_{\text{host}} \times 0.42 = 1.256 \times 10^{-3} \text{ M}$$

$$C'_{\text{guest}} = C^{\circ}_{\text{guest}} - C'_{\text{comp}} = 1.854 \times 10^{-3} \text{ M}$$

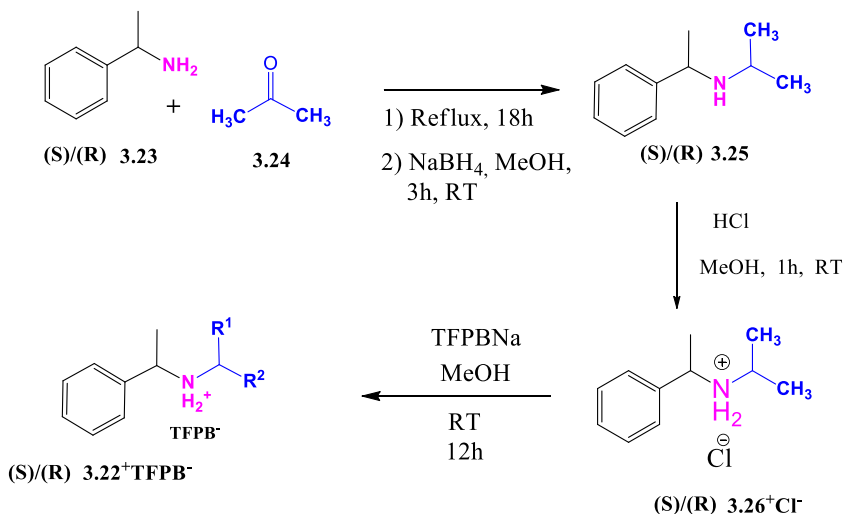
In g/100mL:

$$C'_{\text{comp}} = 1.256 \times 10^{-3} \text{ M} \times \text{MW}_{\text{comp}} / 10 = 0.268 \text{ g/100mL}$$

$$C'_{\text{guest}} = 1.854 \times 10^{-3} \text{ M} \times \text{MW}_{\text{guest}} / 10 = 0.199 \text{ g/100mL}$$

λ	α_{tot}	$[\alpha]_{\text{guest}}$	α_{guest}	α_{comp}	$[\alpha]_{\text{comp}}$
589	-0.030	0.8	0.0022	-0.0322	-2.0
546	-0.0686	-4.8	-0.0128	-0.0588	-20.8
435	-0.153	-14.3	-0.0384	-0.1146	-42.8
405	-0.195	-19.6	-0.0527	-0.1423	-53.1

Synthesis of derivatives (R)/(S)-3.22⁺TFPB⁻

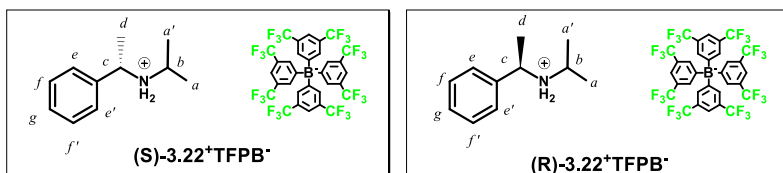


(R)/(S)- α -Methylbenzylamine (0.010 mol) was dissolved into acetone (40 mL) and the reaction mixture was stirred at reflux for 18 h. The reaction mixture was then cooled to room temperature and the excess of ketone was removed under reduced pressure.

The resulting imine (0.010 mol) was dissolved in dry MeOH (20 mL) under a nitrogen atmosphere and NaBH₄ (0.10 mol) was added at 0 °C and then the mixture was allowed to warm at room temperature. The solution was kept under stirring for 3 h. The solvent was removed under reduced pressure and the residue partitioned between AcOEt (30 mL) and an aqueous saturated solution of NaHCO₃ (30 mL). The organic layer was dried over MgSO₄ and the solvent was removed under

reduced pressure, to give derivative **(R)/(S)-3.25** as a yellow viscous liquid. The compound was used for the next step without further purification. The crude product (0.010 mol) was dissolved in Et₂O (20 mL) at room temperature and an aqueous solution of HCl (37% w/w, 0.011 mol) was added dropwise. The mixture was kept under stirring for 1 h, until the formation of a white precipitate. The solid was collected by filtration, purified by crystallization with Exane/MeOH and dried under vacuum, to give derivative **(R)/(S)-3.26⁺Cl⁻** as a white solid.

Derivative **(R)/(S)-3.26⁺Cl⁻** was dissolved in dry MeOH (C= 0.2 M), then sodium tetrakis[3,5-bis(trifluoromethyl)phenyl]borate (1.1 eq) was added and the mixture was kept under stirring overnight in the dark. The solvent was removed and deionized water was added, obtaining a brown precipitate that was filtered off and dried under vacuum to give derivatives **(R)/(S)-3.22⁺TFPB⁻**

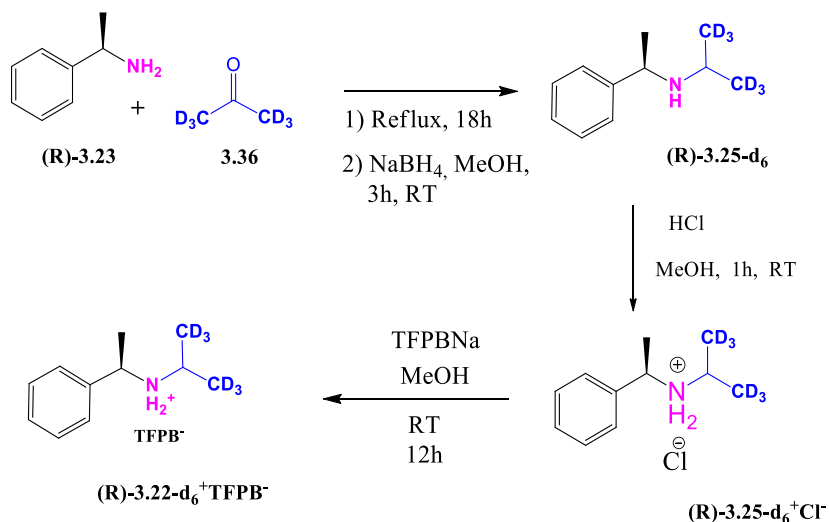


Derivative (S)-3.22⁺TFPB⁻: (0.090 g, 0.22 mmol, 95%).
ESI(+) MS: $m/z = 164.14$ (M⁺). **¹H NMR** (400 MHz, CDCl₃,

298 K): δ 1.24 and 1.29 (d, $J = 6$, 6H, $H_{a-a'}$), 1.66 (d, $J = 7$, 3H, H_d), 4.32 (m, $J = 6$, 1H, H_b), 4.41 (q, $J = 6$, 1H, H_c), 7.22 (d, $J = 7$, 2H, $H_{e-e'}$), 7.46-7.53 (overlapped 3H, $H_{f-f'-g} + 4H$, ArH^{TFPB}), 7.69 (s, 8H, ArH^{TFPB}); ^{13}C NMR (100 MHz, CD_3OD , 298 K) δ 19.1, 19.4, 20.0, 50.4, 57.8, 117.8, 120.7, 123.4, 126.1, 126.5, 128.6, 128.8, 129.0, 129.3, 129.6, 130.6, 131.4, 135.0, 161.1, 161.6, 162.1, 162.6.

Derivative (R)-3.22⁺TFPB⁻: (0.090 g, 0.22 mmol, 95%)

Synthesis of derivative (R)-3.22-d₆⁺ TFPB⁻

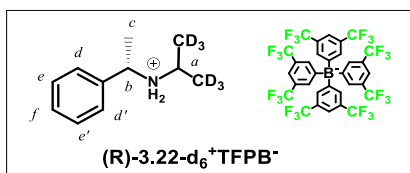


(R)- α -Methylbenzylamine (1.2g, 0.010 mol), Ti(IV)i-OPr₄ (8.5g, 0.030 mol) and deuterated acetone (0.030 mol) were mixed together and stirred for 2h.

The resulting mixture was diluted with MeOD (10 mL) under a nitrogen atmosphere and NaBH₄ (0.020 mol) was added at 0 °C and then the mixture was allowed to warm at room temperature. The solution was kept under stirring for 3 h.

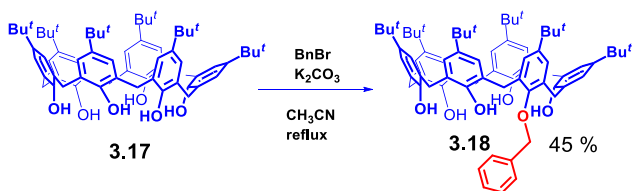
The solvent was removed under reduced pressure and the residue partitioned between AcOEt (30 mL) and an aqueous saturated solution of NaHCO₃ (30 mL). The organic layer was dried over MgSO₄ and the solvent was removed under reduced pressure, to give derivative (R)-**3.25-d₆** as a yellow viscous liquid. The compound was used for the next step without further purification. The crude product (0.010 mol) was dissolved in Et₂O (20 mL) at room temperature and an aqueous solution of HCl (37% w/w, 0.011 mol) was added dropwise. The mixture was kept under stirring for 1 h, until the formation of a white precipitate. The solid was collected by filtration, purified by crystallization with Exane/MeOH and dried under vacuum, to give derivative (R)-**3.25-d₆⁺Cl⁻** as a white solid.

Derivative (R)-**3.25-d₆⁺Cl⁻** was dissolved in dry MeOH (C= 0.2 M), then sodium tetrakis[3,5-bis(trifluoromethyl)phenyl]borate (1.1 eq) was added and the mixture was kept under stirring overnight in the dark. The solvent was removed and deionized water was added, obtaining a brown precipitate that was filtered off and dried under vacuum to give derivatives (R)-**3.22-d₆⁺TFPB⁻**.



Derivative (R)-3.22-d₆⁺TFPB⁻: (0.090 g, 0.22 mmol, 95%).
ESI(+) MS: $m/z = 170.18$ (M⁺). **¹H NMR** (400 MHz, CD₃OD, 298 K): δ 1.64 (d, $J = 7$, 3H, H_c), 3.09 (s, 1H, H_a), 4.49 (q, $J = 7$, 1H, H_b), 7.47-7.59 (overlapped, 5H, ArH, + 12H, ArH^{TFPB}). **¹³C NMR** (100 MHz, CD₃OD, 298 K) δ 19.8, 51.0, 58.5, 118.2, 121.1, 123.8, 126.5, 126.9, 129.1, 129.3, 129.4, 129.7, 130.0, 131.1, 131.9, 134.0, 135.4, 161.5, 162.0, 162.5, 163.0.

Synthesis of derivative **31**



To a suspension of 20 g (21 mmol) of *p*-tert-butylcalix[6]arene in 1.1 L of dry CH₃CN were added 2.8 g (1 eq.) di K₂CO₃.

The mixture was kept under stirring at reflux for 3h and

benzyl bromide (2.4 mL, 1eq) was added.

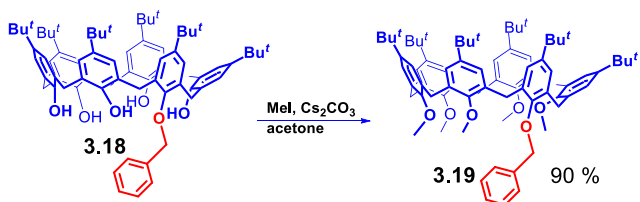
The mixture was kept under stirring at reflux for 3 h again and then the crude product was treated with NH_3 (30 %) and HCl (1 N).

The residue was extracted with CH_2Cl_2 and purified by silica gel chromatography (petroleum ether/ CH_2Cl_2). 10 g of derivative **3.18** were recovered with a yield of 45%.

ESI(+) **MS**: $m/z = 1063.70$ (MH^+). **^1H NMR** (250 MHz, CDCl_3 , 298 K): δ 10.02 (s, *OH*, 2H), 9.82 (s, *OH*, 1H), 9.12 (s, *OH*, 2H), 7.78 (m, ArH_{Bn} , 2H), 7.64 (m, ArH_{Bn} , 2H), 7.45 (m, ArH_{Bn} , 1H), 7.17-7.09 (overlapped, ArH_{calix} , 12H), 5.21 (s, $\text{CH}_2\text{Ar}_{Bn}$, 2H), 4.45 e 3.54 (AX, ArCH_2Ar , $J=13.4$ Hz, 4H), 4.27 e 3.56 (AX, ArCH_2Ar , $J=14.0$ Hz, 4H), 4.02 e 3.39 (AX, ArCH_2Ar , $J=13.9$ Hz, 4H), 1.29 -1.28 (s, $\text{C}(\text{CH}_3)_3$, 36H), 1.23 (s, $\text{C}(\text{CH}_3)_3$, 9H), 1.19 (s, $\text{C}(\text{CH}_3)_3$, 9H).

^{13}C NMR (63 MHz, CDCl_3 , 298 K): δ 149.6, 149.4, 148.4, 148.3, 146.7, 144.6, 143.7, 143.1, 136.6, 132.7, 129.3, 128.6, 127.6, 127.4, 127.2, 127.0, 126.9, 126.4, 126.2, 125.9, 125.6, 78.1, 34.5, 34.2, 34.1, 33.5, 32.9, 31.8 (2).

Synthesis of derivative **3.19**

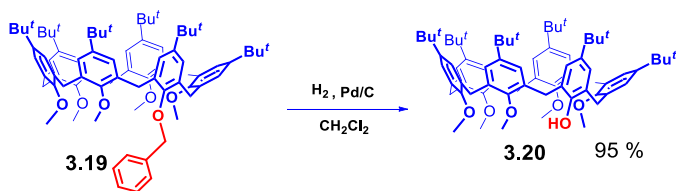


5.7 g of derivative **3.18** were mixed with Cs_2CO_3 (45 g, 30 eq.) in 0.30 L of acetone and kept under stirring at reflux for 1.5 h. The reaction mixture was cooled at room temperature and MeI 29 ml (100 eq) was added and the mixture kept at reflux for 12 h. the solvent was removed under reduced pressure. After usual work-up 5,2 g of derivative **3.19** were recovered (90% yield).

ESI(+) **MS**: $m/z = 1133.80$ (MH^+). **^1H NMR** (250 MHz, CDCl_3 , 298 K): δ 7.55- 6.9 (overlapped, $\text{ArH}_{\text{calix}}$ e ArH_{Bn} , 16H), 4.88 (s, $\text{CH}_2\text{Ar}_{\text{Bn}}$, 2H), 4.46 e 3.68 (AX, ArCH_2Ar , $J=14.7$ Hz, 4H), 4.18 e 3.82 (AX, ArCH_2Ar , $J=15.3$ Hz, 4H), 4.05 e 3.54 (AX, ArCH_2Ar , $J=14.2$ Hz, 4H), 3.20 (s, OCH_3 , 6H), 2.78 (s, OCH_3 , 3H), 2.53 (s, OCH_3 , 6H), 1.25 -1.24 (s, $\text{C}(\text{CH}_3)_3$, 27H), 1.03 -0.97 (s, $\text{C}(\text{CH}_3)_3$, 18H).

^{13}C NMR (63 MHz, CDCl_3 , 298 K): δ 154.5, 154.4, 153.7, 152.2, 146.0, 145.8 (2), 138.0, 134.0, 133.7, 133.5, 133.4, 133.3, 128.6, 127.9, 127.4, 127.0, 126.9, 125.3, 125.2, 124.7, 77.4, 74.5, 60.2, 60.1, 60.0, 34.3, 34.2, 31.6, 31.5, 31.4.

Synthesis of derivative **3.20**

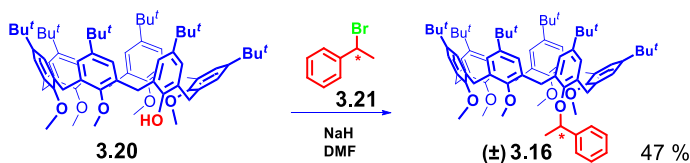


To a solution of 5.22 g of **3.19** in 0.10 L of CH_2Cl_2 Pd/C was added and the mixture kept under stirring at RT for 12 h.

The crude product was filtered with celite and the solvent removed under reduced pressure. The derivative **3.20** was recovered with a 95% yield (5,00 g).

ESI(+) MS: $m/z = 1043.71$ (MH^+). **^1H NMR** (250 MHz, CDCl_3 , 298 K): δ 7.38 (s, OH), 7.12- 7.11 (overlapped, ArH_{calix} , 2H), 7.04- 7.01 (overlapped, ArH_{calix} , 6H), 6.89 (s, ArH_{calix} , 2H), 6.80 (s, ArH_{calix} , 2H), 3.97 e 3.94 (broad, ArCH_2Ar , 8H), 3.82 (broad, ArCH_2Ar , 4H), 3.52 (s, OCH_3 , 3H), 3.07 (s, OCH_3 , 12H), 1.19 -1.17 (s, $\text{C}(\text{CH}_3)_3$, 45H), 1.12 (s, $\text{C}(\text{CH}_3)_3$, 9H). **^{13}C NMR** (63 MHz, CDCl_3 , 298 K): δ 154.6, 154.2, 153.3, 149.7, 146.7, 146.0, 145.3, 142.2, 133.9, 133.6, 133.4, 132.8, 127.3, 126.7, 126.5, 126.3, 125.9, 125.6, 124.9, 77.5, 61.1, 60.8, 34.4, 34.2, 34.1, 31.6 (2), 31.4.

Synthesis of derivative (\pm)-**3.16**



NaH (0.072g, 3.0 mmol) was added to a solution of derivative **3.20** (0.31g, 0.30 mmol) in dry DMF (15 mL) and stirred for 1h.

The mixture was allowed to cool at room and benzylbromide (0.17g, 1.00 mmol) was added. The resulting mixture was kept at 80°C for 12h under a nitrogen atmosphere, then the solvent was removed under reduced pressure and the mixture was partitioned between CH₂Cl₂ and H₂O.

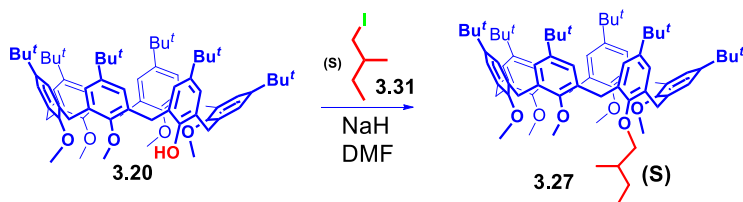
The organic layer was washed with 1N HCl (30 mL), brine (30 mL), and dried over Na₂SO₄. The crude product was purified by column chromatography (SiO₂; CH₂Cl₂) to give (0.16g, 0.14 mmol) of derivative (±)-**3.16** as a white solid.

ESI(+) MS: $m/z = 1147.81$ (MH⁺), **¹HNMR** (400 MHz, CDCl₃, 298 K): δ 7.53-6.75 (overlapped, 17H, ArH_{calix} + ArH_{Bn}), 5.06 (q, $J = 8$, 1H, CH_{Bn}), 4.64 and 3.63 (AX, $J = 13.4$ Hz, 2H, ArCH₂Ar), 4.27 and 3.69 (AX, $J = 14$ Hz, ArCH₂Ar, 2H), 4.25 and 3.59 (AX, $J = 14$ Hz, ArCH₂Ar, 2H), 4.16 and 3.00 (AX, $J = 13.6$ Hz, ArCH₂Ar, 2H), 4.12 and 3.84 (AX, $J = 13.9$ Hz, ArCH₂Ar, 2H), 4.12 and 3.77 (AX, $J = 13.9$ Hz, ArCH₂Ar, 2H), 3.36 (s, overlapped, OCH₃, 6H), 2.75 (s, OCH₃, 3H), 2.52 (s, OCH₃, 3H), 2.35 (s, OCH₃, 3H), 1.68

(d, $J = 8$, 3H, CH_{3Bn}), 1.34 (s, $C(CH_3)_3$, 9H), 1.29 and 1.28 (s, overlapped, $C(CH_3)_3$, 18H), 1.00 and 0.98 (s, overlapped $C(CH_3)_3$, 18H), 0.92 (s, $C(CH_3)_3$, 9H)

^{13}C NMR (100 MHz, $CDCl_3$, 298 K): δ 154.5, 154.4, 154.4, 153.6, 151.3, 145.8, 145.7, 145.4, 143.3, 134.2, 134.0, 133.8, 133.6, 133.6, 133.5, 133.4, 133.4, 128.4, 127.8, 127.1, 126.7, 124.9, 124.3, 124.1, 81.0, 77.4, 60.3, 60.2, 60.0, 59.9, 34.3, 34.2, 34.2.

Synthesis of derivative **3.27**



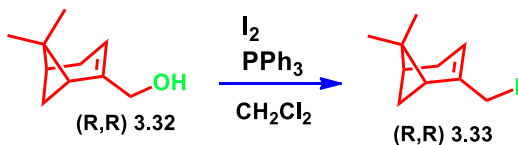
NaH (0.024g, 1.0 mmol) was added to a solution of derivative **3.20** (0.10g, 0.10 mmol) in dry DMF (15 mL) and stirred for 1h.

The mixture was allowed to cool at room and (S)-(+)-1-iodo-2-methylbutane (0.99g 0.5 mmol) was added. The resulting mixture was kept at $80^\circ C$ for 12h under a nitrogen atmosphere, then the solvent was removed under reduced pressure and the mixture was partitioned between CH_2Cl_2 and H_2O .

The organic layer was washed with 1N HCl (30 mL), brine (30 mL), and dried over Na₂SO₄. The crude product was purified by column chromatography (SiO₂; CH₂Cl₂) to give derivative **3.27** as a white solid (0.87g, 0.078 mmol, 78%)

ESI(+) MS: $m/z = 1130.77$ [M+NH₄]⁺, **¹H NMR** (300 MHz, CDCl₃, 298 K): δ 7.27-7.26 (overlapped, ArH, 2H), 7.13-7.11 (overlapped, ArH, 4H), 6.86 (br s, ArH, 2H), 6.84 (br s, ArH, 2H), 6.76 (br s, ArH, 2H), 3.94-3.70 (br, ArCH₂Ar + OCH₂CH(CH₃)CH₂CH₃, 14H), 3.28 (s, OCH₃, 6H), 2.71 (s, OCH₃, 3H) 2.47 (s, OCH₃, 6H), 1.95 (m, OCH₂CH(CH₃)CH₂CH₃, 1H), 1.69 (m, OCH₂CH(CH₃)CH₂CH₃, 2H), 1.30 (s, overlapped, C(CH₃)₃, 18H), 1.27 (s, overlapped, C(CH₃)₃, 9H), 1.11 (br, d, $J = 9$, OCH₂CH(CH₃)CH₂CH₃, 1H), 1.00 (s, overlapped, C(CH₃)₃, 18H), 0.98 (br, m, OCH₂CH(CH₃)CH₂CH₃, 3H), 0.91 (s, C(CH₃)₃, 9H); **¹³C NMR** (75 MHz, CDCl₃, 298 K): δ 154.4 (2), 153.6, 152.2, 145.8, 145.6, 133.9, 133.7, 133.6 (2), 133.5, 133.3, 127.6, 127.0, 125.0, 124.2, 60.2, 60.1, 60.0, 36.2, 34.3, 34.2, 32.1, 31.7, 31.4(2), 30.6, 30.3, 29.9, 29.5, 26.4, 22.9, 16.9, 14.3, 11.7.

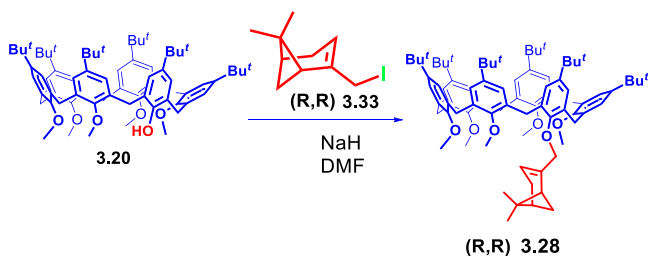
Synthesis of derivative 3.33

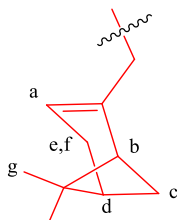


(R)-Myrtenol (3.0 g, 0.020 mol) was dissolved in DMF (80 mL) and I₂ (22g, 0.087 mol) and PPh₃ (20g, 0.079 mol) were added and the mixture was kept at 40°C for 2h.

DMF was removed under reduced pressure and the mixture partitioned between CH₂Cl₂ and H₂O. the organic layer was washed with brine and dried over Na₂SO₄. The crud product was used directly for the next step without any purification (0.52g, 2.0 mmol 10%)

Synthesis of derivative 41





NaH (0.05g, 2.0 mmol) was added to a solution of derivative **3.20** (0.20g, 0.20 mmol) in dry DMF (10 mL) and stirred for 1h.

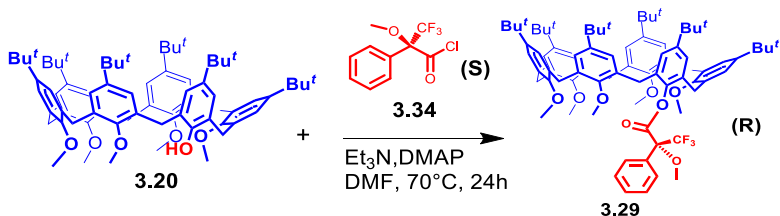
The mixture was allowed to cool at room and derivative **3.33** (0.27g, 1.0 mmol) was added. The resulting mixture was kept at 80°C for 12h under a nitrogen atmosphere, then the solvent was removed under reduced pressure and the mixture was partitioned between CH₂Cl₂ and H₂O.

The organic layer was washed with 1N HCl (30 mL), brine (30 mL), and dried over Na₂SO₄. The crude product was purified by column chromatography (SiO₂; CH₂Cl₂) to give derivative **3.28** as a white solid (0.16g, 0.14mmol, 75%).

ESI(+) MS: $m/z = 1194.75 [M+NH_4]^+$, **¹H NMR** (300 MHz, TCDE, 353 K): δ 7.39 (br s, ArH, 2H), 7.28-7.26 (overlapped, ArH, 4H), 7.02 (s, ArH, 2H), 6.98 (s, ArH, 2H), 6.94 (s, ArH, 2H), 5.90 (br s, H_a, 1H), 4.59 and 3.61 (AX, $J = 14$ Hz, ArCH₂Ar, 2H), 4.40 (s OCH₂, 2H), 4.39 and 3.77 (AX, $J = 15$ Hz, ArCH₂Ar, 2H), 4.27 and 3.87 (AX, $J = 15$ Hz, ArCH₂Ar, 2H), 3.49 (s, OCH₃, 3H), 3.47 (s, OCH₃, 3H), 2.87 (s, OCH₃, 3H), 2.73(s, OCH₃, 3H), 2.68 (s, OCH₃, 3H), 2.61 (br m, H_b,

1H), 2.52 (overlapped H_c+H_e, 3H), 2.30 (br s, H_f, 1H), 1.47 (s, C(CH₃)₃, 9H), 1.46 (s, C(CH₃)₃, 9H), 1.42 (s, C(CH₃)₃, 9H), 1.16 (s, overlapped, C(CH₃)₃, 18H), 1.08 (s, C(CH₃)₃, 9H), 1.01 (br s H_g, 6H). ¹H NMR (75 MHz, CDCl₃, 298 K) 154.9, 154.2, 152.8, 146.3, 146.2, 145.4, 134.5, 134.4, 134.2, 134.1, 133.8 (2), 127.5, 125.6, 124.8, 120.0, 77.9, 75.9, 60.5, 44.3, 41.6, 38.9, 35.3, 34.9, 34.7, 32.4, 32.2, 31.2, 32.0, 31.9, 31.1, 30.9, 27.0, 25.9, 21.9.

Synthesis of derivative **3.29**

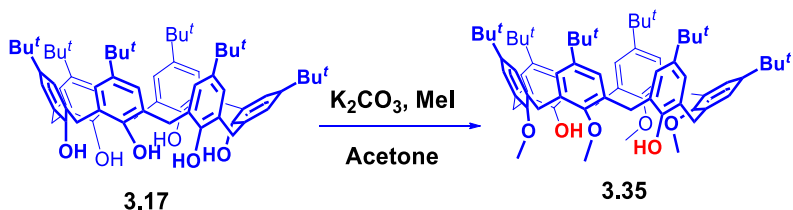


An oven-dried flask was charged with derivative **3.20** (0.10g, 0.10 mmol), DMAP (3.7mg, 0.030 mmol), and triethylamine (1.0 mL) in DMF (5.0 mL). Finally, (S)-Mosher's acid chloride (47 mg, 0.20 mmol) was added and the reaction mixture was stirred at 70 °C for 12 h. The reaction mixture was cooled to room temperature followed by standard workup procedure using dichloromethane for extraction. The crude product was purified by silica gel column chromatography (CH₂Cl₂: CH₃OH, 98:2, v/v) to yield 0.12 g (0.12g, 0.093

mmol, yield: 93%) of derivative **3.29** as white solids.

ESI(+) **MS**: $m/z = 1259.74$ $[M+H]^+$, **1H NMR** (300 MHz, $CDCl_3$, 353 K): δ 7.93 (br m, $ArH_{Moshier(para)}$, 1H), 7.58 (overlapped $ArH_{Moshier(meta)}$ + $ArH_{Moshier(orto)}$, 4H), 7.35 (br m, ArH_{calix} , 2H), 7.30-7.28 (overlapped, ArH_{calix} , 6H), 6.99- 6.94 (overlapped, ArH_{calix} , 6H), 4.44 and 3.73 (AX, $J=10$ Hz, $ArCH_2Ar$, 2H), 4.36 and 3.75 (AX, $J=12$ Hz, $ArCH_2Ar$, 2H), 4.06 and 3.46 (AX, $J=15$ Hz, $ArCH_2Ar$, 2H), 4.33-4.22 and 3.82-3.49 (overlapped $ArCH_2Ar$, 6H), 3.89 (s, OCH_3 -Moshier, 3H), 3.63 (s, OCH_3 , 3H) 3.51 (s, OCH_3 , 3H), 2.80 (s, OCH_3 , 3H), 2.67 (s, OCH_3 , 3H), 2.57 (s, OCH_3 , 3H), 1.50 (s, $C(CH_3)_3$, 9H), 1.46 (s, $C(CH_3)_3$, 9H), 1.44 (s, $C(CH_3)_3$, 9H), 1.41 (s, $C(CH_3)_3$, 9H), 1.13 (s, $C(CH_3)_3$, 9H), 1.04 (s, $C(CH_3)_3$, 9H); **^{13}C NMR** (75 MHz, $CDCl_3$, 353 K): δ 165.9, 155.3, 155.1, 154.2, 149.5, 146.6, 146.4, 144.1, 134.2, 134.0, 133.9, 133.6, 133.5, 132.8, 132.3, 130.6, 129.3, 128.7, 128.3, 128.2, 128.0, 127.8, 127.7, 125.6, 125.3, 125.2, 125.1, 60.7, 60.6, 56.5, 34.8, 34.7, 32.2, 32.0, 31.8, 31.3, 31.1.

Synthesis of derivative **3.35**

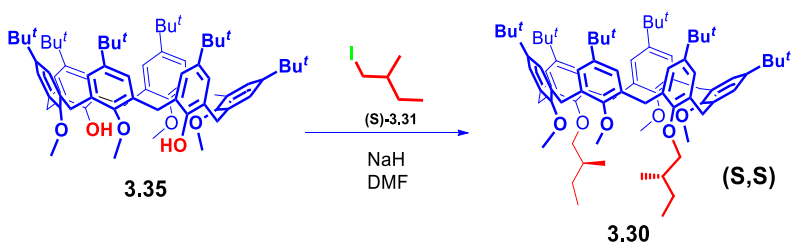


A mixture of *p*-*tert*-butylcalix[6]arene (1.0 g, 1.0 mmol), K₂CO₃ (4.1 mmol) and MeI (320 μL, 5.1 mmol) in dry acetone (70 mL) was heated at 70°C in an autoclave for 20 h. The mixture was poured into 10% HCl (100 mL), and the aqueous layer was extracted with CH₂Cl₂ (2 x 50 mL), washed with brine (2 x 50 mL), dried over Na₂SO₄ and evaporated to dryness.

The crude product was purified by column chromatography (SiO₂; Hexane/THF, 9:1) to give derivative **3.35** as a white solid (0.39 g, 35%).

ESI(+) MS: *m/z* = 1028.41 (M⁺). **¹H NMR** (300 MHz, CDCl₃, 298 K): δ 8.03 (s, ArH, 4H), 7.06 (m, ArH, 8H), 6.70 (s, ArH, 4H), 3.97 (br s, ArCH₂Ar, 4H), 3.87 (br s, ArCH₂Ar, 8H), 3.14 (s, OCH₃, 6H), 1.18 (s, C(CH₃)₃, 36H), 0.94 (s, C(CH₃)₃, 18H); **¹³C NMR** (75 MHz, CDCl₃, 298 K) δ 153.4, 149.6, 146.8, 142.0, 134.2, 132.4, 127.5, 126.7, 126.3, 124.1, 61.7, 34.4, 34.0, 31.6, 31.5, 31.2, 31.0.

Synthesis of derivative **3.30**



NaH (0.024 g, 1.0 mmol) was added to a solution of derivative **3.35** (0.10 g, 0.10 mmol) in dry DMF (15 mL) and stirred for 1h.

The mixture was allowed to cool at room and (S)-(+)-1-iodo-2-methylbutane (0.20 g, 1.0 mmol) was added. The resulting mixture was kept at 80°C for 12 h under a nitrogen atmosphere, then the solvent was removed under reduced pressure and the mixture was partitioned between CH₂Cl₂ and H₂O. The organic layer was washed with 1N HCl (30 mL), brine (30 mL), and dried over Na₂SO₄. The crude product was purified by column chromatography (SiO₂; CH₂Cl₂) to give derivative **3.30** as a white solid (0.11g, 0.096 mmol, 96%).

ESI(+) MS: $m/z = 1286.88$ [M+NH₄]⁺. **¹H NMR** (400 MHz, CDCl₃, 298 K): δ 7.24 (br s, ArH, 4H), 6.92 (br s, ArH, 8H), 4.23 and 3.60 (br AX, ArCH₂Ar, 6H), 3.87 (br AX, ArCH₂Ar, 6H), 3.67 (br m, OCH₂CH(CH₃)CH₂CH₃, 4H), 2.72 (br s, OCH₃, 12H), 1.97 and 1.71 (m, OCH₂CH(CH₃)CH₂CH₃, 2H), 1.21 (s, C(CH₃)₃, 36H), 1.11 (d, $J = 7$, OCH₂CH(CH₃)CH₂CH₃, 6H), 1.02 (s, C(CH₃)₃, 18H), 0.98 (t, $J = 7$, OCH₂CH(CH₃)CH₂CH₃, 6H); **¹³C NMR** (75 MHz, CDCl₃, 298 K) δ 155.0, 152.9, 146.4, 146.3, 134.8, 134.4, 134.3, 127.6, 126.6, 125.4, 78.7, 60.5, 36.9, 35.0, 34.9, 32.3, 32.1, 31.5, 31.3, 27.2, 17.6, 12.4.

General procedure for MS experiments (isotopic effect)

Sample preparation

Calixarene derivatives ($1.9 \cdot 10^{-3}$ mmol) were dissolved in 0.5 mL of CHCl_3 ($3.8 \cdot 10^{-3}$ M solution). Then, the appropriate **TFPB⁻** salts **(R)-3.22⁺TFPB⁻** ($3.8 \cdot 10^{-3}$ mmol, $7.6 \cdot 10^{-3}$ M) and **(R)-3.22-d₆⁺TFPB⁻** ($3.8 \cdot 10^{-3}$ mmol, $7.6 \cdot 10^{-3}$ M) were added and the mixture was stirred for 15 min. Then, the solution was diluted at a concentration of 300 μM with CH_2Cl_2 before the MS injection.

MS conditions

Sample concentration 300 μM ; flow rate 2-4 $\mu\text{L}/\text{min}$; sample cone: 25 V; HV 2500 V; source temperature and temperature of desolvation gas were kept constant at 40 °C, no nebulizer gas was used for the experiments.

$I_{\text{R}}/I_{\text{R-d}_n}$ evaluation

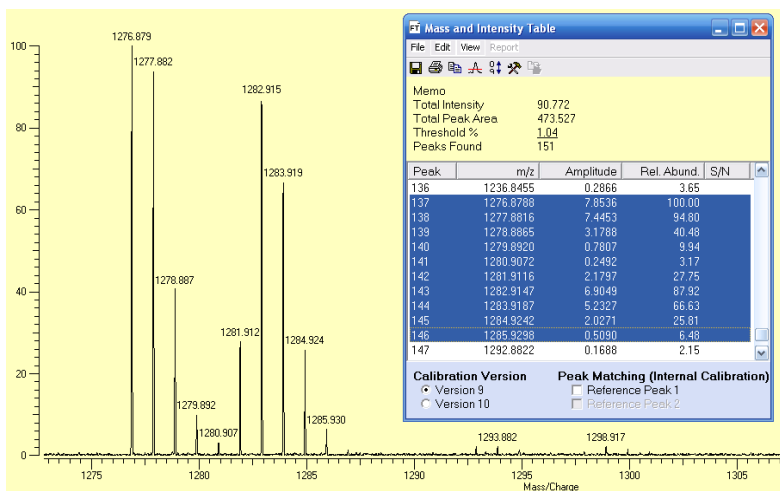
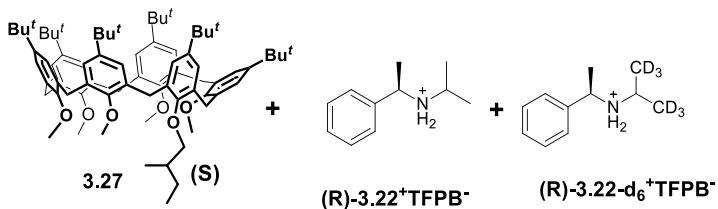
The deuterated axle is a mixture of partially deuterated compounds so $I_{\text{R-d}_n}$ can be evaluated as the sum of the intensity of each peak related to the deuterated compounds.

This operation is valid assuming that no significant differences and isotopic effect occur between the partially deuterated compounds (d_4 and d_5) and the fully deuterated one (d_6). The intensity of the non-deuterated compounds, is then evaluated as the sum of each peak related to its distribution.

The corresponding peak intensities are pasted from the

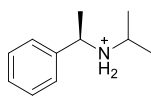
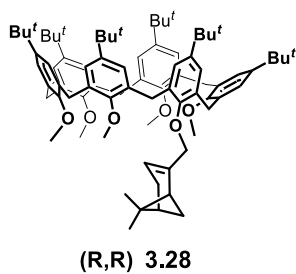
Omega software controlling the mass spectrometer to the spreadsheet, which calculates the intensity of each peak.

a) 1:2:2 mixture of **3.27**, (R)-**3.22⁺TFPB⁻** and (R)-**3.22-d₆⁺TFPB⁻**

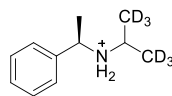


	Peak	<i>m/z</i>	Rel. Abund.
Non-Deuterated Complex	A	1340,9037	100,00
	A+1	1341,9070	94,80
	A+2	1342,9116	40,48
	A+3	1343,9166	9,94
	A+4	1344,9262	3,17
		$I_R =$	248,39
Deuterated Complex	A(D5)	1345,9369	27,75
	A (D5)+1 + A (D6)	1346,9401	87,92
	A (D5)+2 + A (D6)+1	1347,9440	66,63
	A (D5)+3 + A (D6)+2	1348,9493	25,81
	A (D5)+4 + A (D6)+3	1349,9548	6,48
	A (D6)+4	1350,9563	0,00
		$I_{Rdn} =$	214,59
		$I_R/I_{Rdn} =$	1,16

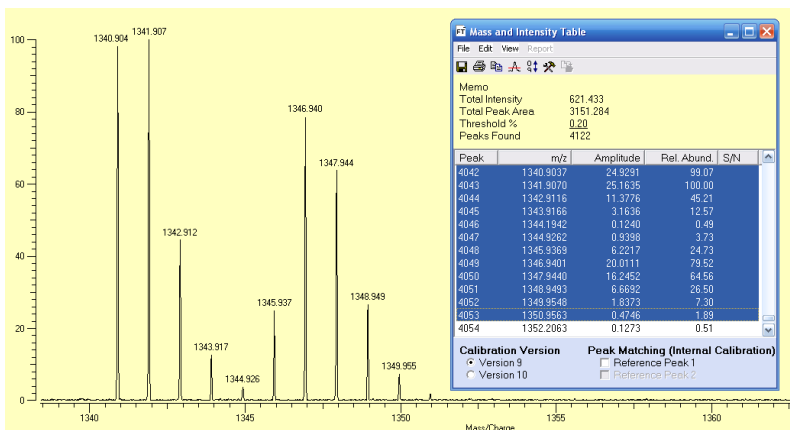
b) 1:2:2 mixture of **3.28**, (R)-**3.22**⁺TFPB⁻ and (R)-**3.22-d**₆⁺TFPB⁻



(R)-**3.22**⁺TFPB⁻

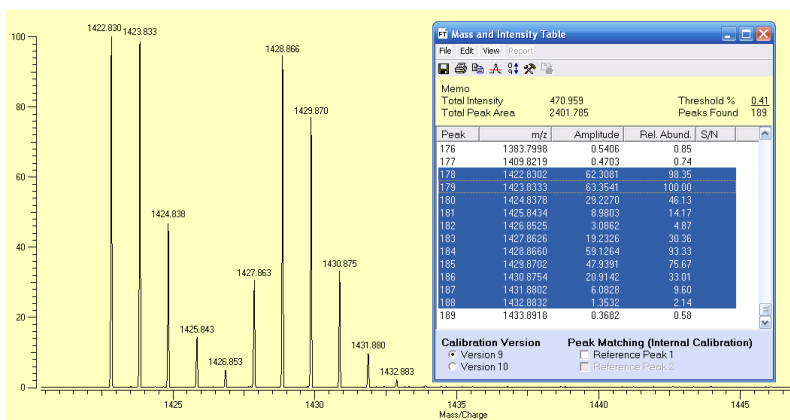
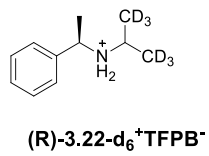
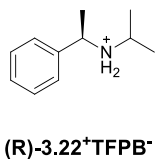
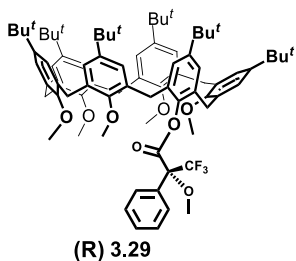


(R)-**3.22-d**₆⁺TFPB⁻



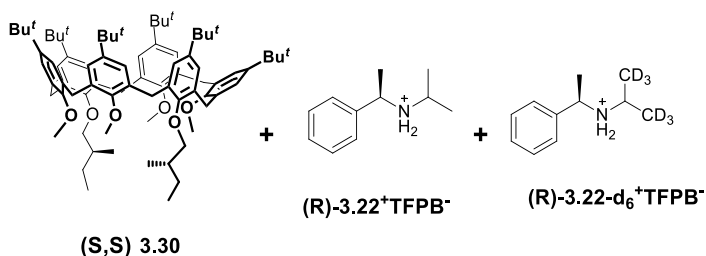
	Peak	m/z	Rel. Abund.
Non-Deuterated Complex	A	1340,9037	99,07
	A+1	1341,9070	100,00
	A+2	1342,9116	45,21
	A+3	1343,9166	12,57
	A+4	1344,9262	3,73
		I_R =	260,58
Deuterated Complex	A(D5)	1345,9369	24,73
	A (D5)+1 + A (D6)	1346,9401	79,52
	A (D5)+2 + A (D6)+1	1347,9440	64,56
	A (D5)+3 + A (D6)+2	1348,9493	26,50
	A (D5)+4 + A (D6)+3	1349,9548	7,30
	A (D6)+4	1350,9563	1,89
		I_{Rdn} =	204,50
		I_R/I_{Rdn} =	1,27

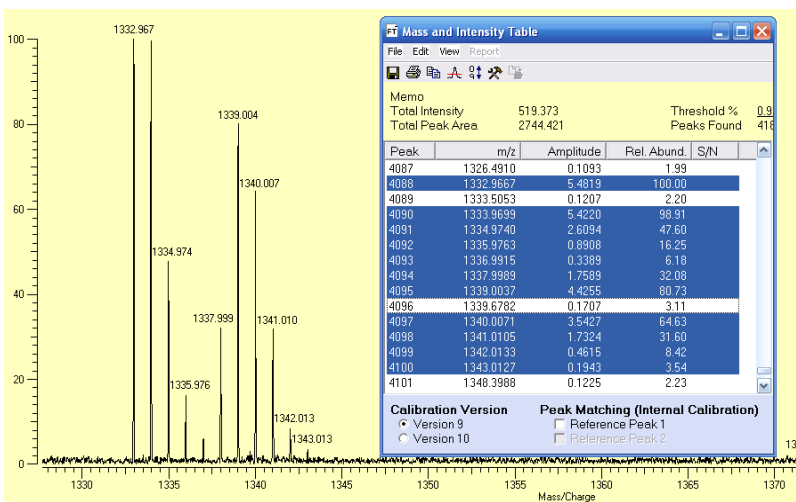
c) 1:2:2 mixture of **3.29**, (R)-**3.22**⁺**TFPB**⁻ and (R)-**3.22-d**₆⁺**TFPB**⁻



	Peak	<i>m/z</i>	Rel. Abund.
Non-Deuterated Complex	A	1340,9037	98,35
	A+1	1341,9070	100,00
	A+2	1342,9116	46,13
	A+3	1343,9166	14,17
	A+4	1344,9262	4,87
		$I_R =$	263,52
	Peak	<i>m/z</i>	Rel. Abund.
Deuterated Complex	A(D5)	1345,9369	30,36
	A (D5)+1 + A (D6)	1346,9401	93,33
	A (D5)+2 + A (D6)+1	1347,9440	75,67
	A (D5)+3 + A (D6)+2	1348,9493	33,01
	A (D5)+4 + A (D6)+3	1349,9548	9,60
	A (D6)+4	1350,9563	2,14
		$I_{Rdn} =$	244,11
		$I_R/I_{Rdn} =$	1,08

d) 1:2:2 mixture of **3.30**, (R)-**3.22**⁺TFPB⁻ and (R)-**3.22-d**₆⁺TFPB⁻





	Peak	m/z	Rel. Abund.
Non-Deuterated Complex	A	1340,9037	100,00
	A+1	1341,9070	98,91
	A+2	1342,9116	47,60
	A+3	1343,9166	16,25
	A+4	1344,9262	6,18
		$I_R =$	268,94
Deuterated Complex	A(D5)	1345,9369	32,08
	A(D5)+1 + A(D6)	1346,9401	80,73
	A(D5)+2 + A(D6)+1	1347,9440	64,63
	A(D5)+3 + A(D6)+2	1348,9493	31,60
	A(D5)+4 + A(D6)+3	1349,9548	8,42
	A(D6)+4	1350,9563	3,54
		$I_{Rdn} =$	221,00
		$I_R/I_{Rdn} =$	1,22

General procedure for MS experiments (chiral recognition effect)

Calixarene derivatives ($1.9 \cdot 10^{-3}$ mmol) were dissolved in 0.5 mL of CHCl_3 ($3.8 \cdot 10^{-3}$ M solution). Then, the appropriate **TFPB**⁻ salts **(S)-35**⁺ ($3.8 \cdot 10^{-3}$ mmol, $7.6 \cdot 10^{-3}$ M) and **(R)-35-d₆**⁺ ($3.8 \cdot 10^{-3}$ mmol, $7.6 \cdot 10^{-3}$ M) were added and the mixture was stirred for 15 min. Then, the solution was diluted at the desired concentration with CH_2Cl_2 just before the MS analysis. **MS condition:** sample concentration 300 μM ; flow rate 2-4 $\mu\text{L}/\text{min}$; sample cone: 25 V; HV 2500 V; source temperature and temperature of desolvation gas were kept constant at 40 °C, no nebulizer gas was used for the experiments.

I_S/I_{R-d_n} evaluation

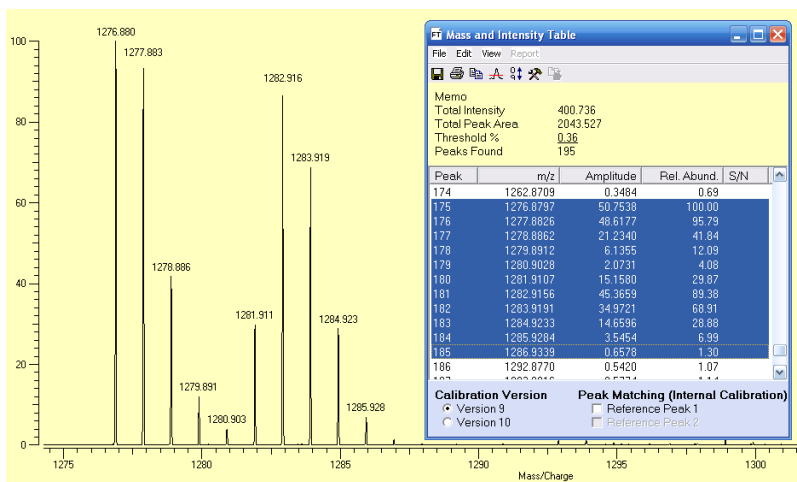
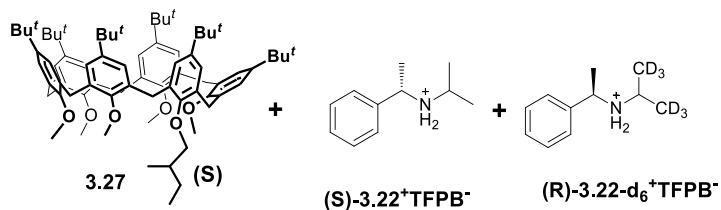
The deuterated axle is a mixture of partially deuterated compounds so **I_{Sdn}** can be evaluated as the sum of the intensity of each peak related to the deuterated compounds.

This operation is valid assuming that no significant differences and isotopic effect occur between the partially deuterated compounds (d_4 and d_5) and the fully deuterated one (d_6). The intensity of the non-deuterated compounds, is than evaluated as the sum of each peak related to its distribution.

The corresponding peak intensities are pasted from the Omega software controlling the mass spectrometer to the spreadsheet, which calculates the intensity of each peak and

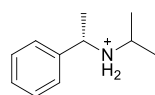
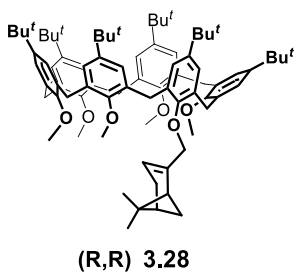
the I_S/I_{R-d_6} .

a) 1:2:2 mixture of **3.27**, (**S**)-**3.22⁺TFPB⁻** and (**R**)-**3.22-d₆⁺TFPB⁻**

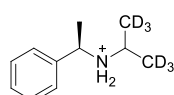


	Peak	<i>m/z</i>	Rel. Abund.
Non-Deuterated Complex	A	1340,9037	100,00
	A+1	1341,9070	95,79
	A+2	1342,9116	41,84
	A+3	1343,9166	12,09
	A+4	1344,9262	4,08
		$I_R =$	253,80
	Peak	<i>m/z</i>	Rel. Abund.
Deuterated Complex	A (D5)	1345,9369	29,87
	A (D5)+1 + A (D6)	1346,9401	89,38
	A (D5)+2 + A (D6)+1	1347,9440	68,91
	A (D5)+3 + A (D6)+2	1348,9493	28,88
	A (D5)+4 + A (D6)+3	1349,9548	6,99
	A (D6)+4	1350,9563	1,30
		$I_{Rdn} =$	225,33
		$I_R/I_{Rdn} =$	1,13

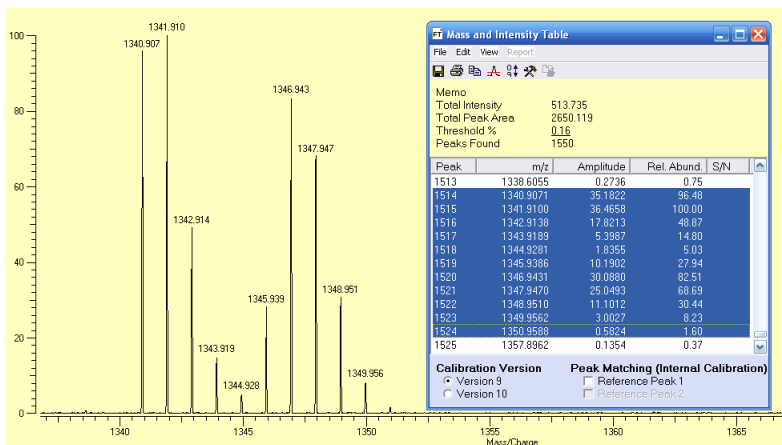
b) 1:2:2 mixture of **3.28**, (S)-**3.22**⁺TFPB⁻ and (R)-**3.22-d**₆⁺TFPB⁻



(S)-**3.22**⁺TFPB⁻

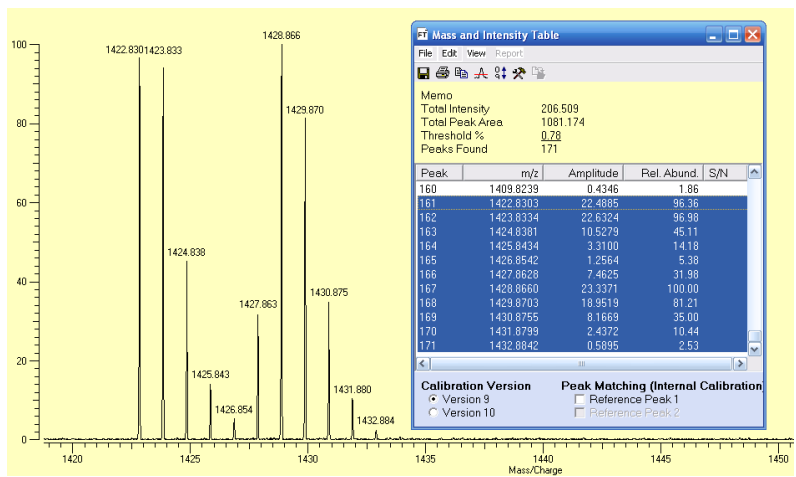
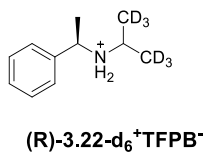
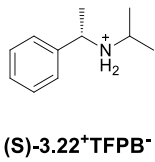
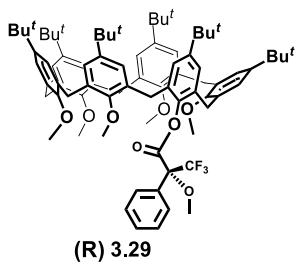


(R)-**3.22-d**₆⁺TFPB⁻



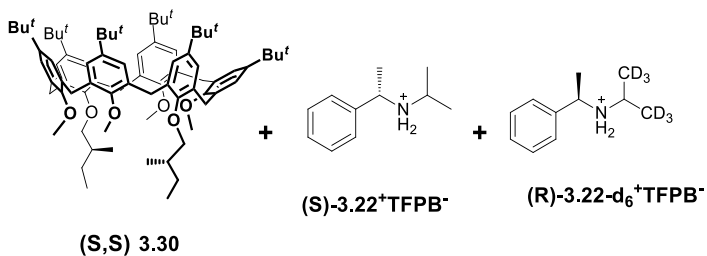
	Peak	m/z	Rel. Abund.
Non-Deuterated Complex	A	1340,9037	96,48
	A+1	1341,9070	100,00
	A+2	1342,9116	48,87
	A+3	1343,9166	14,80
	A+4	1344,9262	5,03
		$I_R =$	265,18
Deuterated Complex	A(D5)	1345,9369	27,94
	A (D5)+1 + A (D6)	1346,9401	82,51
	A (D5)+2 + A (D6)+1	1347,9440	68,69
	A (D5)+3 + A (D6)+2	1348,9493	30,44
	A (D5)+4 + A (D6)+3	1349,9548	8,23
	A (D6)+4	1350,9563	1,60
		$I_{Rdn} =$	219,41
		$I_R/I_{Rdn} =$	1,21

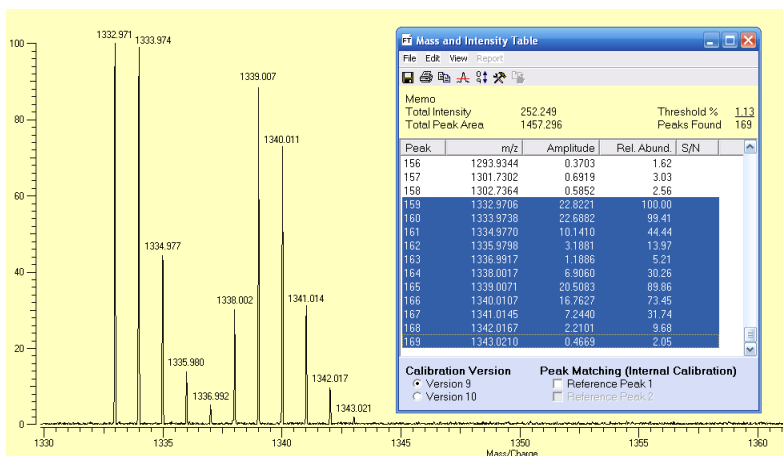
c) 1:2:2 mixture of **3.29**, (S)-**3.22**⁺TFPB⁻ and (R)-**3.22**-**d**₆⁺TFPB⁻



	Peak	<i>m/z</i>	Rel. Abund.
Non-Deuterated Complex	A	1340,9037	96,36
	A+1	1341,9070	96,98
	A+2	1342,9116	45,11
	A+3	1343,9166	14,18
	A+4	1344,9262	5,38
		$I_R =$	258,01
Deuterated Complex	A (D5)	1345,9369	31,98
	A (D5)+1 + A (D6)	1346,9401	100,00
	A (D5)+2 + A (D6)+1	1347,9440	81,21
	A (D5)+3 + A (D6)+2	1348,9493	35,00
	A (D5)+4 + A (D6)+3	1349,9548	10,44
	A (D6)+4	1350,9563	2,53
		$I_{Rdn} =$	261,16
		$I_R/I_{Rdn} =$	0,99

d) Derivative **42** mixed with (S)-**35**⁺ and (R)-**35-d**₆⁺





	Peak	<i>m/z</i>	Rel. Abund.
Non-Deuterated Complex	A	1340,9037	100,00
	A+1	1341,9070	99,41
	A+2	1342,9116	44,44
	A+3	1343,9166	13,97
	A+4	1344,9262	5,21
		I_R =	263,03
Deuterated Complex	A (D5)	1345,9369	30,26
	A (D5)+1 + A (D6)	1346,9401	89,86
	A (D5)+2 + A (D6)+1	1347,9440	73,45
	A (D5)+3 + A (D6)+2	1348,9493	31,74
	A (D5)+4 + A (D6)+3	1349,9548	9,68
	A (D6)+4	1350,9563	2,05
		I_{Rdn} =	237,04
		I_R/I_{Rdn} =	1,11

CHAPTER IV

SYNTHESIS OF NEW CALIXARENE AND RESORCINARENE BASED CHIRAL HOSTS

4.1 CHIRALITY AND INHERENT CHIRALITY IN CALIXARENES AND RESORCINARENES

In the previous chapter we showed the importance of the chiral recognition and the use of some chiral calix[6]arenes hosts towards the ammonium guests recognition.

These hosts were synthesised by the functionalization of the scaffold using chiral substituent.

Contrary, this chapter reports the pursuit of new potential chiral hosts by means of the study and the synthesis of some chiral macrocycles using achiral substituents.

The structure and properties of calixarenes and resorcinarenes can be easily varied functionalizing the hydroxyl groups at the *lower rim* or introducing substituents on the aromatic scaffold. This property makes them a versatile building block with regard to structure and function.

The addition of chirality to calixarenes and resorcinarenes is an exciting enhancement of their potential as ligands for chiral catalysis and enantioselective processes.

4.1.1 Inherently chiral calixarenes

The introduction of “inherent chirality” into calixarene scaffolds by asymmetric functionalization with achiral substituents is more challenging and interesting

The term “inherent chirality” was defined for the first time by Böhmer⁵⁵ for chiral calixarenes and then it was extended to all that compounds that do not match with other type of chirality

The inherent chirality definition was reformulated by Mandolini and Schiaffino and subsequently revised by Szumna that now states: “*inherent chirality arises from the introduction of a curvature in an ideal planar structure that is devoid of perpendicular symmetry planes in its bidimensional representation*”.

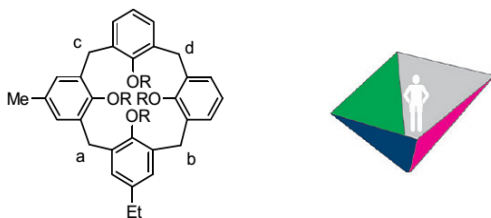


Figure 4.1 Inherent chirality in calix[4]arene.

To designate inherent chirality two type of notations, $(cR)/(cS)$ and $(P)/(M)$, were suggested.

In the case of calix[4]arenes, once the carbons of the bridges

⁵⁵ V. Böhmer, D. Kraft, M. Tabatabai, *J. Incl. Phenom. Macro. Chem.* **1994**, *19*, 17-39.

are labelled as *a*, *b*, *c*, and *d* according to standard stereochemistry rules, an ideal observer standing on the concave side of the calixarene will see the three highest priority atoms *a*, *b*, and *c*.

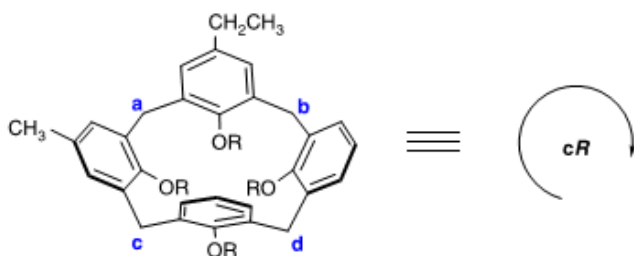


Figure 4.2 Mandolini's assignment rules.

The (*cR*) and (*cS*) description indicates respectively a clockwise and counterclockwise priority of their sequence while *c* stands for curvature.

Similarly, the (*P*)/(*M*) one does it as *P* or *M*, respectively. The latter notation was promoted by Szumna especially for concave molecules like calixarenes and resorcinarenes.

There are mainly two methods to synthesise inherently chiral calixarenes: the condensation of different phenolic units⁵⁶ (**Figure 4.3**) and the asymmetric functionalization of the calixarene skeleton such as *O*-alkylation or esterification of

⁵⁶ a) V. Böhmer, L. Merkel, U. Kunz, *J. Chem. Soc., Chem. Commun.*, **1987**, 12, 896–897; b) H. Casabianca, J. Royer, A. Satrallah, A. Taty-C, J. Vicens, *Tetrahedron Lett.* **1987**, 28, 6595–6596; c) G. D. Andreotti, V. Böhmer, J. G. Jordon, M. Tabatabai, F. Uguzzoli, W. Vogt, A. Wolfft, *J. Org. Chem.* **1993**, 58, 4023–4032.

phenolic OH on the lower rim and and *para*- and *meta*-substitution of phenolic units on the upper rim.⁵⁷

The condensation method was used only for calix[4]arene because the process is tedious and yields are low.

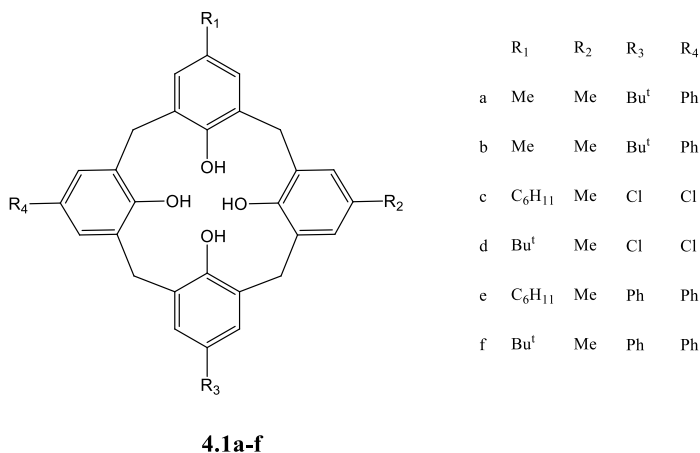


Figure 4.3 Calix[4]arenes obtained by condensation of different phenolic units

On the other hand Reinhoudt synthesized *meta*-substituted inherently chiral calix[4]arenes from *para*-acetamido substituted calix[4]arenes (**Figure 4.4**)

⁵⁷ S. Y. Li, Y. W. Xu, J. M. Liu, C. Y. Su, *Int. J. Mol. Sci.* **2011**, *12*, 429-455.

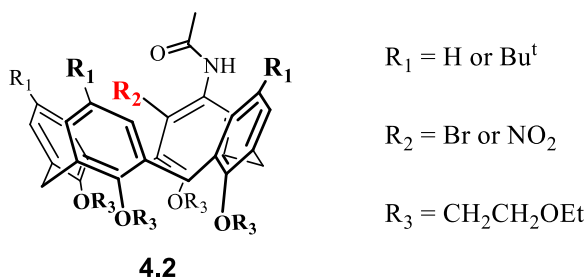


Figure 4.4 *meta*-substituted inherently chiral calix[4]arenes

In particular there is a preference of the *meta*-substitution over the *para*-substitution because of the activation of the *meta*-position by the *para*-acetamido group.⁵⁸

A series of inherently chiral calix[4]arenes, asymmetrically functionalized on the phenolic *meta*-position, were prepared by Neri et al. through the so called “*p*-bromodienone route”.⁵⁹

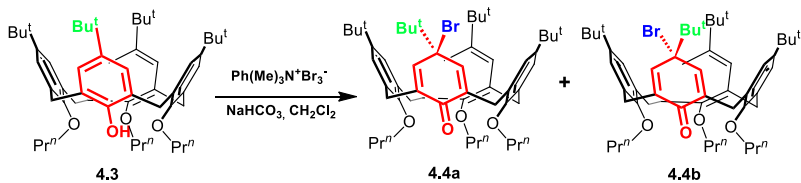
4.1.2 *Meta*-functionalization of Calixarenes: the “*p*-bromodienone route”

The first example of calixarene *p*-bromodienone derivatives **4.4a** and **4.4b** was reported by Neri et al. by treatment of the tripropoxy-*p*-*tert*-butylcalix[4]arene **4.3** with trimethylphenylammonium tribromide and a saturated

⁵⁸ W. Verboom, P. J. Bodewes, G. van Essen, P. Timmerman, G. J. van Hummel, S. Harkema, D. N. Reinhoudt, *Tetrahedron* **1995**, *51*, 499–512.

⁵⁹ F. Troisi, T. Pierro, C. Gaeta, M. Carratù, P. Neri, *Tetrahedron Lett.* **2009**, *50*, 4416–4419.

solution of NaHCO_3 (**Scheme 1**).⁶⁰



Scheme 4.1 Synthesis of *p*-bromoderivatives **4.4a-b**

Successively the same authors reported the Ag^+ -mediated nucleophilic substitution of bromine in **4.4a** and **4.4b** with alcohols, the successive re-aromatization gives *p*-alkoxycalixarene derivatives (**Scheme 4.2**).

In this procedure, the mixture of *p*-bromodienone-tripropoxycalix[4]arene **4.4a** and **4.4b** was treated with an alcoholic solution of AgClO_4 for 2 h at 0 C. Soon after the addition, a yellow precipitate of AgBr was formed⁶¹, and *p*-alkoxycalix[4]arene derivatives **4.5a-k** were obtained in good yields.⁶²

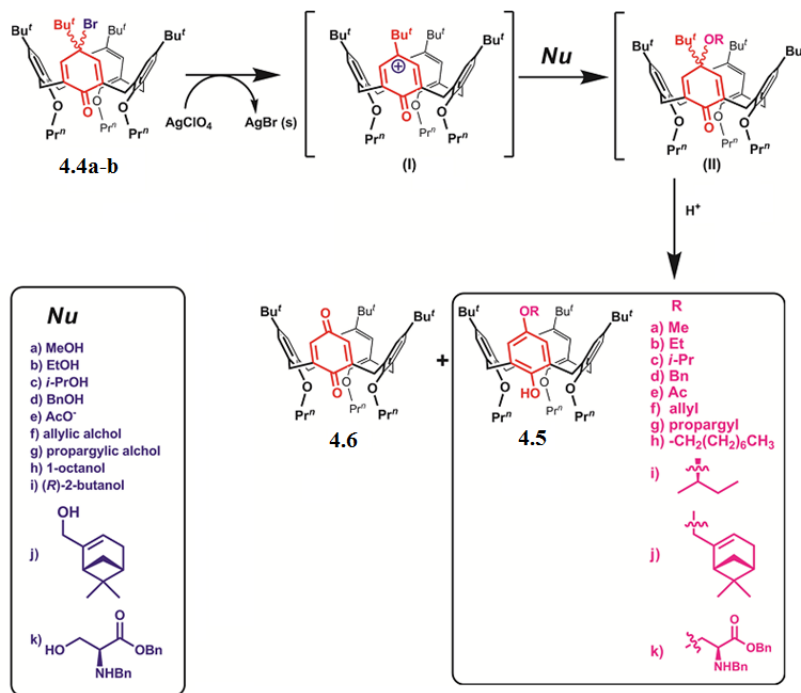
The formation of the *p*-substitued adduct suggested the initial formation of the aryloxenium carbocation **I**, which reacted with methanol to give the intermediate **II** (**Scheme 4.2**). The subsequent de-*tert*-butylation and rearomatization yield to *p*-

⁶⁰ C. Gaeta, M. Martino, P. Neri, *Tetrahedron Lett.* **2003**, *44*, 9155–9159.

⁶¹ F. Troisi, T. Pierro, C. Gaeta, P. Neri, *Org. Lett.* **2009**, *11*, 697–700.

⁶² C. Gaeta, F. Troisi, C. Talotta, T. Pierro, P. Neri, *J. Org. Chem.* **2012**, *77*, 3634–3639.

alkoxycalix[4]arene **4.5a-k**.⁶³



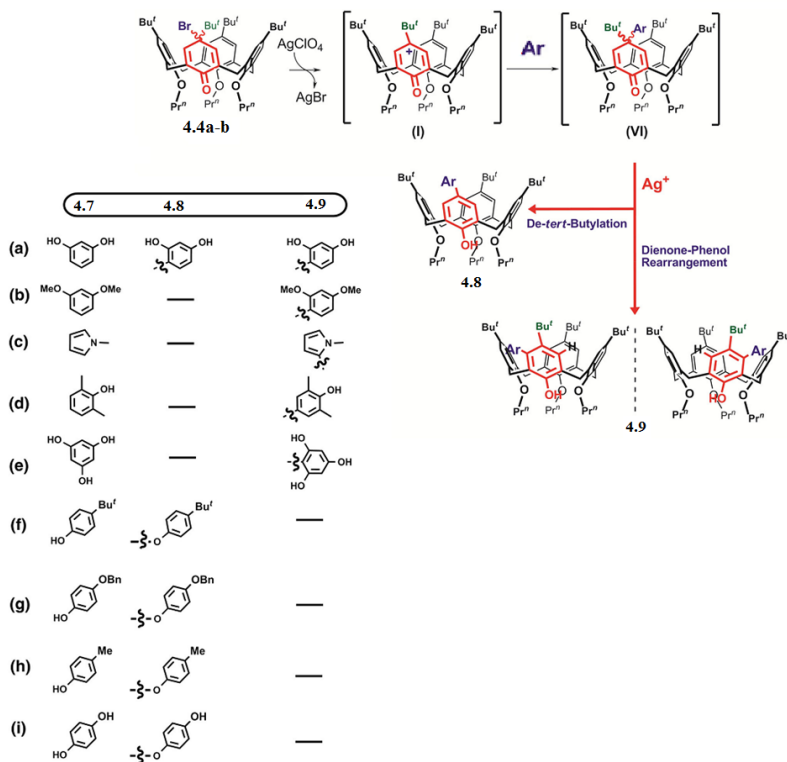
Scheme 4. 2 *p*-bromodienone route with different nucleophiles

An important aspect in the *p*-bromodienone route was observed using activated aromatic rings as nucleophiles.⁵⁹

The reaction with activated aromatic nucleophiles such as resorcinol, pyrrole and 2,6-dimethylphenol led mainly to asymmetrical C–C *meta*-substituted derivatives **4.9a-e** through a dienone–phenol rearrangement of the intermediate

⁶³ C. Gaeta, F. Troisi, C. Talotta, T. Pierro, P. Neri, *J. Org. Chem.* **2012**, *77*, 3634–3639.

dienone derivative (**Scheme 4.3**)⁶⁴.



Scheme 4.3. *p*-bromodienone route with aromatic nucleophiles

The *meta*-substituted derivatives represented typical examples of inherently chiral calixarenes, as they had a three-dimensional asymmetrical structure.

Thus the *p*-bromodienone route provided a good way to obtain inherently chiral calix[4]arenes.

⁶⁴ F. Troisi, T. Pierro, C. Gaeta, M. Carratù, P. Neri, *Tetrahedron letters* **2009**, *50*, 4416-4419.

4.1.3 Chiral and inherently chiral resorcinarenes

The asymmetric *O*-alkylation strategy that is used to synthesise inherently chiral calix[4]arene can be also applied to resorcin[4]arenes.

The inherent chirality can arise from a C_1 , C_2 or C_4 symmetry. C_4 -symmetric adducts result as preferential product, due to the stabilisation of their structures by the maximum number of intramolecular hydrogen bonds.

Resorcinarene **A** (**Figure 4.5**), with four methoxy groups, was obtained exploiting an acid catalysed condensation between 3-methoxyphenol and aldehydes (80% yield).⁶⁵

The Mannich reaction of a resorcinarene with primary amines and formaldehyde was used for preparing tetrabenzoxazines **B**⁶⁶ and then a Mannich reaction modification was used for the synthesis of the inherently chiral resorcinarenes **C** and **D**.⁶⁷

⁶⁵ M. J. McIldowie, M. Mocerino, B. W. Skelton, A. H. White, *Org. Lett.* **2000**, *2*, 3869.

⁶⁶ a) Y. Matsushita, T. Matsui, *Tetrahedron Lett.* **1993**, *46*, 7433-7436; b) R. Arnecke, V. Böhmer, E. F. Paulus, W. Vogt, *J. Am. Chem. Soc.* **1995**, *117*, 3286-3287.

⁶⁷ a) W. Iwanek, M. Urbaniak, B. Gawdzik, V. Schurig, *Tetrahedron: Asymmetry* **2003**, *14*, 2787-2792; b) W. Iwanek, R. Fröhlich, P. Schwab, V. Schurig, *Chem. Commun.* **2002**, 2516-2517.

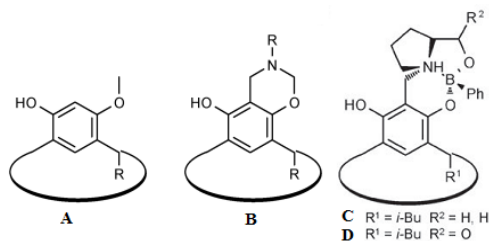


Figure 4. 5. Inherently chiral resorcin[4]arenes.

4.2 AIMS

Considering the importance of the chiral recognition in supramolecular chemistry, another aim of this PhD project has been the study and the synthesis of new macrocycles as powerful host toward ammonium guests recognition.

Therefore the goal was to explore the *p*-bromodienone route on the calix[6]arene scaffold to synthesize chiral and not chiral hosts.

The exploration of new hosts had also the goal of studying inherently chiral resorcinarenes by means of their synthesis separation and chirality identification.

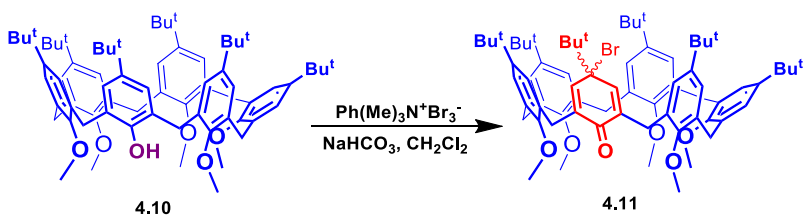
4.2 RESULTS AND DISCUSSION

4.2.1 Synthesis of calixarene hosts via *p*-bromodienone route

With the intent in mind to synthesise new inherently chiral calix[6]arene hosts it was decided to verify the feasibility of the *p*-bromodienone route on partially *O*-alkylated calix[6]arene derivatives.

It was decided to perform the oxidation of the phenol ring of the mono-ol derivative, synthesised as described in the previous section.

Thus the mono-ol was treated (in CH₂Cl₂ at 25 °C) with trimethylphenylammonium tribromide and a saturated solution of NaHCO₃ producing in quantitative yield the first example of calix[6]arene *p*-bromodienone derivative.⁶⁸



Scheme 4. 4. Synthesis of derivative **4.11**

The structure of **4.11** was assigned by means of spectral

⁶⁸ M. De Rosa, A. Soriente, G. Concilio, C. Talotta, C. Gaeta, P. Neri, *J. Org. Chem.* **2015**, *80*, 7295–7300.

analysis.

The ^1H NMR spectrum of *p*-bromodienone derivative **4.11** in CDCl_3 at 298 K (600 MHz) showed signals in agreement with the *p*-bromodienone derivative's structure.

There was the presence of 3 singlets in a 2:2:1 ratio at 1.23, 1.16, and 1.11 ppm, respectively, due to *t*-butyl groups on anisole rings; a broad singlet at 0.86 ppm due to *t*-butyl group on the oxidized *p*-bromodienone ring and a broad singlet at 6.60 ppm due to the dienone H atoms.

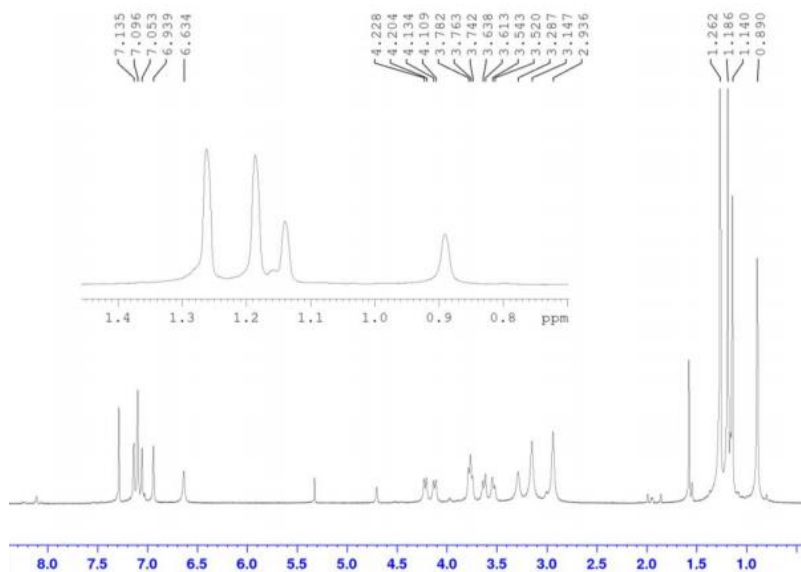


Figure 4.6. ^1H NMR spectrum of derivative **4.11** (600 MHz, CDCl_3 , 298 K).

While the ^{13}C NMR spectrum revealed the $\text{C}=\text{O}$ and $\text{C}-\text{Br}$ signals at 183.7 and 71.3 ppm, respectively.

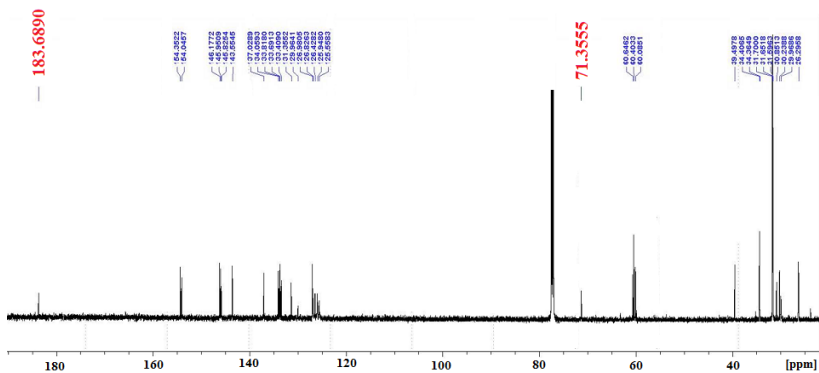


Figure 4.7. ^{13}C NMR spectrum of derivative **4.11** (150 MHz, CDCl_3 , 298 K).

In the synthesis of calix[4]arene *p*-bromodienone they obtained two stereoisomers, namely, the *exo* and *endo* ones, referring to the relative orientation of the Br atom with respect to the calix[4]arene cavity. An analogous stereoisomerism should be expected for calix[6]arene *p*-bromodienone, but its rapid *cone-to-cone* inversion (even with respect to the NMR timescale) led to the mutual interconversion between *exo*- and *endo*-**4.11** stereoisomers

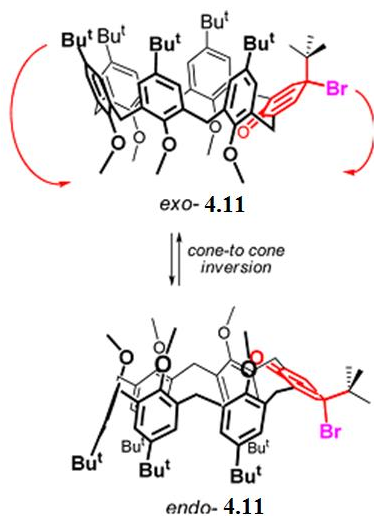
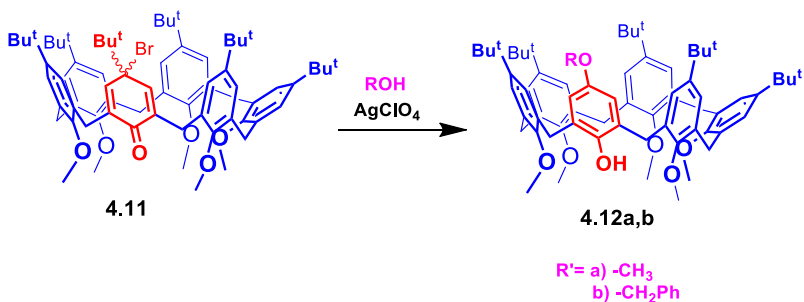


Figure 4. 8. *Cone-to-cone* inversion of derivative **4.11**

The ^1H NMR showed a temperature dependent behaviour due to the *through-the-annulus* rotation of the anisole and *p*-bromodienone rings.

The lowering of the temperature at 233 K gave a very complicated ^1H NMR spectrum corresponding to the presence of the two *exo*-/*endo* stereoisomers in different conformations. At this point the *p*-bromodienone route was preliminarily tested with small and simple *O*-nucleophiles such as methanol and benzyl alcohol.



Scheme 1. *p*-bomodienone route

The derivative **4.11** was treated with a methanolic solution of AgClO₄ at 0°C to give *p*-methoxycalix[6]arene **4.12a** in 20% yield, after usual workup.

The ESI(+) mass spectrum confirmed the molecular formula, while the C_s molecular symmetry was assigned by pertinent signals in the ¹H and ¹³C NMR spectra.

In particular, from the ¹H NMR spectrum there was a clear displacement of a *t*-Bu group by a methoxyl one, which was corroborated by the presence of four singlets due to OMe groups.

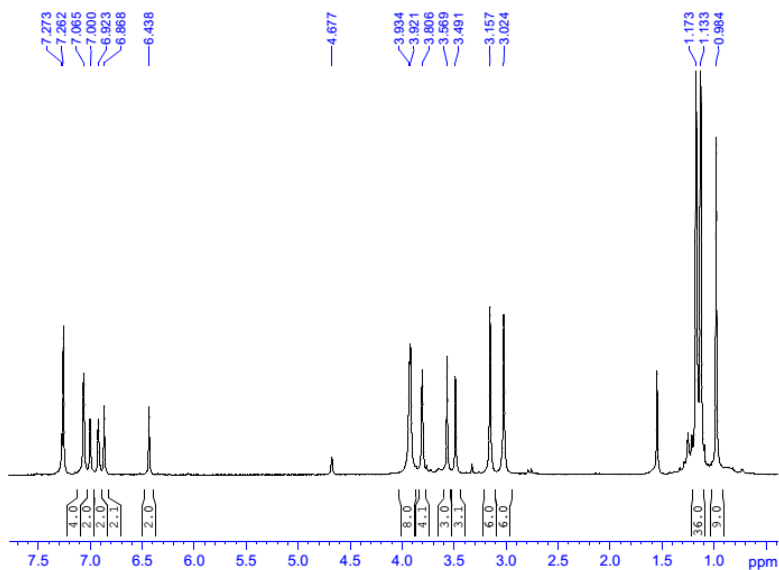


Figure 4.9. ^1H NMR spectrum of derivative **4.12a** (400 MHz, CDCl_3 , 298 K).

The reaction of the derivative with benzylic alcohol was conducted by treating the *p*-bromodienone derivative **4.11** with BnOH in the presence of AgClO_4 in DME as solvent. The obtaining of the desired product was confirmed by spectral analysis, in particular the ^1H NMR spectrum of **4.12b** showed the singlet at 4.73 ppm due to OCH_2Ph group, which was indicative of the displacement of the t-Bu group.

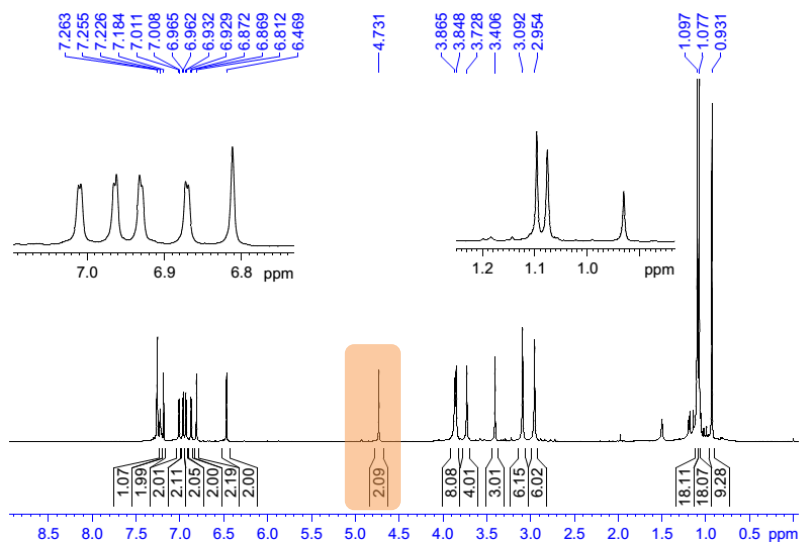


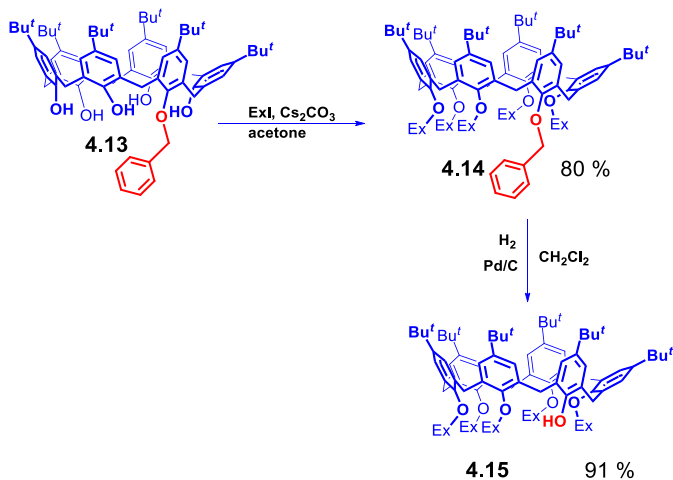
Figure 4.10. ^1H NMR spectrum of derivative **4.12b** (400 MHz, CDCl_3 , 298 K).

The ^{13}C NMR spectrum of **4.12b** confirmed the C_s molecular symmetry by the presence of three signals due to ArCH_2Ar groups at 29.7, 30.3, and 31.2 ppm, three signals due to $-\text{C}(\text{CH}_3)_3$ C atoms at 31.3, 31.4, and 31.6 ppm, and one resonance at 70.2 ppm due to OCH_2Ph group.

At this point, to extend the generality of the *p*-bromodienone route on calix[6]arene macrocycle, it was decided to test another calixarene scaffold.

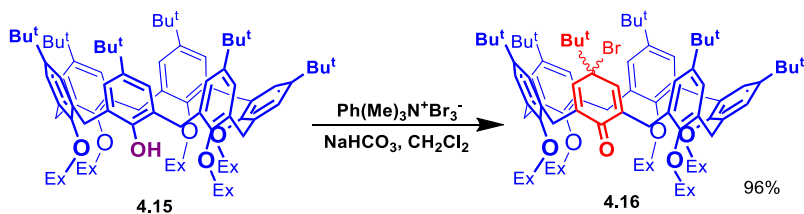
Thus the derivative **4.13** was exhaustively alkylated by treatment with Cs_2CO_3 and 1-iodohexane in acetone as solvent, to give derivative **4.14** in 80% yield. Successively, the benzyl group at the *endo* rim of **4.14** was removed by hydrogenolysis (H_2 and Pd/C) to give pentahexyloxy-mono-ol

4.15 in 91% yield.



Scheme 4.5 Synthesis of derivative **4.15**

Treatment of pentahexyloxycalix[6]arene-mono-ol **4.15** under conditions analogous to the synthesis of **4.11** led to the formation of derivative **4.16** in 96% yield.

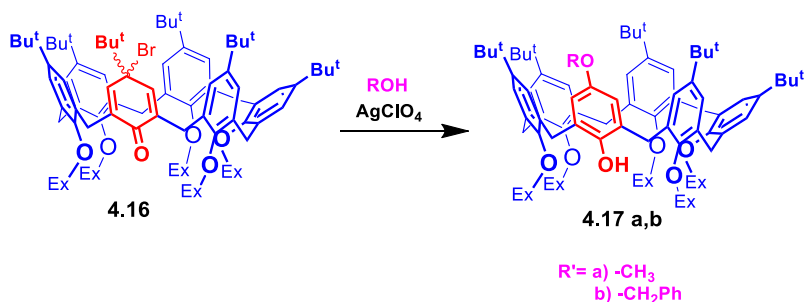


Scheme 4.6 Synthesis of derivative **4.16**

The ESI(+) mass spectrum confirmed the molecular formula of **4.16**. The ^1H NMR spectrum in TCDE at 298 K showed 4

broad singlets due to *t*-butyl groups at 0.71 (9H), 0.99 (18H), 1.13 (9H), and 1.31 (18H) ppm, while broad signals were present in the methylene region indicating a slow conformational interconversion on the NMR time scale.

Analogously to *p*-bromodienone derivative **4.11**, the treatment of **4.16** with a methanolic solution of AgClO₄ afforded *p*-methoxycalix[6]arene **4.17a** in 15% yield, while its treatment with benzylic alcohol afforded derivative **4.17b** in 17% yield (**Scheme 4.7**).

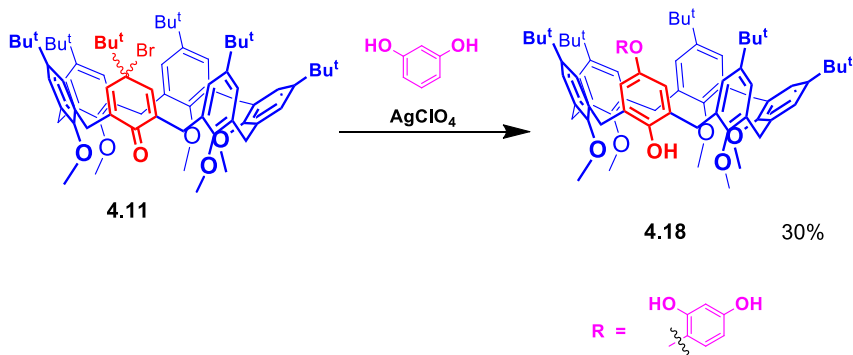


Scheme 4.7 Synthesis of derivative **4.17a-b**

As already reported in the introduction section, the *p*-bromodienone route with active aromatic substrates (e.g: resorcinol) gives a *meta* substitution after a dienone-phenol rearrangement.

At this point the *p*-bromodienone route was tested with resorcinol with the intent to verify, also in this case, the *meta* substitution, obtaining an inherently chiral host.

Thus, the treatment of **4.11** with resorcinol and a cold solution of AgClO_4 afforded *meta*-substituted calix[6]arene **4.18** in 30% yield.



Scheme 4.8. Synthesis of derivative **4.18**

1D and 2D NMR spectra were in agreement with the asymmetrical structure of **4.18**, in which the resorcinol and *t*-Bu groups were, respectively, *meta*- and *para*-linked to the calixarene phenol ring.

In fact, five of the expected six *t*-Bu singlets (two accidentally isochronous) were present in the ^1H NMR spectrum (CDCl_3 , 400 MHz, 298 K) of **4.18** at 1.12, 1.15(18H), 1.19, 1.21, and 1.33 ppm, while five singlets due to ArCH_2Ar groups were present at 3.83, 3.97, 4.07, 4.10 (4H), and 4.12 ppm, which correlated in the HSQC spectrum with carbon resonances at 31.8, 32.6, 30.2 (2C), 30.3, and 29.9 ppm.

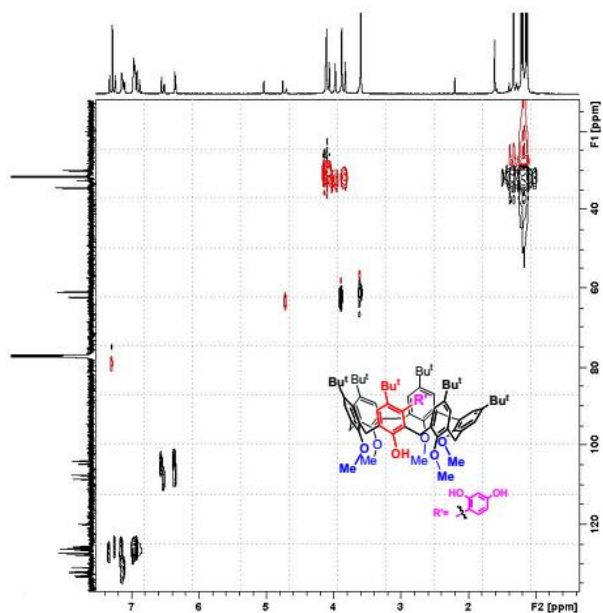


Figure 4. 11 HSQC spectrum of **4.18** (600 MHz, CDCl₃, 298 K).

In addition, the ¹³C NMR spectrum evidenced five signals due to -C(CH₃)₃ atoms at 31.50, 31.51 (2C), 31.54, 31.56, and 31.77 ppm, and four signals due to OMe groups at 60.93, 60.98(2C), 62.27, and 62.34 ppm, which correlated in the HSQC spectrum with singlets at 3.60 (9H), 3.87, and 3.88 ppm.

The asymmetric structure of **4.18** coupled with its three-dimensional nature makes it inherently chiral, and consequently, it should be formed as a racemic mixture.

A rapid *cone-to-cone* inversion of the calix[6]arene skeleton of **4.18** leads to the interconversion between the two enantiomers.

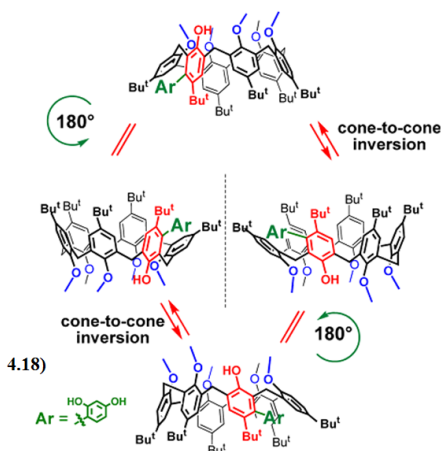


Figure 4.12. *Cone-to-cone* inversion of derivative **4.18**.

The inherently chiral derivative **4.18** was also tested in complexation experiments with some alkylbenzylammonium·TFPB⁻ guests but unfortunately it did not give the formation of the [2]pseudorotaxane desired.

This was probably due to the encumbrance of the resorcinol group that did not allow the entrance of the guest into the calixarene cavity.

4.2.2 Synthesis of inherently chiral resorcin[4]arene

The research of new potential chiral hosts went on with the synthesis of some inherently chiral resorcin[4]arenes.

With this intent in mind it was used the regioselective *O*-

substitution procedure already experimented by Neri et al.⁶⁹

However this synthetic procedure gives chiral resorcinarenes in racemic form. Thus the use of these compounds as supramolecular chiral hosts or building blocks requires their separation and identification of their chirality.

Therefore the synthesis of inherently chiral resorcin[4]arenes was followed by HPLC separation and EDC analyses supported by computational techniques.⁷⁰

The regioselective *O*-substitution procedure started with resorcin[4]arene octol **4.19**. It was subjected to alkylation with an excess of benzylbromide (10 equiv) in the presence of K₂CO₃ (4 equiv) as the weak base in acetone at reflux.

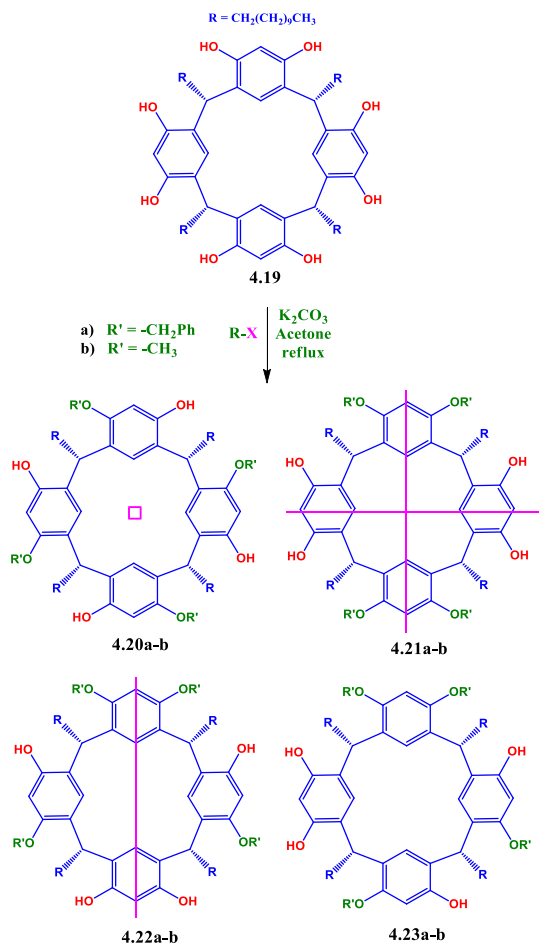
Column chromatography of the crude reaction mixtures afforded four *tetra-O*-benzylated derivatives, namely, **4.20a** (8%), **4.21a** (26%), **4.22a** (9%), and **4.23a** (23%) and four *tetra-O*-methylated derivatives (Scheme 16).

In the same way resorcin[4]arene octol **4.19** was subjected to alkylation with methyl iodide (50 equiv) in the presence of K₂CO₃ (4 equiv) at reflux.

Column chromatography of the crude reaction mixtures afforded four *tetra-O*-methylated derivatives, namely, **4.20b** (9%), **4.21b** (25%), **4.22b** (11%), and **4.23b** (30%) (Scheme 16).

⁶⁹ F. Farina, C. Talotta, G. Gaeta, P. Neri, *Org. Lett.* **2011**, *13*, 4842–4845.

⁷⁰ a) N. Berova, *Comprehensive Chiroptical Spectroscopy*, Ed., Wiley, Hoboken, NJ, **2012**; b) J. Autschbach, *Chirality* **2009**, *21*, E116–E152.



Scheme 4 9 Synthesis of the inherently chiral derivative **4.20a-b**, **4.20a-b**, **4.20a-b** and **4.20a-b**

Structure assignment for the *O*-substituted resorcin[4]arenes counted essentially on spectral analysis.

The tetra-substitution was confirmed by ESI(+) MS spectra, while the assignment of the substitution pattern was based on a careful analysis of ^1H and ^{13}C NMR data assisted by 2D NMR experiments.

The chirality of the derivative **4.20a** in particular its C_4 symmetry was proved by the presence in the ^1H NMR spectrum of one signal for the bridging methine groups, two singlets for the upper and lower ArH protons, and one resonance for benzylic OCH_2 groups.

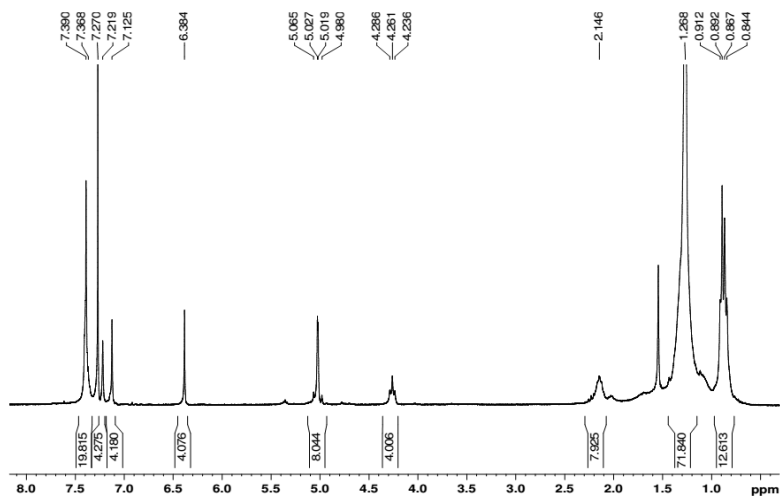


Figure 4.13 ^1H NMR spectrum of derivative **4.20a** (300 MHz, CDCl_3 , 298 K).

The unsymmetrical 1,2,4,6-substitution pattern of **4.23a**, evidenced by eight ArH singlets, was also assigned by considering the presence of four isolated OH signals (7.08, 6.98, 6.86, and 6.82 ppm) only compatible with the 1,2,4,6-tetrasubstitution (**Figure 4.14**).

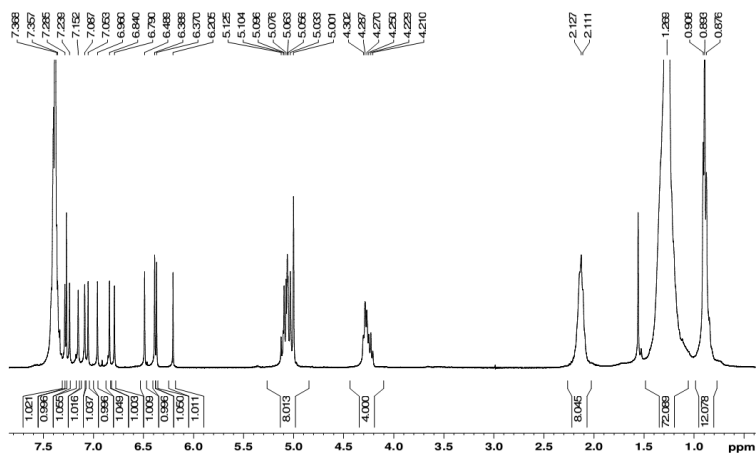
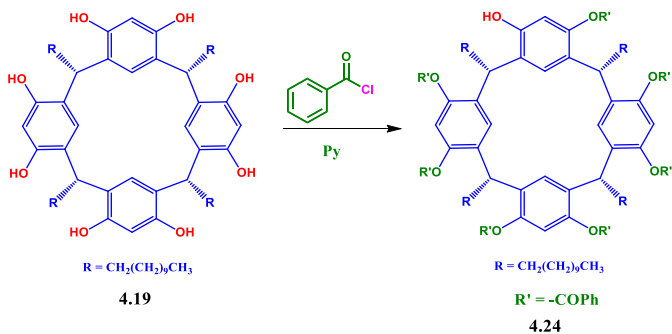


Figure 4. 14 ^1H NMR spectrum of derivative **4.23a** (400 MHz, CDCl_3 , 298 K).

The *epita-O*-substituted resorcinarene is another type of inherent chiral derivative and it was synthesised with the aroylation of the resorcin[4]arene octol.

Thus, the aroylation of resorcin[4]arene **4.19** with benzoyl chloride (10 equivalent) in pyridine was then used for the synthesis of the inherently chiral derivative **4.24** (Scheme 17).



Scheme 4. 10. Synthesis of the inherently chiral derivative **4.24**
 The derivative **4.24** was fully characterised, by MS and NMR

spectroscopy as in the previous cases for the other derivatives.

4.2.3 HPLC-EDC analysis and Computational Spectroscopy

According to the “racemic approach”⁷¹, the semi-preparative resolution of the enantiomers of compounds **4.20a**, **4.20b**, and **4.23b** was performed by enantioselective HPLC using a Chiralpak AD column in normal-phase conditions (*n*-hexane/2-propanol mixtures, proportions ranging from 97:3 to 99:1 v/v, flow rates 1 mL min⁻¹).

The resolution of derivatives **4.23a** was performed using a Lux Amylose-2 column in normal-phase conditions (*n*-hexane/methanol 96:4 v/v, flow rates 1 mL min⁻¹), while the resolution of derivatives **4.24** was performed using a Lux Cellulose-1 column in normal-phase conditions (*n*-hexane/2-propanol 97:3 v/v, flow rates 1 mL min⁻¹),

The ECD analysis were performed investigating the hyphenation of enantioselective HPLC with a ECD spectropolarimeter with the possibility of on-line measurements.

The so called “stopped-flow” technique allows a reliable on-line ECD analysis with limited loss in spectral resolution and the additional advantage of reduced amounts of racemate

⁷¹ E. R. Francotte, *J. Chromatogr. A* **2001**, 906, 379-397.

necessary for the analysis: under optimized conditions, in general, sub-milligram quantities of racemate may be sufficient depending on the spectroscopic properties of the analyte.

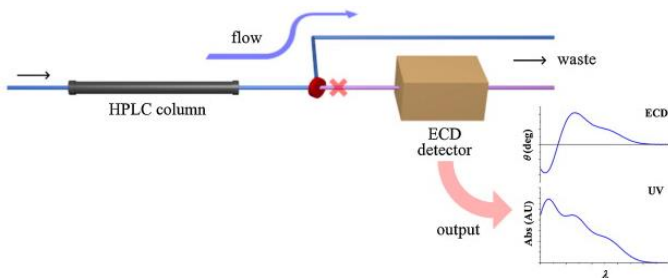


Figure 4.15 Schematic representation of stopped-flow HPLC-ECD system.

Moreover, on-line ECD analysis allowed avoiding fraction collection/solvent evaporation cycles, where impurities in the mobile phase components can be accumulated and degradation can be promoted, affecting the reliability of the subsequent off-line ECD analysis.

The HPLC-ECD analysis were a result of a collaboration with the prof. Bertucci's group from Università di Bologna; the interpretation of the ECD analysis is summarized in the graphic below.

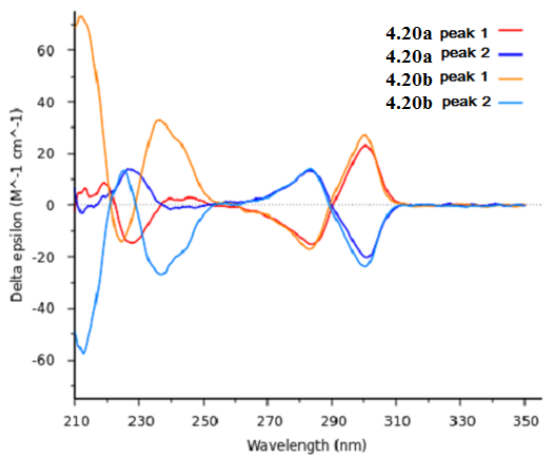


Figure 4. 16 ECD spectra of **4.20a** and **4.20b** (1,3,5,7-*O*-substitution pattern).

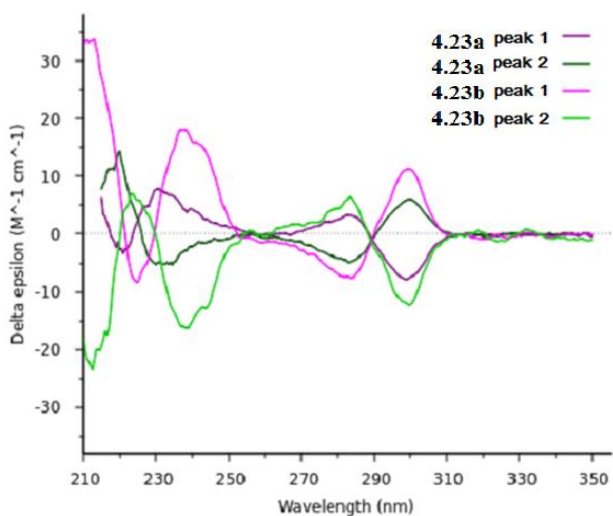


Figure 4. 17 ECD spectra of **4.23a** and **4.23b** (1,2,4,6-*O*-substitution pattern).

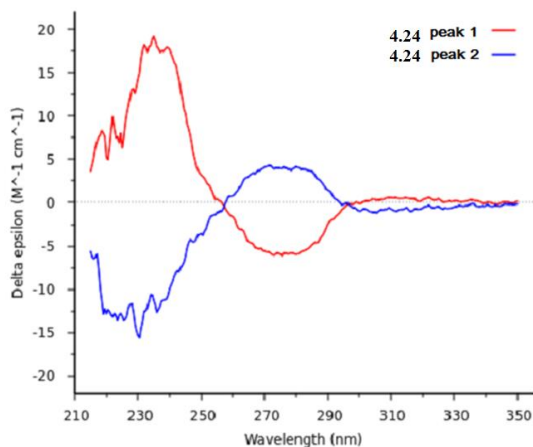


Figure 4. 18 ECD spectra of **4.24**

The recorded spectra displayed an excellent signal-to-noise ratio and limited baseline drift even at shorter wavelengths.

The enantiomers of tetra-*O*-substituted calix[4]resorcinarenes show a CD exciton couplet centred at the absorption maximum of the aromatic 1L_b transitions, due to the coupling between resorcinol rings in the calix[4]resorcinarene skeleton, Methyl substituents did not contribute to the CD profile of calix[4]resorcinarenes, whose CD intensity is only affected by the *O*-substitution pattern.

Benzyl groups contribute to the CD profile of calix[4]resorcinarenes in the short-wavelength spectral region. The ECD spectra have then been computed by TDDFT at the B3LYP/6-31++G* and PBE0/6-31++G* levels and were a result of a collaboration with the prof. Zanasi's group from Università degli Studi di Salerno.

The spectrum below is only an example of the good agreement between the experimental CD curve and the theoretical one calculated for the derivative R (*M*) **4.20a**.

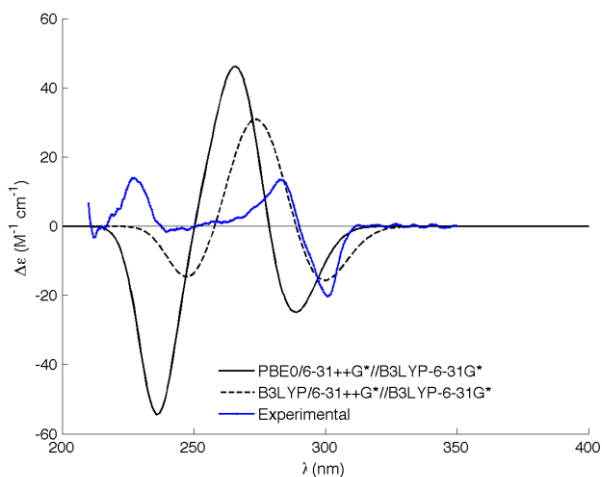


Figure 4. 19 Experimental and theoretical CD curve calculated for the derivative R (*M*) **4.20a**

4.3 CONCLUSION

In this part it was studied the *p*-bromodienone route for the first time on the calix[6]arene scaffold demonstrating that this strategy of functionalization is also effective for the functionalization of the calix[6]arene macrocycle.

Therefore, through this route it was possible to introduce alcoholic *O*-nucleophiles at the calix[6]arene *exo* rim.

In addition, the *p*-bromodienone route with activated aromatic substrates allowed the first example of *meta* functionalization of a calix[6]arene macrocycle giving rise to an unprecedented *meta*-substituted inherently chiral calix[6]arene derivative.

Some other inherently chiral hosts resorcinarene based were synthesised using a regioselective *O*-substitution procedure.

This synthetic strategy gave the chiral hosts in racemic mixture and for this reason any application of them required the separation and identification of their chirality.

The HPLC separation as well as the ECD analysis and interpretation was realised in collaboration with the prof. Bertucci's group from University of Bologna.

The ECD spectra have then been studied by computational calculations in collaboration with the prof. Zanasi's group from University of Salerno.

4.4 EXPERIMENTAL SECTION

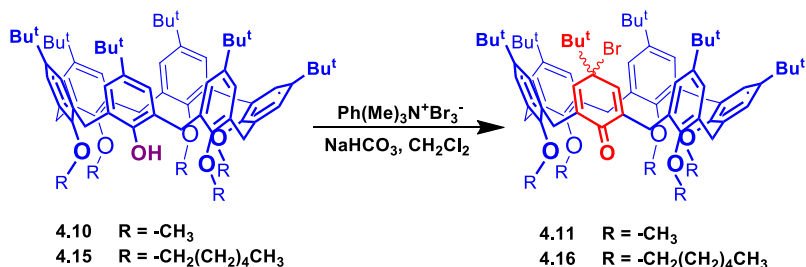
ESI(+) –MS measurements were performed on a quadrupole mass spectrometer equipped with electrospray ion source, using a mixture of H₂O/CH₃CN (1:1) and 5% HCOOH as solvent. Flash chromatography was performed on Merck silica gel (60, 40-63 μm). All chemicals were reagent grade and were used without further purification. Anhydrous solvents were purchased from Aldrich. When necessary compounds were dried in vacuum over CaCl₂. Reaction temperatures were measured externally. Reactions were monitored by TLC on Merck silica gel plates (0.25 mm) and visualized by UV light, or by spraying with H₂SO₄-Ce(SO₄)₂ or phosphomolybdic acid.

1D and 2D NMR spectra were recorded on a Bruker Avance-600 spectrometer [600 (1H) and 150 MHz (13C)], Bruker Avance-400 spectrometer [400 (1H) and 100 MHz (13C)] and Bruker Avance-300 spectrometer [300 (1H) and 75 MHz (13C)]; chemical shifts are reported relative to the residual solvent peak (CHCl₃: δ 7.26, CDCl₃: δ 77.23; CD₃OH: δ 4.87, CD₃OD: δ 49.0). HSQC spectra were performed with gradient selection, sensitivity enhancement, and phase-sensitive mode using Echo/Antiecho-TPPI procedure. A typical experiment comprised 20 scans with 113 increments of 2048 points each. Derivatives **4.19**, **4.20a-b**, **4.21a-b**, **4.22a-b**, **4.23a-b** and

4.24 were synthesized according to a literature procedure⁶⁹

The spectroscopic analysis was performed using the stopped-flow HPLC-CD technique on an HPLC system consisting of a Jasco PU- 980 pump, a LG-2080-02 ternary gradient unit, a DG-2080-53 degasser a Jones (Lakewood, CO) model 7955 column chiller, a Rheodyne (Cotati, CA) 7725i syringe loading injector, and a 20 μ L sample loop; this system was connected to the Jasco J-810 spectropolarimeter, equipped with a 10 mm path length HPLC flow cell and a Rheodyne 7010 injector setup as a three-way valve for stopped-flow measurements.

General Procedure for the Synthesis of *p*-bromodienone derivatives **4.11** and **4.16**



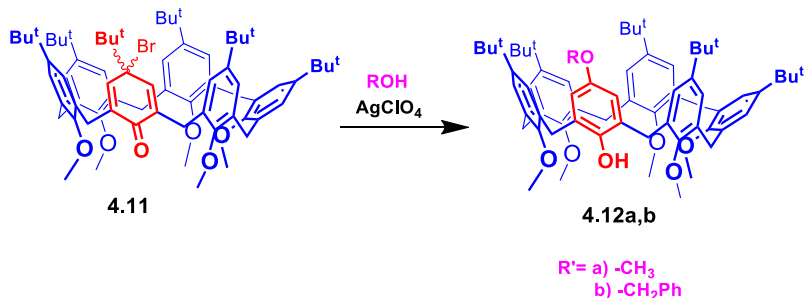
A solution of phenyltrimethylammonium tribromide (0.13 g, 0.36 mmol) in CH₂Cl₂ (5.0 mL) was added dropwise over 15 min to a stirred solution at 0 °C of the appropriate pentaalkoxy-calix[6]arene-mono-ol **4.10** or **4.15** (0.24 mmol) in CH₂Cl₂ (24 mL). Then, 25 mL of a saturated aqueous solution of NaHCO₃ was added and the resulting mixture was stirred for 15 min at room temperature. The organic phase was separated and washed with an aqueous solution of Na₂SO₃ (10% wt) and H₂O. The organic phase was dried over Na₂SO₄ and filtered, and the solvent was removed under reduced pressure, to give the corresponding calix[6]arene *p*-bromodienone derivative **4.11** or **4.16** in quantitative yield.

Derivative **4.11** (0.26 g, 99%). **ESI(+)** **MS**: *m/z* = 1143 (MNa⁺), 1159 (MK⁺). **¹H NMR** (600 MHz, CDCl₃, 298 K): δ 0.86 [s, -C(CH₃)₃, 9H], 1.11 [s, C(CH₃)₃, 9H], 1.16 [s, -C(CH₃)₃, 18H], 1.23 [s, C(CH₃)₃, 18H], 2.90 (br s, OCH₃,

6H), 3.11 (br s, OCH₃, 6H), 3.25 (br s, OCH₃, 3H), 3.51 and 3.60 (AB, ArCH₂Ar, J = 15.0 Hz, 4H), 3.71 and 4.09 (AB, ArCH₂Ar, J = 14.8 Hz, 4H), 3.74 and 4.20 (AX, ArCH₂Ar, J = 14.6 Hz, 4H), 6.60 (s, C=CH, 2H), 6.91 (br s, ArH, 2H), 7.03 (br s, ArH, 2H), 7.07 (br s, ArH, 4H), 7.11 (br s, ArH, 2H). ¹³C NMR (150 MHz, CDCl₃, 298 K): δ 26.3, 30.0, 30.2, 30.8, 31.59, 31.6, 31.7, 34.3, 34.4, 39.5, 60.1, 60.4, 60.6, 71.3, 125.5, 125.9, 126.4, 126.8, 127.0, 130.0, 131.3, 133.4, 133.7, 133.8, 134.0, 137.0, 143.5, 145.8, 145.9, 146.2, 146.2, 154.0, 154.3, 183.7.

Derivative 4.16 (0.34 g, 96%). **ESI(+)** MS: m/z = 1494 (MNa⁺). ¹H NMR (300 MHz, TCDE, 298 K): δ 0.71 [broad, -C(CH₃)₃, 9H], 0.89 [br s, O(CH₂)₅CH₃, 15H], 0.99 [s, -C(CH₃)₃, 18H], 1.13 [s, -C(CH₃)₃, 9H], 1.16 - 1.19 (overlapped, OCH₂CH₂CH₂CH₂CH₂CH₃, 30H), 1.31 [s, -C(CH₃)₃, 18H], 1.52 - 1.98 (overlapped, OCH₂CH₂CH₂CH₂CH₂CH₃, 10H), 2.92 - 2.95 (broad, OCH₂CH₂CH₂CH₂CH₂CH₃, 2H), 2.98 - 3.46 (overlapped, ArCH₂Ar + OCH₂CH₂CH₂CH₂CH₂CH₃, 14H), 4.28 - 4.34 (overlapped, ArCH₂Ar, 6H), 6.61 - 7.07 (overlapped, ArH + C=CH, 12H). ¹³C NMR (150 MHz, CDCl₃, 298 K): δ 14.4, 14.5, 22.8, 22.9, 26.0, 26.2, 29.7, 29.9, 30.5, 30.7, 31.7, 31.8, 32.1, 32.3, 34.3, 38.9, 83.9, 74.2, 126.7, 126.2, 126.5, 127.0, 127.6, 131.1, 132.8, 133.2, 134.1, 136.6, 144.3, 145.1, 145.5, 153.5, 154.1, 183.7.

General Procedure for the Synthesis of Derivatives **56a–b**.



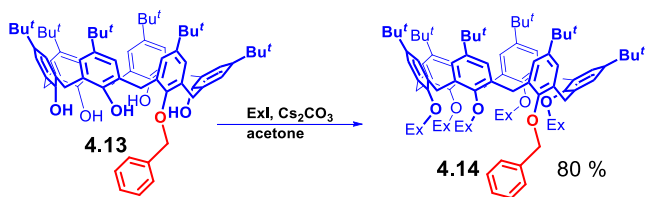
A solution of AgClO₄ (0.048 g, 0.23 mmol) in the appropriate alcohol (1.6 mL of methanol or benzylic alcohol) was cooled at 0 °C and added to solid **4.11** (0.13 g, 0.12 mmol). The reaction mixture was allowed to warm at room temperature and stirred in the dark overnight. The solvent was removed under reduced pressure, and the residue was solubilized in CH₂Cl₂ (10 mL). The organic phase was washed 3 times with water, dried on Na₂SO₄, and filtered, and the solvent was removed under reduced pressure.

Derivative 4.12a. The crude product was purified by preparative thin layer chromatography, eluent n-hexane/diethyl ether/methanol 80/20/1 (v/v) to give **4.12a** as a white solid, 0.025 g, yield 20%. **ESI(+)** MS: m/z = 1017 (MH⁺). **¹H NMR** (400 MHz, CDCl₃, 298 K): δ 0.98 [s, -C(CH₃)₃, 9H], 1.13 [s, -C(CH₃)₃, 18H], 1.17 [s, -C(CH₃)₃, 18H], 3.02 (s, OCH₃, 6H), 3.15 (s, OCH₃, 6H), 3.49 (s, OCH₃, 3H), 3.57 (s, OCH₃, 3H), 3.81 (s, ArCH₂Ar, 4H), 3.93 (br

s,ArCH₂Ar, 8H), 6.44 (s, ArH, 2H), 6.87 (s, ArH, 2H), 6.92 (s, ArH,2H), 7.00 (s, ArH, 2H), 7.06 (s, ArH, 4H), 7.27 (s, OH, 1H). ¹³C NMR (CDCl₃, 100 MHz, 298 K): δ 30.5, 31.4, 31.5, 31.7, 34.2, 34.3,55.3, 60.6, 60.9, 113.2, 125.6, 126.3, 126.5, 129.0, 132.5, 133.2, 133.4,133.6, 133.8, 145.4, 145.8, 145.9, 146.7, 152.6, 153.2, 154.1, 154.4.

Derivative 4.12b . The crude product was purified by column chromatography on silica gel using CHCl₃/n-hexane (96/4, v/v) as eluent to give **4.12b** as a colourless solid, 0.040 g, 30% yield. **ESI(+)** **MS**: m/z = 1093 (MH⁺). **¹H NMR** (600 MHz, CDCl₃,298 K): δ 0.93 [s, -C(CH₃)₃, 9H], 1.08 [s, -C(CH₃)₃, 18H], 1.10 [s, C(CH₃)₃, 18H], 2.95 (s, OCH₃, 6H), 3.09 (s, OCH₃, 6H), 3.41 (s,OCH₃, 3H), 3.73 (s, ArCH₂Ar, 4H), 3.85 (bs, ArCH₂Ar, 8H), 4.73 (s,OCH₂Ph, 2H), 6.47 (s, ArH, 2H), 6.81 (s, ArH, 2H), 6.87 and 7.01(AB, ArH, J = 2.04 Hz, 4H), 6.93 and 6.96 (AB, ArH, J = 2.04 Hz,4H), 7.18 -7.21 (overlapped, OCH₂C₆H₅ + OH, 6H). **¹³C NMR** (150MHz, CDCl₃, 298 K): δ 29.7, 30.3, 31.2, 31.3, 31.4, 31.6, 31.9, 34.05,34.1, 60.3, 60.7, 70.2, 114.2, 125.4, 125.7, 125.9, 126.1, 126.4, 127.5,127.7, 128.4, 128.6, 128.7, 132.2, 133.0, 133.2, 133.4, 133.6, 133.7,137.4, 145.2, 145.6, 146.0, 146.5, 151.8, 153.0, 154.0, 154.3.

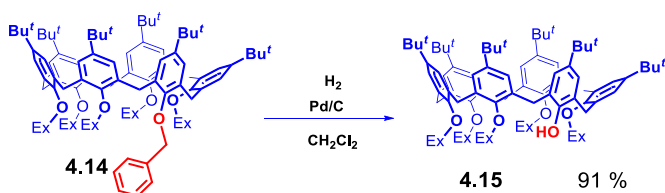
Synthesis of Derivative **37**



Cs_2CO_3 (9.8 g, 30 mmol) was added, under stirring, to a solution of compound **4.13** (1.2 g, 1.1 mmol) in dry acetone (60 mL), and the mixture was heated at reflux. After 30min, 1-iodohexane (15 g, 10 mL, 70 mmol) was added and the resulting mixture was kept at reflux under stirring for 48 h. The reaction was allowed to cool at room temperature and the solvent removed under reduced pressure. The crude product was solubilized in CH_2Cl_2 , washed with aqueous 1N HCl and brine, and then dried over Na_2SO_4 . The solvent was evaporated to dryness, and the product was crystallized from $\text{MeOH}/\text{CH}_2\text{Cl}_2$ to give **4.14** as a pale yellow solid (1.32g, 80% yield). **ESI(+)** **MS**: $m/z = 1485$ (MH^+), 1507 (MNa^+), 1522 (MK^+). **^1H NMR** (300 MHz, TCDE, 383 K): δ 0.77 [broad, $\text{O}(\text{CH}_2)_5\text{CH}_3$, 15H], 0.94 [s, $-\text{C}(\text{CH}_3)$, 9H], 0.95 [s, $-\text{C}(\text{CH}_3)$, 18H], 1.04 [s, $-\text{C}(\text{CH}_3)$, 27H], 1.10–1.25 (overlapped, $\text{OCH}_2\text{CH}_2\text{CH}_2\text{CH}_2\text{CH}_2\text{CH}_3$, 30H), 1.35–1.60 (overlapped, $\text{OCH}_2\text{CH}_2\text{CH}_2\text{CH}_2\text{CH}_2\text{CH}_3$, 10H), 3.28 (broad, $\text{OCH}_2\text{CH}_2\text{CH}_2\text{CH}_2\text{CH}_2\text{CH}_3$, 4H), 3.39 (broad, $\text{OCH}_2\text{CH}_2\text{CH}_2\text{CH}_2\text{CH}_2\text{CH}_3$, 4H), 3.48 (t, $\text{OCH}_2\text{CH}_2\text{CH}_2\text{CH}_2\text{CH}_2\text{CH}_3$, J = 6.5 Hz, 2H), 3.79 (broad s,

ArCH₂Ar, 12H), 4.67 (s, OCH₂Ph, 2H), 6.77 (s, ArH, 2H), 6.83 (s, ArH, 4H), 6.90 (s, ArH, 4H), 6.94 (s, ArH, 2H), 7.16 –7.21 (overlapped, OCH₂C₆H₅, 3H), 7.30 –7.35 (m, OCH₂C₆H₅, 2H). **¹³CNMR** (75 MHz, TCDE, 383 K): δ 12.2, 20.8, 24.2, 28.1, 28.3, 28.4, 28.9, 29.7, 30.0, 32.1, 71.7, 73.0, 123.7, 123.9, 124.3, 124.6, 124.8, 125.6, 126.4, 131.1, 131.2, 136.5, 143.1, 143.6, 150.9, 151.6, 152.0.

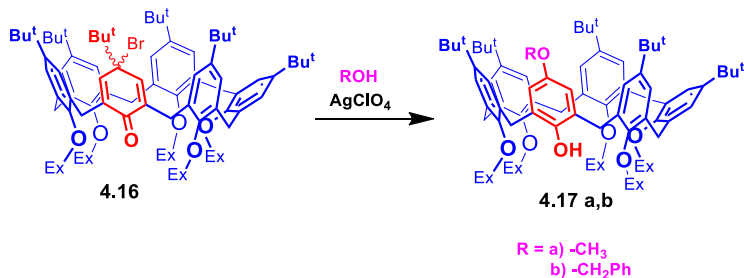
Synthesis of Derivative **4.15**



A solution of **4.14** (1.3 g, 0.89 mmol) in CHCl₃ (80 mL) was added of Pd/C, and the mixture stirred for 12h under H₂ at 25 °C. The catalyst was filtered on a Celite pad, and the filtrate was evaporated under vacuum. Precipitation of the residue from methanol gave pure **4.15** as a yellow solid (1.13 g, 91% yield). **ESI(+)** MS: m/z = 1417 (MNa⁺), 1434 (MK⁺). **¹H NMR** (300 MHz, TCDE, 383 K): δ 0.70 [s, –C(CH₃), 9H], 0.77 [broad, O(CH₂)₅CH₃, 15H], 0.94 [s, –C(CH₃), 9H], 1.12 [s, –C(CH₃), 18H], 1.15 [s, –C(CH₃), 18H], 1.06 –1.40 (overlapped, OCH₂CH₂CH₂CH₂CH₂CH₃, 30H), 1.59 –1.70 (overlapped, OCH₂CH₂CH₂CH₂CH₂CH₃, 10H), 3.09 (broad

t, $\text{OCH}_2\text{CH}_2\text{CH}_2\text{CH}_2\text{CH}_2\text{CH}_3$, 4H), 3.60 (t, $\text{OCH}_2\text{CH}_2\text{CH}_2\text{CH}_2\text{CH}_2\text{CH}_3$, $J = 7.2$ Hz, 2H), 3.71 –3.76 (overlapped, $\text{ArCH}_2\text{Ar} + \text{OCH}_2\text{CH}_2\text{CH}_2\text{CH}_2\text{CH}_2\text{CH}_3$, 16H), 6.41, (br s, ArH,2H), 6.54 (br s, ArH, 2H), 6.57 (br s, OH, 1H), 6.77 (s, ArH, 2H), 6.91 (s, ArH, 2H), 6.96 (br s, ArH, 2H), 7.00 (br s, ArH, 2H). $^{13}\text{CNMR}$ (75 MHz, TCDE, 383 K): δ 11.9, 12.0, 20.6, 20.9, 24.0, 27.9,28.4, 28.6, 29.5, 29.6, 29.8, 30.0, 32.0, 32.1, 71.7, 122.7, 123.0, 124.4,124.5, 125.3, 130.2, 131.2, 131.8, 140.1, 142.6, 143.0, 143.1, 144.0,149.3, 149.9, 151.7, 152.4.

General Procedure for the Synthesis of Derivatives **4.17a-b**.



A solution of AgClO_4 (0.048 g, 0.23 mmol) in the appropriate alcohol (1.6 mL) at 0 °C was added to the solid *p*-bromodienone derivative **4.16** (0.18 g, 0.12 mmol). The reaction mixture was allowed to warm at room temperature and stirred in the dark overnight. The solvent was removed under reduced pressure, and the residue was solubilized in

CH₂Cl₂ (10 mL). The organic phase was washed 3 times with water, dried on Na₂SO₄, and filtered, and the solvent was removed under reduced pressure.

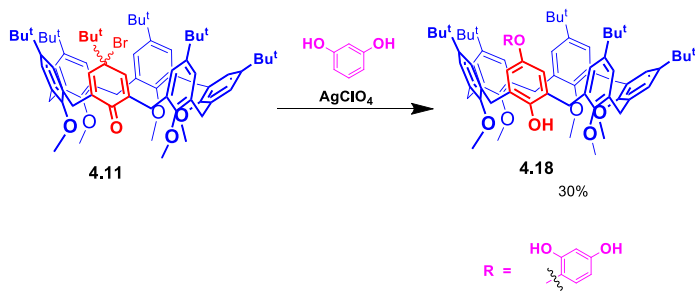
Derivative 4.17a. The crude product was purified by column chromatography on silica gel using CHCl₃/n-hexane 96/4 as eluent to give **4.17a** as a white solid, 0.025 g, 15% yield.

ESI(+)MS: m/z = 1369 (MH⁺), 1391 (MNa⁺). **¹H NMR** (300 MHz, TCDE, 393 K): δ 0.79 [broad, O(CH₂)₅CH₃, 15H], 0.87 [s, -C(CH₃)₃, 18H], 0.99 [s, -C(CH₃)₃, 9H], 1.14 [s, -C(CH₃)₃, 18H], 1.14 -1.73 (overlapped, OCH₂CH₂CH₂CH₂CH₂CH₃, 40H), 3.17 (br t, OCH₂CH₂CH₂CH₂CH₂CH₃, 2H), 3.60 -3.80 (overlapped, ArCH₂Ar+ OCH₂CH₂CH₂CH₂CH₂CH₃, 20H), 3.70 (br s, OCH₃, 3H), 6.63 (b s, ArH, 2H), 6.70 (b s, ArH, 2H), 6.82 (s, ArH, 2H), 6.94 (b s, ArH, 2H), 7.03 (b s, ArH, 4H). **¹³C NMR** (75 MHz, TCDE, 393 K): δ 11.9, 20.5, 20.8, 21.4, 23.9, 24.1, 27.8, 27.9, 29.0, 29.5, 29.7, 32.1, 71.4, 109.4, 127.7, 123.1, 123.3, 123.8, 125.1, 125.2, 127.9, 129.6, 130.2, 131.2, 131.6, 143.0, 143.2, 144.0, 144.4, 150.2, 150.7, 151.6, 152.3.

Derivative 4.17b. The crude product was purified by column chromatography on silica gel using CHCl₃/n-hexane 40/60 as eluent to give **4.17b** as a pale yellow solid, 0.031 g, 17% yield. **ESI(+)** MS: m/z = 1466 (MNa⁺), 1483 (MK⁺). **¹H NMR** (300 MHz, TCDE, 393 K): δ 0.77 -0.80 [overlapped, O(CH₂)₅CH₃ + C(CH₃)₃, 33H], 0.98 [s, -C(CH₃)₃, 9H], 1.12

[s, $-\text{C}(\text{CH}_3)_3$, 18H], 1.08 –1.62 (overlapped, $\text{OCH}_2\text{CH}_2\text{CH}_2\text{CH}_2\text{CH}_2\text{CH}_3$, 40H), 3.16 (br t, $\text{OCH}_2\text{CH}_2\text{CH}_2\text{CH}_2\text{CH}_2\text{CH}_3$, 2H), 3.49- 3.79 (overlapped, $\text{ArCH}_2\text{Ar} + \text{OCH}_2\text{CH}_2\text{CH}_2\text{CH}_2\text{CH}_2\text{CH}_3$, 20H), 4.53 (br s, OH, 1H), 4.82 (s, OCH_2Ph , 2H), 6.50 –6.64 (overlapped, ArH, 6H), 6.80 (br s, ArH, 2H), 6.93 (s, ArH, 2H), 6.99 (s, ArH, 2H), 7.16 –7.23(overlapped, $\text{OCH}_2\text{C}_6\text{H}_5$, 5H). ^{13}C NMR (75 MHz, TCDE, 393 K): δ 17.0, 25.8, 29.1, 33.0, 33.3, 33.7, 34.0, 34.6, 35.0, 37.1, 74.5, 119.6, 127.9, 128.4, 130.1, 130.5, 131.5, 132.8, 134.0, 134.9, 135.4, 136.7, 148.2, 149.1, 155.9, 156.8, 157.4.

Synthesis of derivative **4.18**



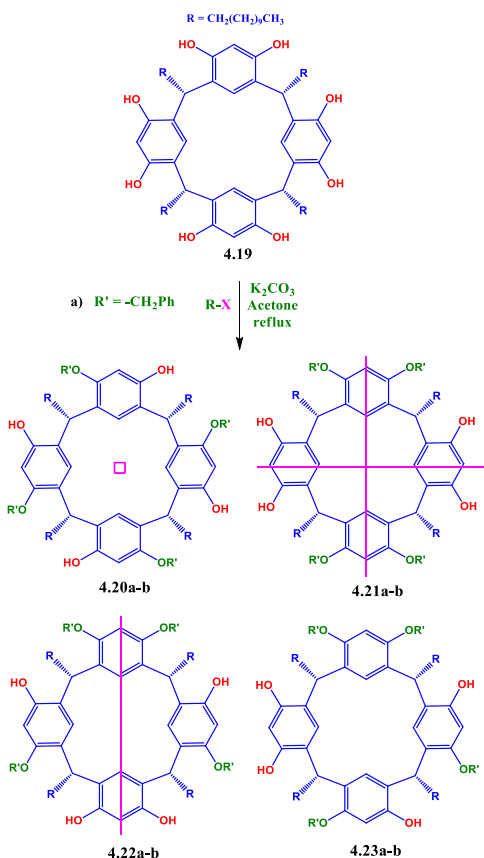
To a solution of *p*-bromodienone **4.11** (0.52 g, 0.47 mmol) in DME (3.0 mL) at 0 °C was added a solution of AgClO_4 (0.19 g, 0.93 mmol) and resorcinol (0.52 g, 4.7 mmol) in DME (4 mL). The reaction mixture was allowed to warm at room

temperature and stirred in the dark overnight. The solvent was removed under reduced pressure, and the residue was solubilized in CH_2Cl_2 (15 mL) and washed with aqueous 1 N HCl and successively with water, dried on Na_2SO_4 , and filtered, and the solvent was removed under reduced pressure. The crude product was purified by column chromatography on silica gel (CH_2Cl_2) to give derivative **4.18** (0.16 g, 30% yield) as a white solid.

ESI(+) MS: $m/z = 1152$ (MH^+). **^1H NMR** (600 MHz, CDCl_3 , 298 K): δ 1.12 [s, $-\text{C}(\text{CH}_3)_3$, 9H], 1.15 [bs, $-\text{C}(\text{CH}_3)_3$, 18H], 1.19 [s, $-\text{C}(\text{CH}_3)_3$, 9H], 1.21 [s, $-\text{C}(\text{CH}_3)_3$, 9H], 1.33 [s, $-\text{C}(\text{CH}_3)_3$, 9H], 3.60 (s, OCH_3 , 9H), 3.83 (s, ArCH_2Ar , 2H), 3.88 (bs, OCH_3 , 6H), 3.97 (s, ArCH_2Ar , 2H), 4.07 (s, ArCH_2Ar , 2H), 4.10 (bs, ArCH_2Ar , 4H), 4.12 (s, ArCH_2Ar , 2H), 4.76 (s, OH, 1H), 5.03 (s, OH, 1H), 6.34 (m, ArH, 1H), 6.36 (bs, ArH, 1H), 6.52 (m, ArH, 1H), 6.55 (m, ArH, 1H), 6.88 – 6.97 (overlapped, ArH, 3H), 7.10 – 7.14 (overlapped, ArH, 3H), 7.24 – 7.32 (overlapped, ArH, 3H), 7.81 (s, ArH, 1H), 8.55 (s, OH, 1H). **^{13}C NMR** (150 MHz, CDCl_3 , 298 K): δ 29.9, 30.2, 30.3, 31.50, 31.51, 31.54, 31.56, 31.8, 32.6, 34.37, 34.41, 34.51, 34.54, 60.93, 60.98, 62.27, 62.34, 104.1, 104.8, 107.5, 108.6, 119.9, 120.1, 125.3, 125.6, 125.7, 125.9, 126.0, 126.1, 126.4, 126.5, 127.1, 127.2, 127.3, 127.7, 131.0, 132.0, 132.3, 132.4, 132.5, 133.2, 133.3, 133.4, 133.5, 133.6, 144.2, 146.3, 146.6, 148.1, 148.3, 152.0,

152.1, 154.6, 154.7, 155.2, 155.7, 155.8, 156.8.

General procedure for the synthesis of derivatives **4.20a** - **4.23a**



A suspension of resorcinarene **4.19** (0.50 g, 0.45 mmol) and K_2CO_3 (0.25 g, 1.8 mmol) was stirred in acetone (30 mL) under reflux. After 1 h BrCH_2Ph (0.54 mL, 4.5 mmol) was

added at room temperature and the mixture was stirred under reflux overnight. The solvent was removed under reduced pressure and the product was extracted in CH_2Cl_2 (50 mL), and washed with 0.1 M HCl (2×30 mL). The organic phase was washed with H_2O (3×20 mL) dried over Na_2SO_4 filtered and evaporated. The crude product was subjected to flash chromatography on deactivated (7.5%) silica gel ($\text{CH}_2\text{Cl}_2/\text{AcOEt}$, 98/2) to give pure **4.20a** and **4.21a** and a mixture of derivatives **4.22a** and **4.23a**, which was separated by preparative TLC (hexane/diethyl ether, 4/6).

Derivative 4.20a.

White solid, 0.036 mmol, 54 mg, yield: 8%. $^1\text{H NMR}$ (300 MHz, CDCl_3 , 298 K): δ 7.38 (m, 20H, CH_2Ph), 7.22 (s, 4H, ArH), 7.12 (s, 4H, OH), 6.38 (s, 4H, ArH), 5.03 and 5.02 (AB, 8H, $J = 11.4$ Hz, OCH_2Ph), 4.26 (t, 4H, $J = 7.6$ Hz, ArCHAr), 2.15 (m, 8H, CHCH_2), 1.27 (m, 72H, $\text{CH}_2(\text{CH}_2)_9\text{CH}_3$), 0.88 (m, 12H, $\text{CH}_2(\text{CH}_2)_9\text{CH}_3$). $^{13}\text{C NMR}$ (75 MHz, CDCl_3 , 298 K): δ 153.1, 152.9, 135.7, 128.8, 128.6, 128.1, 125.2, 124.9, 123.9, 101.8, 71.7, 34.3, 33.3, 32.0, 29.8, 29.5, 28.1, 22.8, 14.2.

Derivative 4.21a. White solid, 0.120 mmol, 174 mg, yield: 26%. $^1\text{H NMR}$ (300 MHz, CDCl_3 , 298 K): δ 7.39 (m, 20H, CH_2Ph), 7.17 (s, 2H, ArH), 7.11 (s, 2H, ArH), 6.78 (s, 4H, OH), 6.49 (s, 2H, ArH), 6.20 (s, 2H, ArH), 5.10 and 5.06 (AB, 8H, $J = 11.4$ Hz, OCH_2Ph), 4.28 (t, 4H, $J = 6.9$ Hz,

ArCHAr), 2.11 (m, 8H, CHCH₂), 1.26 (m, 72H, CH₂(CH₂)₉CH₃), 0.89 (t, 12H, *J* = 6.3 Hz, CH₂(CH₂)₉CH₃). ¹³C NMR (75 MHz, CDCl₃, 298 K): δ 153.4, 152.6, 135.7, 128.9, 128.6, 127.8, 127.3, 126.3, 122.1, 121.9, 103.9, 98.9, 71.9, 34.5, 33.1, 32.0, 29.8, 29.5, 28.0, 22.8, 14.2.

Derivative 4.22a. White solid, 0.041 mmol, 60 mg, yield: 9%. ¹H NMR (400 MHz, CDCl₃, 298 K): δ 7.37 (overlapped, 21H, CH₂Ph + ArH), 7.18 (s, 2H, ArH), 7.10 (s, 1H, ArH), 6.92 (s, 2H, OH), 6.86 (s, 2H, OH), 6.46 (s, 1H, ArH), 6.39 (s, 2H, ArH), 6.21 (s, 1H, ArH), 5.04 (m, 8H, OCH₂Ph), 4.26 (t, 4H, *J* = 7.7 Hz, ArCHAr), 2.14 (m, 8H, CHCH₂), 1.27 (m, 72H, CH₂(CH₂)₉CH₃), 0.89 (m, 12H, CH₂(CH₂)₉CH₃). ¹³C NMR (100 MHz, CDCl₃, 298 K): δ 153.2, 153.1, 152.8, 152.5, 135.7, 135.3, 128.9, 128.7, 127.9, 126.8, 125.8, 124.6, 124.3, 124.2, 123.4, 122.6, 104.6, 101.8, 98.9, 72.0, 71.5, 34.4, 34.1, 33.4, 33.1, 32.0, 29.8, 29.4, 28.0, 22.7, 14.1.

Derivative 4.23a. White solid, 0.104 mmol, 154 mg, yield: 23%. ¹H NMR (400 MHz, CDCl₃, 298 K): δ 7.39 (overlapped, 20H, CH₂Ph), 7.28 (s, 1H, ArH), 7.24 (s, 1H, ArH), 7.15 (s, 1H, ArH), 7.09 (s, 1H, ArH), 7.05 (s, 1H, OH), 6.96 (s, 1H, OH), 6.84 (s, 1H, OH), 6.79 (s, 1H, OH), 6.49 (s, 1H, ArH), 6.39 (s, 1H, ArH), 6.37 (s, 1H, ArH), 6.21 (s, 1H, ArH), 5.06 (overlapped, 8H, OCH₂Ph), 4.26 (overlapped, 4H, ArCHAr), 2.12 (overlapped, 8H, CHCH₂), 1.27 (overlapped, 72H, CH₂(CH₂)₉CH₃), 0.89 (overlapped, 12H,

A mixture of resorcinarene **4.19** (0.50 g, 0.45 mmol) and K_2CO_3 (0.25 g, 1.8 mmol) was stirred in acetone (30 mL) under reflux. After 1 h CH_3I (2.8 mL, 45 mmol) was added at room temperature and the mixture was stirred under reflux for 5 h. The solvent was removed under reduced pressure and the residue partitioned between CH_2Cl_2 (20 mL) and 0.1 M HCl (20 mL). The organic phase was washed with H_2O (3×20 mL) and dried over Na_2SO_4 filtered and evaporated. The crude product was subjected to flash chromatography on deactivated (10%) silica gel ($CH_2Cl_2/AcOEt$, 98/2) to give pure **4.20b** and **4.21b** and a mixture of derivatives **4.22b** and **4.23b** which was separated by preparative TLC (hexane/diethyl ether, 4/6).

Derivative 4.20b. White solid, 0.041 mmol, 47 mg, yield: 9%. 1H NMR (300 MHz, $CDCl_3$, 298 K): δ 7.54 (s, 4H, OH), 7.22 (s, 4H, ArH), 6.35 (s, 4H, ArH), 4.27 (t, 4H, $J = 7.6$ Hz, ArCHAr), 3.84 (s, 12H, OCH_3), 2.19 (m, 8H, $CH_2CH_2CH_2$), 1.27 (m, 72H, $CH_2(CH_2)_9CH_3$), 0.89 (t, 12H, $J = 6.3$ Hz, $C_{10}H_{20}CH_3$). ^{13}C NMR (75 MHz, $CDCl_3$, 298 K): δ 153.6, 152.9, 124.7, 124.6, 123.7, 99.9, 55.8, 33.9, 33.0, 31.9, 29.7, 29.4, 28.1, 22.7, 14.1.

Derivative 4.21b. White solid, 0.113 mmol, 131 mg, yield: 25%. 1H NMR (300 MHz, $CDCl_3$, 298 K): δ 7.19 (s, 4H, ArH), 7.07 (s, 4H, OH), 6.38 (s, 2H, ArH), 6.26 (s, 2H, ArH), 4.28 (t, 4H, $J = 7.5$ Hz, ArCHAr), 3.92 (s, 12H, OCH_3), 2.17 (m, 8H, $CHCH_2CH_2$), 1.26 (m, 72H, $CH_2(CH_2)_9CH_3$), 0.89 (t,

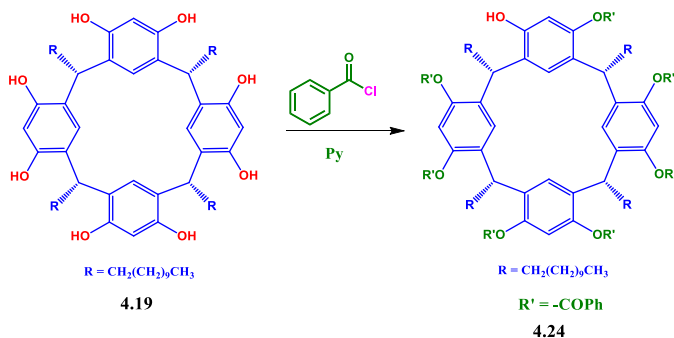
12H, $J = 6.3$ Hz, $C_{10}H_{20}CH_3$). ^{13}C NMR (62.5 MHz, $CDCl_3$, 298 K): δ 153.4, 153.2, 126.4, 125.6, 122.6, 122.2, 104.2, 94.9, 56.2, 34.2, 32.9, 32.0, 29.7, 29.4, 28.0, 22.7, 14.1.

Derivative 4.22b. White solid, 0.049 mmol, 59 mg, yield: 11%. 1H NMR: (250 MHz, $CDCl_3$, 298 K): δ 7.36 (s, 1H, ArH), 7.30 (s, 2H, OH), 7.21 (s, 2H, OH), 7.19 (s, 2H, ArH), 7.12 (s, 1H, ArH), 6.37 (s, 1H, ArH), 6.35 (s, 2H, ArH), 6.28 (s, 1H, ArH), 4.27 (br t, 4H, ArCHAr), 3.91 (s, 6H, OCH_3), 3.83 (s, 6H, OCH_3), 2.18 (m, 8H, $CHCH_2CH_2$), 1.27 (m, 72H, $CH_2(CH_2)_9CH_3$), 0.88 (m, 12H, $C_{10}H_{20}CH_3$). ^{13}C NMR (62.5 MHz, $CDCl_3$, 298 K): δ 153.9, 153.8, 152.8, 152.0, 126.1, 125.5, 124.0, 123.9, 123.9, 123.7, 122.8, 104.7, 99.9, 95.1, 56.2, 55.9, 34.2, 34.1, 33.2, 32.0, 29.8, 29.5, 28.1, 22.8, 14.2.

Derivative 4.23b. White solid, 0.135 mmol, 157 mg, yield: 30%. 1H NMR (400 MHz, $CDCl_3$, 298 K): δ 7.41 (s, 1H, OH), 7.35 (s, 1H, OH), 7.28 (overlapped, 3H, OH + ArH), 7.16 (s, 1H, ArH), 7.15 (s, 1H, ArH), 7.09 (s, 1H, OH), 6.39 (s, 1H, ArH), 6.36 (s, 1H, ArH), 6.34 (s, 1H, ArH), 6.28 (s, 1H, ArH), 4.31-4.26 (overlapped, 4H, ArCHAr), 3.93 and 3.92 (d, 6H, OCH_3), 3.84 and 3.82 (s, 6H, OCH_3), 2.19 (m, 8H, $CHCH_2CH_2$), 1.27 (m, 72H, $CH_2(CH_2)_9CH_3$), 0.90 (overlapped, 12H, $C_{10}H_{20}CH_3$). ^{13}C NMR (62.5 MHz, $CDCl_3$, 298 K): δ 153.9, 153.6, 153.5, 153.1, 153.0, 152.8, 152.6, 126.7, 125.9, 125.1, 124.7, 124.2, 123.7, 123.6, 123.2, 122.8, 122.5, 104.5, 99.96, 99.8, 95.0, 56.2, 55.8, 34.0, 33.1,

33.0, 32.0, 29.7, 29.4, 28.1, 22.7, 14.1.

General procedure for the synthesis of derivative **4.24**



A suspension of resorcinarene **4.19** (0.25 g, 0.23 mmol) and benzoyl chloride (0.32 g, 2.3 mmol), in 5.0 mL of dry pyridine was stirred at room temperature for 10 min. The mixture was dried under vacuum and partitioned between CH₂Cl₂ (30 mL) and 0.1 M HCl (10 mL). The organic phase was washed with H₂O (3×10 mL) and dried. The crude product was purified by flash chromatography on deactivated (10%) silica gel (petroleum ether/CH₂Cl₂, 60/40).

Derivative 4.24; white solid, 0.13 mmol, 0.23 g, yield 55%.

¹H NMR (300 MHz, CDCl₃, 298 K): δ 8.41 (s, 1H, *ArH*), 8.38 (s, 1H, *ArH*), 7.99-7.45 (overlapped, 36H, *ArH*), 7.10 (s, 1H, *ArH*), 7.08 (s, 1H, *ArH*), 6.80 (s, 1H, *ArH*), 6.61 (s, 1H, *ArH*), 6.46 (s, 1H, *ArH*), 6.02 (s, 1H, *OH*), 4.51 (m, 2H, *ArCHAR*), 4.36 (br t, 1H, *ArCHAR*), 4.21 (br t, 1H, *ArCHAR*),

2.07 (m, 4H, CHCH₂CH₂), 1.88 (m, 2H, CHCH₂CH₂), 1.77 (m, 2H, CHCH₂CH₂), 1.19 (m, 72H, CH₂(CH₂)₉CH₃), 0.87 (t, *J* = 6.5 Hz, 12H, C₁₀H₂₀CH₃). ¹³C NMR (62.5 MHz, CDCl₃, 298 K): δ 14.7, 23.2, 28.5, 29.9, 30.2, 30.4, 32.4, 35.1, 35.7, 37.8, 38.0, 90.0, 92.1, 94.2, 112.2, 113.6, 116.6, 118.6, 125.8, 126.1, 128.9, 129.3, 129.6, 129.8, 130.4, 130.5, 130.6, 130.9, 131.5, 131.8, 133.7, 134.0, 134.1, 134.4, 134.7, 135.8, 136.1, 136.6, 137.0, 146.2, 146.3, 146.8, 147.1, 148.7, 148.0, 149.5, 154.6, 163.2, 164.7, 165.0, 166.7, 178.9.

HPLC analysis

Chromatographic conditions employed for stopped-flow measurements

Comp.	Column	Mobile phase	(v/v)	Flow (mL min ⁻¹)	Inj. volume (μ L)	t_r (min)	k_1	k_2	α	R_s
<i>rac</i> -4.20a	Chiralpak AD	<i>n</i> -hexane/2-propanol	99:1	1.0	20	2.780	4.952	6.631	1.339	1.508
					100	3.040	4.383	6.071	1.385	1.595
<i>rac</i> -4.20b	Chiralpak AD	<i>n</i> -hexane/2-propanol	99:1	1.0	20	3.000	1.076	1.562	1.452	1.664
					100	3.047	1.071	1.505	1.406	1.553
<i>rac</i> -4.23a	Lux Amylose-2	<i>n</i> -hexane/methanol	96:4	1.0	20	3.047	1.501	1.792	1.194	1.522
					100	3.047	1.433	1.731	1.208	1.309
<i>rac</i> -4.23b	Chiralpak AD	<i>n</i> -hexane/2-propanol	97:3	1.0	20	2.940	1.746	3.079	1.764	2.731
					100	3.037	1.647	2.926	1.777	2.711
<i>rac</i> -4.24	Lux Cellulose-1	<i>n</i> -hexane/2-propanol	97:3	1.0	20	2.800	2.724	3.821	1.403	1.483
					100	2.793	2.415	3.523	1.458	1.562

All separations were carried out at controlled temperature (15 °C). The 20 μ L injection loop was used during the optimization of chromatographic conditions, while the 100 μ L injection loop was used for stopped-flow measurements.

ECD analysis (in collaboration with Prof. Bertucci and Dott. Tedesco from Università di Bologna) and Theoretical Calculations (in collaboration with Prof. Zanasi and Dott. Monaco from Università degli Studi di Salerno)

The enantiomeric fractions were stopped inside the HPLC flow cell during their elution and analysed by full-spectrum ECD spectroscopy in the 350–215 nm spectral range, using a 4 nm spectral bandwidth, a 50 nm min⁻¹ scanning speed, a 1 s data integration time, a 0.2 nm data pitch and three accumulation cycles.

TD-DFT calculations were performed using combinations of the PBE0 and B3LYP functionals with the 6/31++G* basis sets using Gaussian 03.⁷²

⁷² Frisch, M. J.; Trucks, G. W.; Schlegel, H. B.; Scuseria, G. E.; Robb, M. A.; Cheeseman, J. R.; Montgomery, J. A., Jr.; Vreven, T.; Kudin, K. N.; Burant, J. C.; Millam, J. M.; Iyengar, S. S.; Tomasi, J.; Barone, V.;

Mennucci, B.;ossi, M.; Scalmani, G.; Rega, N.; Petersson, G. A.; Nakatsuji, H.; Hada, M.; Ehara, M.; Toyota, K.; Fukuda, R.; Hasegawa, J.; Ishida, M.; Nakajima, T.; Honda, Y.; Kitao, O.; Nakai, H.; Klene, M.; Li, X.; Knox, J. E.; Hratchian, H. P.; Cross, J. B.; Bakken, V.; Adamo, C.; Jaramillo, J.; Gomperts, R.; Stratmann, R. E.; Yazyev, O.; Austin, A. J.; Cammi, R.; Pomelli, C.; Ochterski, J. W.; Ayala, P. Y.; Morokuma, K.; Voth, G. A.; Salvador, P.; Dannenberg, J. J.; Zakrzewski, V. G.; Dapprich, S.; Daniels, A. D.; Strain, M. C.; Farkas, O.; Malick, D. K.; Rabuck, A. D.; Raghavachari, K.; Foresman, J. B.; Ortiz, J. V.; Cui, Q.; Baboul, A. G.; Clifford, S.; Cioslowski, J.; Stefanov, B. B.; Liu, G.; Liashenko, A.; Piskorz, P.; Komaromi, I.; Martin, R. L.; Fox, D. J.; Keith, T.; Al-Laham, M. A.; Peng, C. Y.; Nanayakkara, A.; Challacombe, M.; Gill, P. M. W.; Johnson, B.; Chen, W.; Wong, M. W.; Gonzalez, C.; Pople, J. A.; *Gaussian 03, Revision B.05*; Gaussian, Inc.: Pittsburgh, PA, 2003.